INTERACTIONS BETWEEN ECOSYSTEMS AND DISEASE IN THE PLANKTON OF FRESHWATER LAKES

A Dissertation
Presented to
The Academic Faculty

by

Rachel M. Penczykowski

In Partial Fulfillment
of the Requirements for the Degree
Doctor of Philosophy in the
School of Biology

Georgia Institute of Technology
December 2013

INTERACTIONS BETWEEN ECOSYSTEMS AND DISEASE IN THE PLANKTON OF FRESHWATER LAKES

Approved by:

Dr. Meghan A. Duffy, Advisor
School of Biology
Georgia Institute of Technology

Dr. Terry W. Snell
School of Biology
Georgia Institute of Technology

Dr. Mark E. Hay
School of Biology
Georgia Institute of Technology

Dr. Joshua S. Weitz
School of Biology
Georgia Institute of Technology

Dr. Joseph P. Montoya
School of Biology
Georgia Institute of Technology

Dr. Spencer R. Hall
Department of Biology
Indiana University

Date Approved: September 16, 2013

To Kathy Mosher and Paul du Vair of Madison East High School

ACKNOWLEDGEMENTS

Congratulations to my advisor, Meghan Duffy, for fledging her first graduate student. I thank Meg for her guidance, support, good humor, and patience over the past 5 years. She has been a fantastic teacher and role model. I am particularly grateful to Meg for advocating a common-sense approach to field and lab work, which can be distilled down to the words of *her* advisor: "You can't analyze data if you're dead."

Next, I want to recognize Spencer Hall for his role as Jedi Master and *de facto* co-advisor. Spencer was gracious enough to let me invade his lab at Indiana University (Bloomington, IN) for two field seasons. I thank him for his help with the bag experiments, for including me "as one of [his] peeps" in the field surveys, and for sometimes letting me choose the podcasts to listen to while we counted zooplankton late into the night. I also thank the other members of my thesis committee for valuable feedback along the way: Mark Hay, Joe Montoya, Terry Snell, and Joshua Weitz.

I greatly appreciate the hard work and insights of my collaborators and co-authors: Dave Civitello, Jessica Hite, Julia Kubanek, Brian Lemanski, Jessica Housley Ochs, Marta Shocket, Drew Sieg, and Hema Sundar. These field surveys and experiments would not have been possible without help from many people, including those who assisted in the field and lab at Indiana University: Alisha Betchtel, Kelly Boatman, Annie Bowling, Zach Brown, and Alex Strauss, and at Georgia Tech: Anna and Stuart Auld, Alison Burger, Dylan Grippi, Melanie Heckman, Stephanie Hernandez, Rachel Lasley-Rasher, Kelsey Poulson-Ellestad, and Catherine Searle. An extra special thank you to J. Hite and M. Shocket for their dedication to "Operation *D(aphnia)*-bag 2.0" (Chapter 4).

I am grateful to Shannon Croft and Diane Heath for many helpful conversations about foraging behavior. In addition, I thank Sandy Brovold (University of Minnesota) for analyzing the carbon and nitrogen content of algae, Ben Bolker (McMaster University, Ontario) for help with statistical analysis, and Eric von Elert (University of Cologne, Germany) for advice on culturing *Microcystis*. I acknowledge Bill Jones and the Indiana Clean Lakes Program for lake morphometry data, and appreciate the cooperation of S. Siscoe (Division of Forestry) and R. Ronk (Division of Fish and Wildlife) at the Indiana Department of Natural Resources for access to field sites.

My thanks to the P.E.O. Sisterhood for their monetary support through a P.E.O. Scholar Award, and especially to the women of Atlanta's Chapter B for their kindness and encouragement in the final years of my graduate studies. This research was funded in part by a National Science Foundation Graduate Research Fellowship.

I have many wonderful friends to thank for enriching my life and my grad school experience. In particular, I thank Mel Heckman for being an amazing roommate, and for her commitment to our theme parties (e.g., dinos'more, pirate, superhero, *Mega Shark vs. Giant Octopus*, and Mary Martin's *Peter Pan*). To quote the party favor rocks at the Velociraptor Awareness Day Awareness Party: "Hope you had a rock-in' good time!"

Oczywiście, dziękuję bardzo to my family for loving and supporting me during these 22.5 years of school, and for going above and beyond to facilitate my dissertation writing in Madison this summer. I look forward to more Wednesday latte days with you.

Finally, I thank my husband, Dr. James Jackson Potter, for his patience, love, and help in the field/lab/Matlab. Thanks for being game to do this Ph.D. thing with me, and for letting me defend first so that we could be Dr. and Mr. Potterkowski for 3 whole days.

TABLE OF CONTENTS

LIST OF TABLES

LIST OF FIGURES

SUMMARY

I investigated effects of environmental change on disease, and effects of disease on ecosystems, using a freshwater zooplankton host and its fungal parasite. This research involved lake surveys, manipulative experiments, and mathematical models. My results indicate that ecosystem characteristics such as habitat structure, nutrient availability, and quality of a host's resources (here, phytoplankton) can affect the spread of disease. For example, a survey of epidemics in lakes revealed direct and indirect links between habitat structure and epidemic size, where indirect connections were mediated by non-host species. Then, in a mesocosm experiment in a lake, manipulations of habitat structure and nutrient availability interactively affected the spread of disease, and nutrient enrichment increased densities of infected hosts. In a separate laboratory experiment, poor quality resources were shown to decrease parasite transmission rate by altering host foraging behavior. My experimental results also suggest that disease can affect ecosystems through effects on host densities and host traits. In the mesocosm experiment, the parasite indirectly increased abundance of algal resources by decreasing densities of the zooplankton host. Disease in the experimental zooplankton populations also impacted nutrient stoichiometry of algae, which could entail a parasite-mediated shift in food quality for grazers such as the host. Additionally, I showed that infection dramatically reduces host feeding rate, and used a dynamic epidemiological model to illustrate how this parasite-mediated trait change could affect densities of resources and hosts, as well as the spread of disease. I discuss the implications of these ecosystem–disease interactions in light of ongoing changes to habitat and nutrient regimes in freshwater ecosystems.

CHAPTER 1

INTRODUCTION

Changes in climate and land use are altering ecosystems worldwide (Foley et al. 2005, MEA 2005, Fowler et al. 2013). Their effects on ecosystems include altered habitat structure, nutrient regimes, and productivity. One of the many concerns regarding such changes is that they will drive increases in the prevalence or severity of infectious diseases (Harvell et al. 1999, Marcogliese 2001, Burdon et al. 2006, Lafferty 2009). Given the importance of disease to wildlife conservation (e.g., McCallum et al. 2009, Kilpatrick et al. 2010), agriculture and aquaculture (e.g., Power 1987, Sumpter and Martin 2004, Pulkkinen et al. 2010), and human health (e.g., Daszak et al. 2000, MEA 2005), ecologists and epidemiologists have focused much effort on uncovering environmental and ecological drivers of disease. Indeed, there is now a substantial body of literature on how environmental and ecological context influence both the spread of disease and the consequences of disease for hosts (e.g., Johnson et al. 2010b, Keesing et al. 2010, Rohr et al. 2011).

At the same time, ecologists are beginning to recognize that effects of disease can propagate beyond host populations (Tompkins et al. 2011, Hatcher et al. 2012). By altering host densities or traits, parasites may indirectly affect resources, competitors, or predators of hosts (Lafferty and Morris 1996, Burdon et al. 2006, Holdo et al. 2009). In addition, because parasites consume host resources, and can themselves be eaten, a significant proportion of food web links may directly involve parasites (Lafferty et al. 2006, Preston et al. 2012). Therefore, parasites could play major roles in influencing how energy and nutrients flow through ecosystems. This raises the intriguing possibility that changes to climate and land use could drive patterns of parasitism, which could in turn affect how ecosystems respond to environmental forcing. In this dissertation, I investigate

how ecosystems shape disease, and how disease may shape ecosystems, using a model freshwater host-parasite-resource system.

Ecosystems affect disease

Chapters 2–4 of my dissertation focus on roles of habitat structure and nutrient availability in the spread of disease. Features of habitat, such as size or connectedness, can affect disease transmission through several mechanisms (Ostfeld et al. 2005). For example, larger habitat patches might support greater densities of hosts, which could lead to larger epidemics of diseases with density-dependent transmission (Anderson and May 1992). Alternatively, larger habitats might allow for greater biodiversity, including species that inhibit the spread of disease (e.g., through a 'dilution effect'; Keesing et al. 2006). In some systems, more fragmented or structured habitats might segregate hosts from parasites, leading to reduced transmission (Smith et al. 2002, Collinge et al. 2005, Johnson et al. 2009b), while more connected habitats promote host-parasite contact (McCallum et al. 2003). In other systems, habitat fragmentation or juxtaposition of different habitat types may lead to increased transmission at edges (Plowright et al. 2011). Thus, to assess how habitat structure should affect disease, we need to understand features of the host-parasite system, including the mode of transmission, relative motility of the host and parasite, and how habitat structure affects ecological drivers of disease.

Nutrient availability can influence the spread of disease through effects on ecosystem productivity and the quantity and quality of resources for hosts. As with habitat structure, increased nutrient supply might enhance or depress the spread of disease, depending on characteristics of the host-parasite system and the community in which it is embedded (Johnson et al. 2010b). In some systems, nutrient enrichment might stimulate the abundance or nutritional quality of resources for hosts. This could lead to higher infection prevalence if host density increases, or if better fed hosts produce more parasite propagules (Johnson et al. 2007, Seppälä et al. 2008). On the other hand, more

abundant resources, or resources with certain chemical properties, could lessen the spread of disease by improving the overall condition or immune function of hosts (Ali et al. 1998, Babin et al. 2010, Cotter et al. 2011). The quantity and quality of resources in the environment can also dictate the rate at which hosts forage (Krebs et al. 1974, Plath and Boersma 2001, Cruz-Rivera and Hay 2003, Darchambeau and Thys 2005), as well as the types of habitat in which they search for food (Hutchings et al. 2001, Johnson et al. 2009a). This may affect disease transmission for the broad array of hosts that become exposed to parasites while foraging (e.g., Hutchings et al. 2001, Dwyer et al. 2005, Fels 2005, de Roode et al. 2008, Johnson et al. 2009a).

Because they share similar drivers (e.g., changes in climate and land use), habitat structure and the quantity or quality of resources for hosts may be altered simultaneously in many ecosystems. Therefore, as part of my dissertation, I studied not only the influence of each of these environmental changes on disease spread, but also the potential for interactive effects between them.

Diseases affect ecosystems

Ecologists increasingly recognize that parasites are ubiquitous (Lafferty et al. 2008, Gachon et al. 2010), and can have major effects on populations (May 1983, Hudson et al. 1998, Duffy and Sivars-Becker 2007) and communities (Park 1948, Tompkins et al. 2003, Hatcher and Dunn 2011). Yet we are only beginning to understand the role of parasites at the ecosystem level (Hudson et al. 2006, Tompkins et al. 2011, Hatcher et al. 2012). How do parasites affect the movement of energy and nutrients through ecosystems? Could parasites modulate how ecosystems respond to changes in climate or land use? Chapters 3 and 4 of my dissertation lay some groundwork for answering these questions.

One way that parasites may affect the flow of energy and nutrients through ecosystems is by impacting host densities (Lafferty et al. 2008, Hatcher et al. 2012). For

diseases of primary producers, disease-mediated density reductions may directly affect productivity or nutrient cycling (Burdon et al. 2006, Gachon et al. 2010, Rhodes and Martin 2010). For hosts at higher trophic levels, parasites can indirectly affect resources through trophic cascades (Duffy 2007, Holdo et al. 2009). Parasite-mediated density reductions may also affect food web fluxes through indirect effects on competitors or consumers of hosts (Park 1948, Tompkins et al. 2003, Ferrer and Negro 2004). Such density-mediated effects of disease are most likely to be detected for parasites that cause strong negative effects on host fecundity or survivorship, particularly if the host is either a dominant or keystone species in the community.

However, parasites that do not reduce host density may still affect food webs and ecosystem functioning through effects on host traits. Regardless of their effects on host fecundity or survivorship, parasites typically alter other host traits (Moore 1995). For example, host strategies for resisting or compensating for infection may involve changes in activity levels, foraging rates, or diet (Hart 1990, Lefèvre et al. 2010). In addition, within-host parasite growth can affect host size, morphology, behavior, or nutrient content (Wood et al. 2007, Forshay et al. 2008, Careau et al. 2010). Many parasites also manipulate host behavior or habitat use to increase the probability of transmission (Lafferty and Morris 1996, Lefèvre et al. 2009, Sato et al. 2012). These types of parasite-mediated trait changes could have major implications for the transfer of energy and nutrients through food webs and ecosystems (Thomas et al. 1998, Bernot and Lamberti 2008, Hernandez and Sukhdeo 2008a, Sato et al. 2011).

Dissertation overview

Study system

I studied interactions between ecosystems and disease using a host–parasite system in the plankton of freshwater lakes. The host, *Daphnia dentifera*, is a dominant

zooplankton grazer in small, thermally stratified lakes in temperate North America (Tessier and Woodruff 2002). This host species ingests free-living spores of the fungal parasite, *Metschnikowia bicuspidata*, while non-selectively foraging in the water column (Ebert 2005, Hall et al. 2007b). In a successful infection, the parasite pierces the gut wall of its host and reproduces in the hemolymph (Ebert 2005). As new spores proliferate throughout the host's body, the parasite can cause large reductions in host growth, fecundity, and survivorship (Hall et al. 2009c). Infective spores are released into the water only after death of the host (Ebert 2005). In the Midwestern USA, epidemics typically occur between July and December (Hall et al. 2011, Overholt et al. 2012).

Chapters 2, 3, and 4: Ecosystems affect disease

In Chapter 2 of my dissertation, I use a field study to investigate potential direct and indirect links between habitat and the spread of disease. Using data from a survey of epidemics in 18 lakes, I illustrate connections between lake size, productivity, light environment, thermal stratification of the water column, ecological drivers of disease, and the timing and overall size of epidemics. Chapter 3 describes an experiment in which I manipulated resource quality for hosts, where a 'high quality' green alga yielded faster somatic growth of hosts compared to a 'low quality' cyanobacterium. I show that the cyanobacterium depressed transmission potential by reducing host foraging rate, thereby decreasing the rate of parasite encounter. This resource quality manipulation is relevant to large-scale ecosystem change because cyanobacteria are generally favored by climate warming and nutrient enrichment (Carey et al. 2012, O'Neil et al. 2012). In Chapter 4, I present a mesocosm experiment in which I tested for interactions between altered habitat structure (i.e., disruption of thermal stratification achieved by manually mixing the water column) and nutrient enrichment on disease. I found that nutrient enrichment and disrupted stratification can jointly promote the spread of disease, and that nutrient enrichment in particular can fuel large densities of infected hosts. Data from a survey of

epidemics in lakes over multiple years are consistent with the interpretation that high densities of infected hosts may seed larger future epidemics.

Chapters 4 and 5: Diseases affect ecosystems

The results of the mesocosm experiment in Chapter 4 also highlight the potential for disease to modulate effects of environmental forcing on ecosystems. Specifically, parasite-mediated reductions in host density allowed for greater algal abundance in the low nutrient compared to the high nutrient treatment. In addition, epidemics altered nutrient stoichiometry of algae (relative to disease-free control mesocosms) in both high and low nutrient treatments. Finally, in Chapter 5, I show that infection reduces host feeding rates. I develop a mathematical model to describe the mechanism for this trait change, and I use that model to estimate the potential reduction in average feeding rates of adult hosts during natural epidemics. Then I use a dynamic epidemiological model to explore how this disease-mediated reduction in feeding rate could affect densities of hosts and resources, as well as the spread of disease.

CHAPTER 2

HABITAT STRUCTURE AND ECOLOGICAL DRIVERS OF DISEASE[1]

Abstract

Habitat can influence disease directly, through effects on hosts and parasites, or indirectly, through effects on ecological drivers of disease. We illustrated direct and indirect connections between habitat and outbreaks using a case study in the plankton. We sampled yeast epidemics in 18 populations of the lake zooplankter *Daphnia dentifera*. Lake size drove variation in two types of habitat structure, size of predation refuges and strength of stratification. Those habitat factors, in turn, indirectly linked to epidemics through two pathways involving non-host species. In the first pathway, larger lakes had larger hypolimnetic refuges from vertebrate predation and greater densities of *Daphnia pulicaria*, a completely resistant species that can reduce disease risk for *D. dentifera* hosts by removing parasite spores from the environment. In lakes with more *D. pulicaria*, epidemics started later in autumn and remained smaller. In the second pathway, smaller lakes had shallower penetration of light, which correlated with stronger thermal stratification and higher densities of an invertebrate predator (*Chaoborus*) that spreads disease by releasing spores from infected hosts. Lakes with weaker stratification had fewer of these predators and smaller epidemics. In the second pathway, deeper light penetration may also decrease disease by imposing direct mortality on spores. Thus, this

---

[1] Adapted from: Penczykowski, R. M., S. R. Hall, D. J. Civitello, and M. A. Duffy. in press. Habitat structure and ecological drivers of disease. Limnology and Oceanography.

case study shows how habitat structure could influence epidemics through direct and indirect effects on the host–parasite system. Understanding these multiple mechanisms can enhance prediction of disease outbreaks as habitat modification continues in lakes and other ecosystems worldwide.

Introduction

Infectious diseases and habitat alteration are changing ecosystems worldwide (Daszak et al. 2000, Foley et al. 2005). Furthermore, these two factors may interact: habitat alteration may catalyze further spread of epidemics (Patz et al. 2004, Ostfeld et al. 2005). But how does habitat structure drive disease mechanistically? That is, through which direct and indirect pathways does habitat structure influence epidemics? Direct effects of habitat on disease arise through several mechanisms: the size, shape, and connectedness of habitat patches can determine host densities and dispersal rates, contact rates between hosts and free-living parasite stages, and disease transmission at habitat edges (Patz et al. 2004, Ostfeld et al. 2005). Habitat structure may also indirectly alter density of other species that catalyze or inhibit disease spread (Hall et al. 2010b). For example, habitat might increase or suppress density of 'diluting host' species that remove free-living parasites without becoming infected (Keesing et al. 2006). Furthermore, habitat structure may favor or disfavor predators that selectively cull infected hosts (Duffy et al. 2005). Given the range of possibilities, the challenge becomes delineating mechanistic connections between habitat and drivers of disease spread.

Freshwater ecosystems offer ideal environments in which to connect habitat to disease. Major drivers of habitat structure vary among lakes, including basin size and shape, light penetration, thermal stratification, and dissolved oxygen concentration. In a given lake, some of these factors (e.g., light attenuation, stratification, and hypoxic zones) vary within seasons (Tessier and Welser 1991, Johnson et al. 2009b) and among years (De Stasio et al. 1996, Fee et al. 1996). Human activities, such as those that cause

eutrophication, can also alter habitat structure, e.g., by decreasing light penetration and increasing the extent of hypoxia (Mazumder et al. 1990, Marcogliese 2001). This variation in habitat can determine the density and distributions of many aquatic organisms (Threlkeld 1979, Kitchell and Kitchell 1980, Malinen et al. 2001), including parasites (Marcogliese 2001, Johnson et al. 2009b, Hall et al. 2010b).

Here, we illustrate how habitat links to the timing and size of epidemics via multiple pathways in thermally stratified lakes. In these lakes in the Midwestern USA, a yeast parasite (*Metschnikowia bicuspidata*) infects its host *Daphnia dentifera*, a dominant zooplankton grazer (Tessier and Welser 1991). Yeast epidemics start in late summer and extend until early winter (Cáceres et al. 2006, Hall et al. 2011, Overholt et al. 2012). The yeast kills its infected host, thereafter releasing infectious propagules (spores) into the environment to infect new hosts (Ebert 2005). All mechanisms described here ultimately involve this life stage of the parasite. Spore density, not host density, is a sensitive driver of epidemic size in this system (Cáceres et al. 2006, Hall et al. 2009a, Hall et al. 2010b). Using correlative evidence from an extensive field survey conducted in 2009, we focus on indirect relationships between habitat and disease involving two non-host species (Pathways 1 and 2; Fig. 2.1). We also argue for two potential direct links from habitat to disease involving stratification and its driver (Pathway 2; Fig. 2.1).

The two indirect pathways involve non-host species that we mechanistically connected to yeast epidemics in previous work (Cáceres et al. 2009, Hall et al. 2009a, Hall et al. 2010b). Here, we link these species to large scale habitat structure. Both indirect pathways begin with lake size (indexed as surface area) as an ultimate driver of habitat structure (Fig. 2.1). In Pathway 1, bigger lakes were deeper, and greater depth permitted a larger refuge from vertebrate (fish) predation for large bodied zooplankton (as defined below; Threlkeld 1979, Tessier and Welser 1991). This refuge provided essential habitat for *Daphnia pulicaria*, a zooplankton grazer that consumes yeast spores and removes them from the environment but does not become infected (i.e., it functions

as a completely resistant ‘diluter’ in disease ecology; Keesing et al. 2006, Hall et al. 2009a). Higher density of this diluter species, in turn, delayed the start of epidemics. This delay mattered because epidemics that started earlier grew larger (Hall et al. 2011, Overholt et al. 2012), likely due to thermal mechanisms such as increases in host birth rate, parasite transmission rate, and parasite production with water temperature (Hall et al. 2006b). Pathway 2 also begins with lake size, but then moves along a different, uncorrelated path involving stratification and a predator. Solar radiation (indexed by extinction of photosynthetically active radiation [PAR]) penetrated less deeply into smaller lakes. Because more heat was absorbed in shallower waters, lakes with higher light extinction became more strongly stratified (Kling 1988). These more strongly stratified lakes, in turn, supported higher density of *Chaoborus punctipennis.* This invertebrate predator can spread disease through multiple mechanisms, especially through epilimnetic release of spores via sloppy feeding on hosts (Cáceres et al. 2009, Duffy et al. 2011). Thus, lakes with stronger stratification had larger epidemics. This second pathway has two direct-effect correlates. High light extinction may have shielded spores from damaging solar radiation (ultraviolet [UV] and PAR wavelengths) in the epilimnion (Overholt et al. 2012). Stronger stratification may have retarded the loss of spores through sinking (Brookes et al. 2004, Cáceres et al. 2009). The results of this study show the signature of these mechanisms.

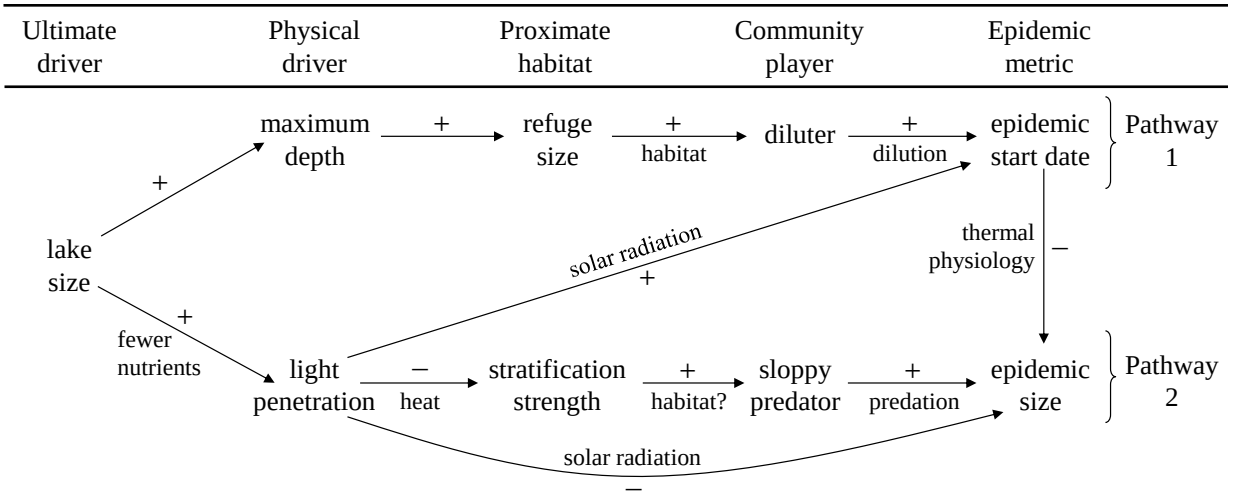

Figure 2.1. Pathways connecting habitat to epidemic metrics. Lake size is the ultimate habitat driver of disease. However, it acts through two physical drivers that influence proximate habitat factors (Figs. 2.2, 2.3), which relate to key community players that shape epidemics (Fig. 2.4). Pathway 1: Larger, deeper lakes have bigger refuges from vertebrate predation that bolster density of a species that can dilute disease, *Daphnia pulicaria*. Higher density of the 'diluter' delays the start date of epidemics, and a later start date can constrain the size of epidemics through thermal physiology. Pathway 2: Light penetrates less deeply in smaller lakes, intensifying stratification. More strongly stratified lakes support higher density of a 'sloppy predator', *Chaoborus punctipennis*, which correlates positively with epidemic size. Direct pathways may also connect solar radiation to epidemic metrics (Fig. 2.5). Positive (+) and negative (-) symbols denote sign of the relationships involved.

Methods

Study system

We studied two *Daphnia* species that are common planktonic grazers in small, thermally stratified lakes in temperate North America (Tessier and Welser 1991). *D. dentifera* and *D. pulicaria* encounter and ingest spores of the yeast parasite *Metschnikowia bicuspidata* (hereafter: yeast) while non-selectively foraging on small algae (Ebert 2005, Hall et al. 2009a). The parasite penetrates the gut wall of its focal host (*D. dentifera*) and multiplies in its hemolymph (Ebert 2005). As it uses host resources to fuel its own reproduction, this parasite reduces host growth, fecundity, and survivorship (Hall et al. 2009c). Parasite spores, once released from the carcasses of dead hosts, can then infect new hosts (Ebert 2005). While yeast epidemics occur in lakes in the upper Midwestern USA (Hall et al. 2011), the diluter species (*D. pulicaria*) resists infection by this parasite (Hall et al. 2009a).

Lake survey

We sampled 18 lakes in southern Indiana (Greene and Sullivan Counties) weekly from August until the first week of December 2009. On every sampling visit, we collected two replicate plankton samples that each contained three pooled tows of a Wisconsin net (13 cm diameter, 153 μm mesh, towed bottom to surface). From one of the plankton samples, we diagnosed infection status of at least 400 live *D. dentifera* under a dissecting scope at 20–50X magnification, following Ebert (2005). Body length of a subset of uninfected adult *Daphnia dentifera* hosts was also measured as an index of fish predation: smaller mean length indicates stronger predation pressure (Kitchell and Kitchell 1980). The other sample was preserved in 60–75% ethanol and counted under a dissecting scope to estimate areal densities of *D. dentifera* (the focal host), *D. pulicaria* (the diluter), and *Chaoborus punctipennis* (the sloppy invertebrate predator). We only

present data on *Chaoborus* large enough to eat *Daphnia* hosts (instars 3+) (Moore 1988).

We calculated two metrics of yeast outbreaks, start date and epidemic size. We defined start date of epidemics as the sampling date on which infection prevalence first exceeded 1%. Based on this definition, 15 of the 18 lakes experienced outbreaks, but two of them started before we began sampling. For those two lakes, we assigned the day of first sampling as the start date. We estimated the size of epidemics by integrating infection prevalence (proportion infected) through time using the trapezoid rule. This metric (integrated prevalence, with units of proportion · days) correlated strongly with maximal prevalence of infection (Pearson correlation, $r = 0.93$, $p < 0.0001$).

To investigate links between lake morphometry and habitat structure, we obtained data on lake surface area and maximum depth from the Indiana Clean Lakes Program (W. W. Jones unpubl.). Fetch was measured as the greatest uninterrupted distance across a lake in the direction of the average prevailing winds. Several key habitat indices stemmed from temperature- and oxygen-based calculations. On each sampling visit, we measured vertical profiles of temperature and dissolved oxygen at 1 m intervals using a Hydrolab multiprobe (Hach Environmental). We vertically interpolated the temperature data to a 0.1 m depth interval (using a piecewise cubic hermite interpolating polynomial, 'pchip'; Matlab version 7.8 R2009a; MathWorks). Then we identified the bottom of the epilimnion (Z_E) as the depth at which temperature decreased by greater than 1°C m^{-1}. Refuge size (Pathway 1) was calculated as the distance between Z_E and a deeper, low oxygen (1 mg L^{-1}) threshold (Z_O) also found with splines (Tessier and Welser 1991). Additionally, we calculated buoyancy frequency at the thermocline – an index of the strength of stratification (Pathway 2) – based on a density criterion. To calculate it, we converted water temperature at each depth j into a density, ρ_j (following Chen and Millero 1977). Buoyancy frequency (N_j) was then calculated as

$$N_j = \sqrt{\frac{g}{\bar{\rho}}\left(\frac{d\rho_j}{dz}\right)} \qquad (2.1)$$

where $\bar{\rho}$ is the mean density of the water column, $d\rho_j/dz$ is the vertical density gradient at depth j, and g is gravitational acceleration (9.81 m s^{-2}). The thermocline occurs at the depth of maximum strength of stratification (N_{max}, cycles per hour [cph]). We used August N_{max}, at the start of epidemic season, as our stratification index. All lakes were strongly stratified (N_{max} > 48 cph) during this period (MacIntyre and Melack 1995).

We estimated penetration of photosynthetically active radiation (PAR) using irradiance data collected at 1 m intervals (0–4 m, duplicate profiles) with a LI-250A light meter (LI-COR). Then, we regressed natural log-transformed irradiance $I(z)$ against depth (z):

$$\ln(I[z]) = a - kz + \varepsilon \quad (2.2)$$

with intercept a and residual errors ε. The slope is the coefficient of light extinction, k (μmol quanta cm^{-2} s^{-1} m^{-1}). Values of $-k$ that are closer to zero indicate deeper light penetration while more negative values of $-k$ indicate shallower light penetration.

We also measured epilimnetic concentrations of total phosphorus (TP) and chlorophyll *a*. TP samples were analyzed on a UV-1700 spectrophotometer (Shimadzu Scientific Instruments) using the ascorbic acid method following persulfate digestion (APHA 1995). We measured chlorophyll *a* using narrow band filters on a Trilogy fluorometer (Turner Designs) following chilled ethanol extraction (Welschmeyer 1994).

Statistical analysis

Statistical analyses were performed in R and Matlab. Linear and nonlinear relationships were assessed using correlations and nonlinear regressions, respectively. To assess the linear relationship between refuge size and epidemic start date including an outlier point, we used the least absolute residual (LAR) method, which is robust to outliers (Neter et al. 1996). In all other cases, we estimated parameters by minimizing sums-of-squares. We log-transformed surface area, zooplankton density, and chlorophyll *a* data to meet assumptions of normality and homoscedasticity. For variables that did not

meet assumptions of normality after transformation (according to the Shapiro–Wilk test), we computed significance of correlations using permutation tests (9999 randomizations) (Bishara and Hittner 2012). We also used permutation tests to compute significance of the nonlinear (exponential: $Y = a \exp[\, bX \,] + \varepsilon$) and LAR regressions. Confidence intervals around parameters were estimated using 10,000 bootstraps.

Results

We first established links between the ultimate habitat driver (lake size), two proximate habitat features (refuge size and stratification strength), and two epidemic metrics (start date and size) along the two pathways (Fig. 2.1). Despite sharing an ultimate driver (lake size), the proximate habitat features in each pathway were uncorrelated (r = -0.07, p = 0.79). Several correlations significantly supported the mechanisms of Pathway 1. Larger lakes, i.e., those with greater surface area, had greater maximum depth (r = 0.59, p = 0.003; Fig. 2.2A). This physical driver, lake depth, created room for larger habitat refuges from fish predation in August (r = 0.91, p < 0.0001; Fig. 2.2B). Lakes with larger refuges, in turn, had later epidemic start dates (LAR regression: p = 0.046; correlation when excluding the outlier denoted with an arrow: r = 0.67, p = 0.009; Fig. 2.2C). Thus, epidemics started later in bigger lakes with larger refuges. Pathway 2 was also supported by several significant correlations. Larger lakes had deeper light penetration in August (r = 0.51, p = 0.018; Fig. 2.2D). Deeper light penetration then correlated with weaker strength of stratification in August (r = -0.55, p = 0.013; Fig. 2.2E). More weakly stratified lakes had smaller epidemics (r = 0.63, p = 0.004; Fig. 2.2F). Thus, lake size drove variation in light penetration, which was a physical driver of stratification strength. Stratification strength, in turn, correlated positively with the size of yeast outbreaks.

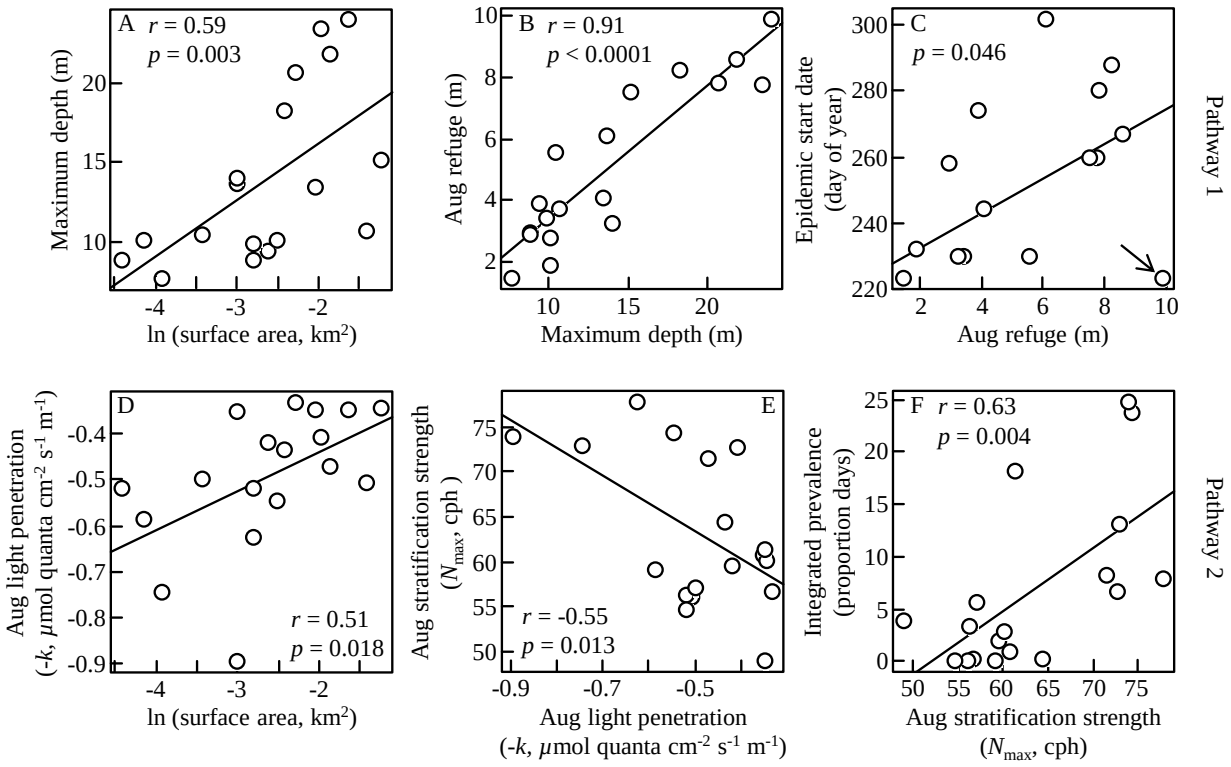

Figure 2.2. Connections between habitat features and key epidemic metrics. (A–C) Pathway 1: (A) Larger lakes had greater maximum depth, and (B) deeper lakes had larger refuges from predation. (C) Epidemics started later in the season in lakes with larger refuges. (The arrow points to an outlier that is referred to in the text; *p*-value stems from LAR regression that includes this data point.) (D–F) Pathway 2: (D) Light penetrated less deeply (i.e., the index of light penetration was more negative) in smaller lakes. (E) When light penetrated less deeply, stratification was stronger in August, near the start of epidemics. (F) Epidemics grew larger in lakes with stronger stratification.

Lake size connected to the two forms of proximate habitat structure through physical drivers (Fig. 2.1). In Pathway 1, lake size correlated with thickness of the predation refuge due to differential response of epilimnetic depth (Z_E, top of refuge) and the 1 mg L^{-1} dissolved oxygen threshold (Z_O, bottom of refuge). The epilimnion was deeper in lakes with larger surface area, *SA* ($r = 0.55$, $p = 0.017$; Fig. 2.3A), longer fetch, *F* (ln[*SA*] and ln[*F*]: $r = 0.74$, $p = 0.0005$; ln[*F*] and Z_E: $r = 0.66$, $p = 0.003$; not shown), and deeper light penetration ($r = 0.59$, $p = 0.002$; not shown). However, depth to the hypoxic zone (Z_O) increased with maximum depth, Z_{max} ($r = 0.88$, $p < 0.0001$; Fig. 2.3B), more steeply than did Z_E ($r = 0.64$, $p = 0.003$; Fig. 2.3B). Since refuge size is $Z_O - Z_E$, larger lakes had bigger refuges (Figs. 2.2B, 2.3B). By contrast, lake size did not correlate with August stratification strength, N_{max} (N_{max} and Z_{max}: $r = 0.12$, $p = 0.32$; N_{max} and ln[*SA*]: $r = -0.04$, $p = 0.89$). In Pathway 2, the positive correlation between lake size and light penetration (Fig. 2.2D) related to nutrient loading and phytoplankton biomass. Smaller lakes had greater total phosphorus (TP) concentrations (ln[*SA*]: $r = -0.50$, $p = 0.035$; Fig. 2.3C). Lakes with higher TP had greater phytoplankton density, indexed as chlorophyll *a* ($r = 0.86$, $p < 0.0001$; Fig. 2.3D). In lakes with more phytoplankton, light penetrated less deeply ($r = -0.72$, $p = 0.002$; Fig. 2.3E).

Each proximate habitat pathway involved a key species (community player; Fig. 2.1) – but not density of the focal host or an index of fish predation. Specifically, density of *D. dentifera* did not correlate with refuge size ($r = -0.12$, $p = 0.65$) and correlated negatively with stratification strength ($r = -0.52$, $p = 0.039$); that is, in the opposite direction from what we would expect if stratification increased disease prevalence by increasing host density. Additionally, the predation index (length of hosts) did not correlate with refuge size ($r = 0.22$, $p = 0.37$) or stratification strength ($r = 0.32$, $p = 0.20$). Furthermore, neither length nor density of hosts correlated with epidemic start date (length: $r = 0.05$, $p = 0.86$; density: $r = 0.35$, $p = 0.22$) or epidemic size (length: $r = 0.28$, $p = 0.13$; density: $r = -0.19$, $p = 0.25$). Instead, two other species were involved. In

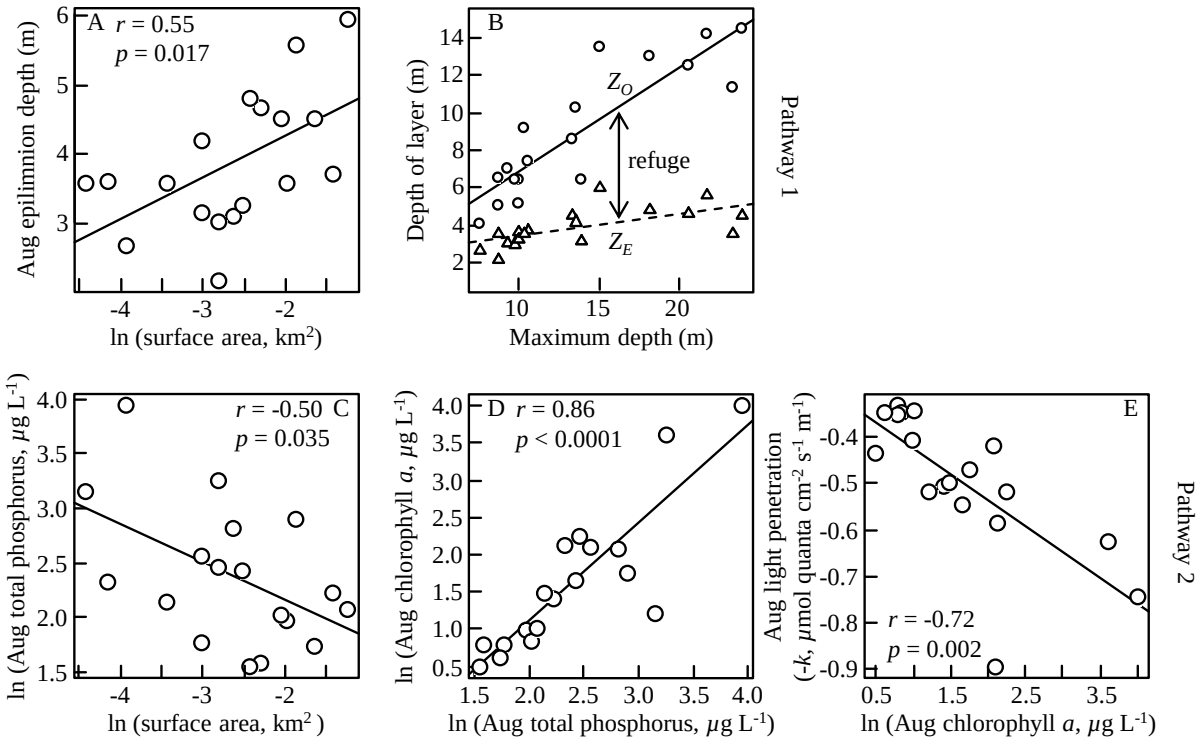

Figure 2.3. (A, B) Pathway 1: Linking lake size to refuge size. (A) Larger lakes had greater epilimnion depth. All else equal, lakes with greater epilimnetic depths should have had smaller refuge layers. (B) However, because depth to the low dissolved oxygen threshold (Z_O, circles, solid regression line) increased more steeply with maximum depth than did depth to the epilimnion (Z_E, triangles, dashed regression line), the refuge layer was larger in bigger, deeper lakes. (C–E) Pathway 2: Linking lake size to light extinction. Bigger lakes had deeper penetration of light through nutrient-to-phytoplankton effects. (C) Smaller lakes had higher total phosphorus in the epilimnion, (D) yielding more phytoplankton (chlorophyll *a*). (E) Light penetrated less deeply into lakes with more chlorophyll *a*.

Pathway 1, the correlation between refuge size and start date was related to the diluter (*Daphnia pulicaria*). Lakes with larger refuges in August had greater densities of the diluter in August ($r = 0.62$, $p = 0.004$; Fig. 2.4A). Lakes with more diluters, in turn, had epidemics that started later (exponential model: $R^2 = 0.50$, $p = 0.008$; Fig. 2.4B). Start date, then, predicted epidemic size. Outbreaks that started earlier in the season grew to larger sizes (exponential model: $R^2 = 0.55$, $p = 0.006$; Fig. 2.4C). Thus, epidemics were smaller overall in lakes with more diluters at the beginning of epidemic season ($r = -0.54$, $p = 0.037$; Fig. 2.4D). However, density of diluters was not significantly correlated with strength of stratification in August, the other proximate habitat feature ($r = -0.36$, $p = 0.08$). Instead, in Pathway 2, stratification strength correlated positively with density of the sloppy predator, *Chaoborus* ($r = 0.58$, $p = 0.012$; Fig. 2.4E). Lakes with more sloppy predators, in turn, had larger epidemics ($r = 0.68$, $p = 0.002$; Fig. 2.4F). However, this predator did not increase with refuge size ($r = -0.17$, $p = 0.51$) and only weakly correlated with start date of epidemics ($r = -0.51$, $p = 0.055$). Densities of the diluter and sloppy predator were also uncorrelated ($r = -0.08$, $p = 0.39$). Thus, the two pathways involved different players: the refuge pathway (1) involved the diluter, while the stratification pathway (2) involved the sloppy predator.

The field data also suggest two possible direct effects on epidemics in Pathway 2 (Fig. 2.1). The first involves light which can damage spores. Specifically, in lakes with deeper penetration of light, epidemics started later ($r = 0.55$, $p = 0.010$; Fig. 2.5A) and were smaller ($r = -0.64$, $p = 0.012$; Fig. 2.5B). The second involves the possibility that the correlation between stratification strength and epidemic size (Fig. 2.2F) reflected a direct relationship between these two variables that was not mediated by the sloppy predator.

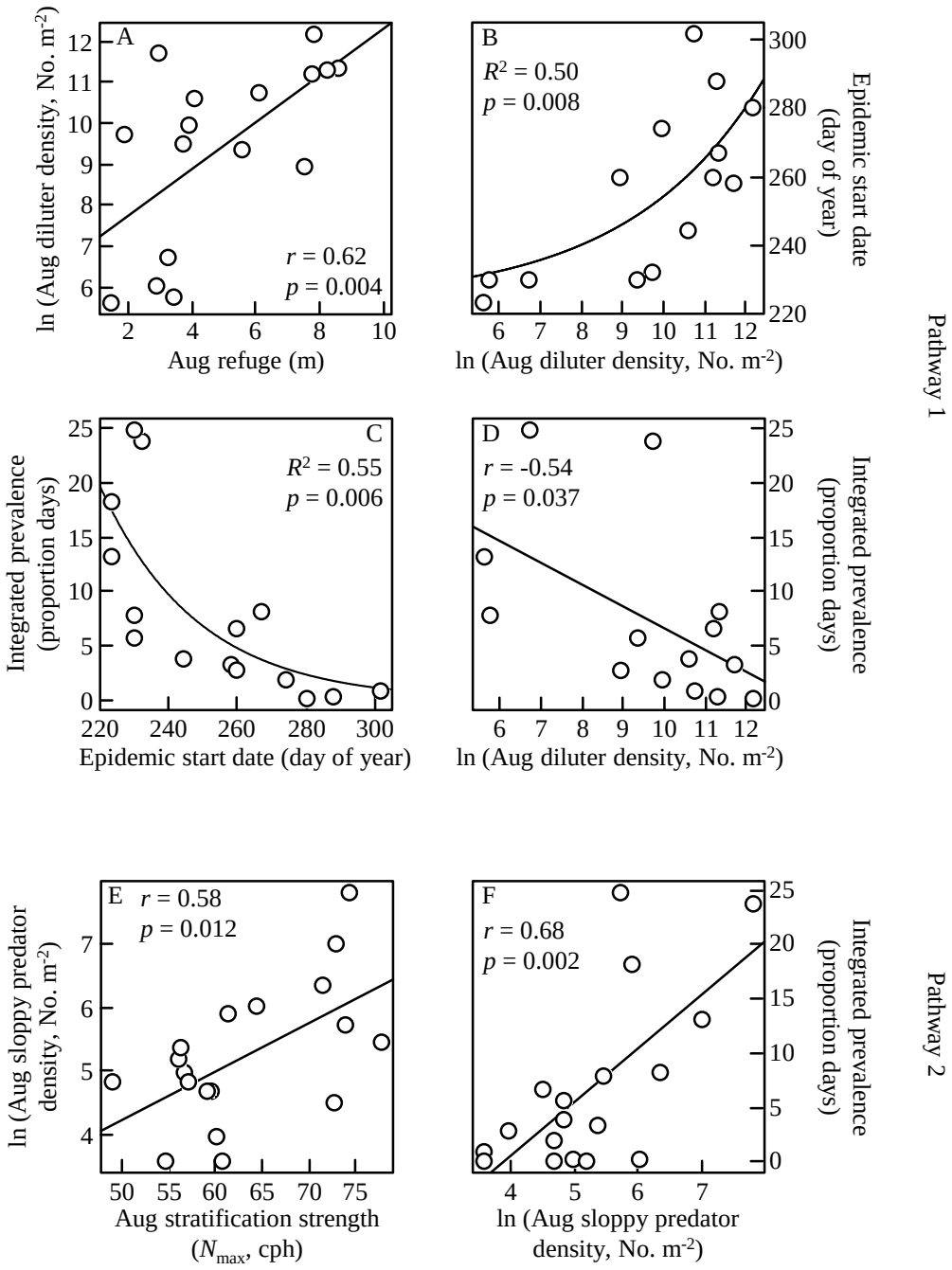

Figure 2.4. (A–D) Pathway 1: An indirect mechanism for the refuge size–start date relationship. (A) Lakes with larger refuges had higher density of the diluter species, *Daphnia pulicaria*. (B) Higher density of this diluter correlated with delayed start of epidemics. (C) Delayed start matters because epidemics that started earlier grew larger. (D) Density of the diluter at the start of epidemics correlated less strongly with the overall size of epidemics. (E, F) Pathway 2: An indirect mechanism for the stratification–epidemic size relationship. (E) More strongly stratified lakes had higher densities of the sloppy predator, *Chaoborus*, and (F) epidemics grew larger with greater density of this sloppy predator.

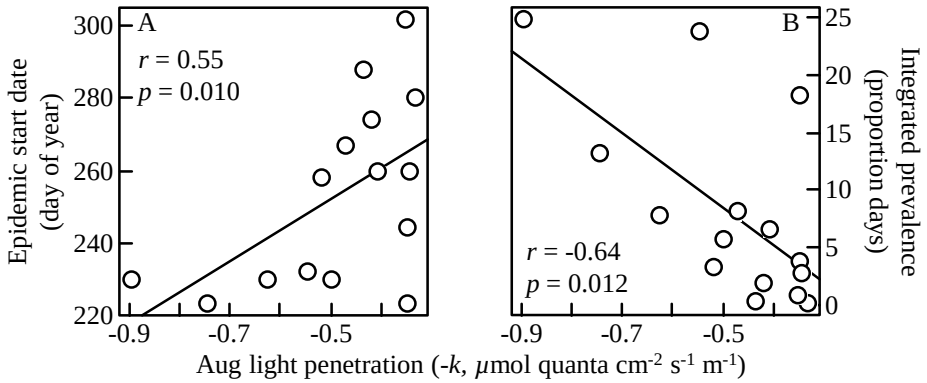

Figure 2.5. Potential direct connections between light environment and epidemic metrics. Deeper light penetration (values of -*k* closer to zero) correlated with (A) later start date of (B) smaller epidemics.

Discussion

The fusion of limnology with community ecology of disease can powerfully link habitat structure to epidemics. Here, variation in the start date and size of epidemics correlated with two features of proximate habitat structure (Fig. 2.1). The pathways connecting habitat to disease originated from physical factors related to lake size. Ultimately, both pathways potentially influenced disease by governing the fate of yeast spores, not host density. In the first pathway, epidemics started earlier in lakes with smaller hypolimnetic refuges and lower density of a diluter (*Daphnia pulicaria*; Hall et al. 2009a). In the second pathway, epidemics became larger in lakes with stronger thermal stratification and higher density of a sloppy predator (*Chaoborus punctipennis*) that can spread disease (Cáceres et al. 2009). Below, we summarize the limnological links between lake size and the proximate habitat factors. Then, we describe each pathway in more detail. Finally, we note how two complementary mechanisms, related to stratification and light (Pathway 2), may also directly affect disease.

Connections between habitat and disease involve some well-studied limnological phenomena. Both refuge size and stratification strength stem from physical drivers

correlated with lake size, specifically surface area. In Pathway 1, bigger lakes had longer fetches and deeper epilimnia, as seen in other studies (Gorham and Boyce 1989, Fee et al. 1996). All else equal, greater epilimnetic depth could compress hypolimnetic refuges. However, depth to the zone of hypoxia increased more steeply with lake size than did epilimnion depth. As a result, bigger lakes had larger refuges, despite their deeper epilimnia. In Pathway 2, smaller lakes had shallower light penetration, which was a likely physical driver of stratification strength (Mazumder et al. 1990, Fee et al. 1996). The light gradient among lakes reflected variation in nutrients and primary producers. Smaller lakes had higher total phosphorus, therefore higher algal biomass. Higher algal biomass, in turn, absorbed more solar radiation in shallower waters. This effect yielded sharper density gradients between warmer, shallower and colder, deeper layers (Kling 1988). Thus, through depth and light drivers, lake size ultimately set up the two habitat–disease pathways.

Before proceeding, we must note that density of the focal host (*D. dentifera*) had little role in these two habitat pathways. Standard epidemiological models predict increasing disease prevalence (i.e., larger epidemics) with increasing host density (Anderson and May 1992). However, August host density did not correlate with refuge size. It did correlate with stratification strength, but in the opposite direction from what we would expect if host density mediated the link between stratification strength and epidemic size: host density was greater in weakly stratified lakes, where epidemics were smaller. Furthermore, August density was not correlated with start date of epidemics or overall epidemic size (*see* also: Cáceres et al. 2006, Hall et al. 2010b). Thus, we focused on other mechanisms that indirectly or directly influenced the fate of yeast spores.

In the first pathway, refuge size correlated with start date and density of a diluter species. Epidemics started later in lakes with larger refuges from fish predation. Considered alone, this pattern seems surprising. Since fish selectively cull infected hosts (Duffy et al. 2005, Johnson et al. 2006), larger refuges might have protected infected

hosts and therefore bolstered epidemics. However, fish predation did not correlate with either epidemic metric. Instead, larger refuges supported higher density of a diluter, *Daphnia pulicaria*. This large-bodied species depends on the refuge to persist with fish predators (Threlkeld 1979, Tessier and Welser 1991). Higher density of this species likely inhibited the start of epidemics via consumption of spores (Hall et al. 2009a). Since *D. pulicaria* does not become infected, it acts as a dead end for the parasite, thereby potentially reducing disease in the more competent host (*D. dentifera*) through a dilution effect (Keesing et al. 2006).

This dilution effect may have delayed the start of outbreaks, but diluter density did not correlate as strongly with the eventual size of epidemics. That is, there was more scatter in the relationship between diluter density and integrated prevalence of infection (Fig. 2.4D), compared to that between diluter density and epidemic start date (Fig. 2.4B). This pattern makes sense based on temporal patterns of diluter density. The diluter should have mitigated disease less effectively later in the season because its density diminished through autumn (not shown). Still, links between habitat, the diluter, and start date of epidemics (Pathway 1) matter for ultimate epidemic size. Outbreaks that started earlier began in warmer waters, and higher temperatures enhance transmission rate and other factors involved in disease spread (Hall et al. 2006b). Conversely, epidemics that started later began in colder waters that inhibit disease spread. Thus, due to thermal physiology and declining water temperatures in autumn, any mechanism that inhibits the start of epidemics can indirectly constrain their size (Hall et al. 2011).

Once epidemics began, a different proximate habitat factor correlated with epidemic size via another community player (Pathway 2). Epidemics grew larger in lakes that started the outbreak season more strongly stratified. More strongly stratified lakes also had higher densities of a sloppy predator (*Chaoborus*) known to spread disease (Cáceres et al. 2009, Duffy et al. 2011). The spreading mechanism here is important for the link to habitat: *Chaoborus* can disperse yeast spores into the epilimnion where both

the host (Threlkeld 1979) and *Chaoborus* (Von Ende 1979) migrate at night. These spores can remain suspended and contact new hosts; otherwise, hosts dying from infection would sink to the lake bottom before spores escaped (Cáceres et al. 2009, Johnson et al. 2009b, Kirillin et al. 2012). But why did lakes with stronger stratification have greater density of *Chaoborus*? We cannot determine causation from our data. It is possible that more strongly stratified lakes had greater oxygen depletion in the hypolimnion, and thus more habitat for *Chaoborus* that was free of fish predators (Malinen et al. 2001). Another possibility is that shallower penetration of solar radiation (i.e., the driver of stronger stratification) protected *Chaoborus* from visual predators and UV damage (Von Ende 1979, Persaud and Yan 2003). Future studies will hopefully address this stratification–*Chaoborus* relationship.

The physical mechanisms involved in Pathway 2 potentially shaped the fate of yeast spores through two other, direct routes. The first possibility involves light itself. As argued above, light penetration can influence habitat structure by shaping the distribution of heat in the water column. Additionally, solar radiation (both UV and PAR) can directly exert deleterious effects on yeast spores (shown experimentally in the lab and field: Overholt et al. 2012). The sensitivity of yeast spores to radiation may at least partly explain why deeper light penetration correlated with later start and smaller size of epidemics. The second possibility involves stratification itself. Stronger stratification might impede sinking of spores out of the water column, away from hosts (Brookes et al. 2004, Cáceres et al. 2009, Hall et al. 2010b). All three mechanisms – sloppy predation, radiation, and sinking – could work together to create more favorable habitat for yeast spores. In strongly stratified lakes, more *Chaoborus* release spores in habitat that provides shielding from radiation and stronger barriers to sinking.

Habitat–disease patterns arise commonly in aquatic systems, and combinations of indirect and direct mechanisms may operate in these other examples as well. For instance, *Daphnia* that use deeper pond habitat to avoid predators have greater risk of

exposure to spores of a bacterial parasite in sediments (Decaestecker et al. 2002). Similarly, whitefish ecotypes that use habitats of different depth host different classes of flatworm parasites (Karvonen et al. 2013). Furthermore, thermal stratification can influence chytrid parasitism in diatoms (Gsell et al. 2013). Habitat structure can also drive variation in host–parasite coevolution, e.g., between snails and their trematode parasites along depth gradients in lakes (King et al. 2009). Even in these examples, spatial distribution of hosts (and thus, infection risk) may ultimately reflect relationships between habitat and other species that drive disease. We hope future studies will continue to unravel interactions between habitat, community context, and disease in an array of aquatic systems.

Our field study connects habitat to disease via indirect community players and through potential direct effects on the parasite. In general, it remains vital to uncover these kinds of mechanisms as humans alter habitats worldwide (Patz et al. 2004, Foley et al. 2005). The intersection of limnology and community ecology of disease can illustrate general principles and also create a predictive framework for lakes themselves. In lakes, climate change and eutrophication alter habitat structure, potentially affecting host–parasite interactions involving diverse taxa (Marcogliese 2001, Ibelings et al. 2011). For example, climate change may alter the timing and strength of thermal stratification, as well as epilimnion depth (De Stasio et al. 1996, Fee et al. 1996). Furthermore, anthropogenic eutrophication can affect stratification and the size of hypolimnetic refuges, through mechanisms involving light penetration, epilimnetic depth, and extent of hypoxic zones (Mazumder et al. 1990, Marcogliese 2001). These and other modifications to aquatic habitats will likely alter disease prevalence through direct and indirect mechanisms. To understand and predict those changes, we must continue to uncover mechanistic links between habitat, ecology, and disease.

CHAPTER 3

POOR RESOURCE QUALITY LOWERS TRANSMISSION POTENTIAL BY CHANGING FORAGING BEHAVIOR[2]

Abstract

Resource quality can have conflicting effects on the spread of disease. High quality resources could hinder disease spread by promoting host immune function. Alternatively, high quality food might enhance the spread of disease through other traits of hosts or parasites. Thus, to assess how resource quality shapes epidemics, we need to delineate mechanisms by which food quality affects key epidemiological traits. Here, we disentangle effects of food quality on "transmission potential" – a key component of parasite fitness that combines transmission rate and parasite production – using a zooplankton host and fungal parasite. We estimated the components of transmission potential (i.e., parasite encounter rate, susceptibility, and yield of parasite propagules) for hosts fed a high quality green alga and a low quality cyanobacterium. The low quality resource decreased transmission potential by stunting host growth and altering foraging behavior. Hosts reared on low quality food were smaller and had lower size-corrected feeding rates. Due to their slower grazing, they encountered fewer parasite spores in the water. Smaller hosts also had lower risk of an ingested spore caused infection (i.e., susceptibility), and yielded fewer parasite propagules. Furthermore, smaller hosts yielded fewer parasite propagules. Hosts switched from high to low quality food during spore

---

[2] Adapted from: Penczykowski, R. M., B. C. P. Lemanski, R. D. Sieg, S. R. Hall, J. H. Ochs, J. Kubanek, and M. A. Duffy. in review. Poor resource quality lowers transmission potential by changing foraging behaviour. Functional Ecology.

exposure also had low transmission potential – despite their large size – because the poor quality resource strongly depressed foraging behavior. A follow-up experiment investigated traits of the low quality resource that might have driven those results. Cyanobacterial compounds that can inhibit digestive proteases of a related grazer likely did not cause the observed reductions in transmission potential. Our study highlights the value of using mechanistic models of disease transmission to inform the design of experiments. Overall, our results show that low quality resources could inhibit the spread of disease through effects on multiple components of transmission potential. These insights improve our understanding of how disease outbreaks in wildlife may respond to shifts in resource quality caused by eutrophication or climate change.

Introduction

Ecologists increasingly recognize that community-level interactions profoundly influence the spread of disease in natural populations (Ostfeld et al. 2008, Keesing et al. 2010). One particularly important interaction is between hosts and their resources. Variation in the abundance or quality of resources may shape parasitism in a diversity of systems (Hutchings et al. 2001, Dwyer et al. 2005, Fels 2005, de Roode et al. 2008). This variation might enhance or diminish the size of epidemics, depending on how resources affect traits of the host and parasite. For example, more plentiful or higher quality food might promote the spread of disease by increasing host density (Anderson and May 1992). Resources can also affect other traits that are central to transmission (Hall et al. 2007b, Beldomenico and Begon 2010) and propagule production (Johnson et al. 2007, Seppälä et al. 2008, Hall et al. 2009c), as described below. Given that key epidemiological traits vary with resources, we need a mechanistic framework to tease apart the various roles of resources in the spread of disease.

As an important step, this framework must delineate effects of food quality on transmission potential – the focus of this paper. Here, transmission potential is the

product of transmission rate and production of parasite propagules from infected hosts. Resource quality could influence components of both parts. Transmission rate is itself the product of host–parasite contact rate (exposure) and the probability of infection upon contact (susceptibility). Resources can alter exposure, particularly for the diverse array of hosts that encounter their parasites while foraging (e.g., mammals–nematodes [Hutchings et al. 2001], gypsy moths–viruses [Dwyer et al. 2005], and butterflies–protozoans [de Roode et al. 2008]). For example, better fed hosts may grow larger, which could lead to more parasite encounters if feeding rate increases with surface area (Kooijman 1986, Kooijman 2010). Food quality can also affect foraging behavior independent of body size. Hosts may compensate for poor food quality by increasing their rate of consumption (Plath and Boersma 2001, Cruz-Rivera and Hay 2003, Darchambeau and Thys 2005, Fink and Von Elert 2006) or by using alternative resources that might increase parasite exposure (Hutchings et al. 2001, Johnson et al. 2009a). Alternatively, undernourished animals may conserve energy by foraging less, thereby decreasing their risk of exposure (Wang et al. 2006). Resources can also influence whether a given dose of parasites results in infection (i.e., susceptibility). This might occur through effects on host physiology (Ali et al. 1998, Hall et al. 2007b) or immune function (Babin et al. 2010, Cotter et al. 2011, Venesky et al. 2012), or through chemical compounds that directly antagonize or facilitate the parasite (Felton and Duffey 1990, Cory and Hoover 2006). While high quality food may sometimes decrease transmission rate, this could be countered by increased parasite production. For instance, better fed hosts may provide more energy and space for growth of parasite propagules (Johnson et al. 2007, Frost et al. 2008b, Hall et al. 2009c). Thus, resource quality might pull the components of transmission potential (exposure, susceptibility, and propagule yield) in opposing directions. This possibility confounds straightforward connections between resources and transmission potential – and therefore, disease spread.

In this study, we quantified links between resource quality and the components of

transmission potential with mechanistic models and experiments built around a focal planktonic host–parasite system. This system involves a zooplankton grazer (*Daphnia dentifera*), a fungal parasite (*Metschnikowia bicuspidata*), and phytoplankton resources of varying quality. In lakes, *Daphnia* are confronted with a wide variety of food quality over space and time (Sterner and Hessen 1994, Tessier and Woodruff 2002, O'Neil et al. 2012). This variation may matter for disease because resource quality affects *Daphnia* traits including rates of ingestion, assimilation, and growth (Demott et al. 1991, Urabe et al. 1997, Ravet et al. 2003, Martin-Creuzburg et al. 2008). These are key epidemiological traits because the host becomes infected by eating fungal spores (Ebert 2005, Hall et al. 2007b), and the parasite uses within-host resources to reproduce (Hall et al. 2009c). Larger, faster feeding hosts encounter more parasites (Hall et al. 2007b, Civitello et al. 2013a). Therefore, resource quality could alter exposure rate through effects on host size or foraging behavior, such as size-corrected feeding rate (Darchambeau and Thys 2005). Food quality might also influence the other component of transmission rate, susceptibility, which varies with body size and other factors (Hall et al. 2007b, Bertram et al. 2013). Additionally, higher quality food could enhance transmission potential by promoting host growth and production of fungal spores (Hall et al. 2009b, Hall et al. 2009c, Duffy et al. 2011).

We quantified the components of transmission potential of hosts using experimental manipulations of resource quality. First, we paired an infection assay with a feeding rate assay to quantify the exposure and susceptibility components of transmission rate. Hosts were fed a high quality green alga (*Ankistrodesmus falcatus*) or a low quality cyanobacterium (*Microcystis aeruginosa*); the latter was expected to reduce somatic growth rate (von Elert et al. 2012). However, these "high quality" and "low quality" treatments could influence host size and/or size-corrected elements of transmission rate. Thus, a third group of hosts was reared on high quality food, but switched to low quality food at the time of spore exposure. This "high-to-low quality" treatment allowed us to

quantify changes in size-corrected traits without a potentially confounding difference in body size (i.e., hosts from high and high-to-low quality treatments were the same size at exposure). For each treatment group, we then multiplied transmission rate and spore yield to calculate transmission potential. A follow-up experiment tested traits of the cyanobacterium (specifically, protease inhibitors; von Elert et al. 2012) that might have rendered it a low quality food. In this second infection assay, we quantified components of transmission potential for hosts fed the high quality green alga ("control") or the green alga coated with organic compounds extracted from the cyanobacterium ("extract"). As before, a "control-to-extract" treatment let us quantify how cyanobacterial compounds modified elements of transmission rate without influencing host size. Thus, by designing experiments based on a mechanistic model of parasite transmission, we were able to assess the role of resource quality – and of specific resource traits – in components of transmission potential.

Methods

Host–parasite system

Daphnia dentifera is a common planktonic grazer in small, stratified lakes of temperate North America (Tessier and Woodruff 2002). *D. dentifera* incidentally ingests spores of the fungal parasite *Metschnikowia bicuspidata* while filter feeding (Hall et al. 2007b, Hall et al. 2009a). The parasite pierces the gut wall of its host and proliferates in the haemolymph (Green 1974, Ebert 2005). As the fungus uses host resources to fuel its own reproduction, it reduces host fecundity and survivorship (Hall et al. 2009b, Hall et al. 2009c). Upon host death, fungal spores are released that can infect new hosts (Ebert 2005). Epidemics of this parasite occur in *D. dentifera* populations throughout the upper Midwestern USA (Hall et al. 2011, Civitello et al. 2013b).

High and low quality resources

We used the green alga *Ankistrodesmus falcatus* as high quality food for hosts (Hall et al. 2007b, Hall et al. 2009b, Duffy et al. 2011). The low quality food was the cyanobacterium *Microcystis aeruginosa* Kützing 1846 (strain NIVA-Cya 43, Norwegian Institute for Water Research Culture Collection, Oslo, Norway) (Lürling and van der Grinten 2003, von Elert et al. 2012). Both are single-celled and edible to *Daphnia*. We cultured both species in 5 L glass vessels of Cyano medium (von Elert and Jüttner 1997). Cells in stationary phase were harvested by centrifugation and either immediately fed to hosts (first experiment) or frozen at -20 °C followed by lyophilization (second experiment; see Appendix A for extraction, fractionation, and coating methods).

Mathematical model of transmission potential

We used mathematical models of the two parts of transmission potential – transmission rate and spore yield – as the framework for testing roles of food quality in disease spread (see also Table 3.1). The first model captures the transmission process over the short time scale relevant to our infection assay (i.e., there are no birth, death, or spore production terms). This model tracks changes in densities of susceptible (*S*) and infected (*I*) hosts, as well as free-living infective stages of the parasite (*Z*):

$$dS/dt = -\beta SZ \quad (3.1.a)$$

$$dI/dt = \beta SZ \quad (3.1.b)$$

$$dZ/dt = -f(S+I)Z. \quad (3.1.c)$$

Susceptible hosts (*S*) become infected (*I*) as they contact spores (*Z*), at rate β (equ. 3.1.a,b). Spores decrease as susceptible and infected hosts consume them at rate *f* (equ. 3.1.c). Infection risk (transmission rate), β, can be decomposed into its components:

$$\beta = uf = \left(\hat{u}L_\beta^2\right)\left(\hat{f}L_\beta^2\right) \quad (3.2)$$

where *u* is per spore susceptibility and *f* is feeding (spore encounter) rate. Both *u* and *f*

can be further broken down into size-corrected parameters, $\hat{u}$ and $\hat{f}$, which both increase with host size (length squared) at the time of exposure, $L_\beta^{\,2}$ (equ. 3.2; Hall et al. 2007b). The size-dependence of *f* occurs because feeding rate of *Daphnia* increases with surface area (Kooijman 1986). Because β increases with size more steeply than $L_\beta^{\,2}$, we assume that *u* also increases with body size (Hall et al. 2007b). Biologically, an increase in *u* with $L_\beta^{\,2}$ may involve gut size; larger hosts have bigger guts that hold more spores and provide a larger surface through which spores can penetrate and infect the host (Hall et al. 2007b). In the first experiment, we estimated each element of transmission rate ($\hat{u}$, $\hat{f}$, and L_β) using data from independent assays of feeding and transmission rate. Then we multiplied these components to estimate β (equ. 3.2).

We modeled the relationship between spore yield (σ) and host size (L_e) at the end of the experiment as

$$\sigma = \sigma_0 + \sigma_1 L_e^3 \tag{3.3}$$

which says that σ increases linearly with host volume at the end of the experiment ($L_e^{\,3}$), with slope σ_1 and intercept σ_0. Then, we defined transmission potential as the product of transmission rate and spore yield, βσ.

Table 3.1. Variables and parameters in the mathematical models of parasite transmission (equ. 3.1) and spore yield (equ. 3.3).

Symbol	Units	Meaning
S	host · L^{-1}	Density of susceptible hosts
I	host · L^{-1}	Density of infected hosts
Z	spore · L^{-1}	Density of spores
t	day	Time
L_β	mm	Length of hosts at exposure to parasites
L_e	mm	Length of hosts at end of experiment
$\hat{u}$	host · $spore^{-1}$ · mm^{-2}	Size-corrected per spore susceptibility of hosts
u	host · $spore^{-1}$	Per spore susceptibility of hosts
$\hat{f}$	L · $host^{-1}$ · day^{-1} · mm^{-2}	Size-corrected feeding (exposure) rate of hosts
f	L · $host^{-1}$ · day^{-1}	Feeding (exposure) rate of hosts
β	L · $spore^{-1}$ · day^{-1}	Transmission rate
σ	spore · $host^{-1}$	Spore yield per infected host at end of experiment
σ_0	spore · $host^{-1}$ · mm^{-3}	Intercept of spore yield model (equ. 3.3)
σ_1	spore · $host^{-1}$	Slope of spore yield model (equ. 3.3)
$\beta\sigma$	L · day^{-1} · $host^{-1}$	Transmission potential

First experiment: Infection assay

We used an infection assay to estimate transmission rate (β) and spore yield (σ) for hosts using three different manipulations of resource quality. We used an isofemale line of *D. dentifera* (host) and a strain of *M. bicuspidata* (parasite) both originally collected from lakes in Barry County, Michigan, USA. To minimize maternal effects, *D. dentifera* were reared in groups of six in 150-mL beakers containing a 100-mL mixture of Artificial *Daphnia* Medium (ADaM; Klüttgen et al. 1994) and filtered water from Lake Lanier (Georgia, USA), and fed 0·73 µg C mL^{-1} day^{-1} (hereafter, "standard" level) of high quality food. Neonate hosts born within a 24 h period were placed in groups of 10 into 150-mL beakers, fed standard levels of either high or low quality food, and kept at 20 °C in a 16:8 h light:dark cycle.

Six-day-old hosts were transferred singly to 50-mL beakers containing 40 mL of medium and exposed to 275 parasite spores mL^{-1} for 24 h. On the day of exposure, half of the individuals reared on high quality food were permanently switched to low quality food (the "high-to-low quality" group). We created this treatment to disentangle effects of resources on body size and size-corrected components of transmission rate. Hosts in the high quality and high-to-low quality groups were similarly sized at exposure. Therefore, a difference in transmission rate between these two groups would reflect differences in size-corrected traits. By contrast, a difference in transmission rate between hosts in low and high-to-low quality treatments would indicate that effects of size at exposure outweighed effects of eating low quality food during and after exposure. Hosts were fed half the standard amount of food during exposure to increase consumption of spores (Hall et al. 2007b).

After spore exposure, we transferred hosts to fresh medium and resumed the standard food level. Hosts were transferred to fresh medium again 4 days later. At 10 days post-exposure to the parasite, we visually examined each individual for infection at

25–50X magnification (Duffy and Sivars-Becker 2007). Hosts were measured from the middle of the eye to the base of the tail at 40X magnification using DP2-BSW software (Olympus America, Center Valley, PA, USA). We transferred infected animals to microcentrifuge tubes, gently smashed each individual using a pestle, and counted the released spores using a hemocytometer at 200X magnification. We started the first experiment with 64 individuals (replicates) per treatment, and 36–38 individuals per treatment survived to the end.

First experiment: Feeding rate assay

We paired the infection assay with an independent assay of feeding rate in order to estimate the contributions of body size ($L_\beta{}^4$) and foraging behavior (i.e., size-corrected feeding rate, $\hat{f}$) to transmission rate (β). On the day of spore exposure, we measured feeding rates of a subset of hosts from the high and low quality treatments; these individuals were not used in the infection assay. Hosts were placed singly in 15-mL centrifuge tubes and fed either high quality food (n = 20 hosts from the high quality treatment) or low quality food (n = 20 hosts from each food treatment). For both food species, we also set up ungrazed controls (n = 10), following Sarnelle and Wilson (2008). During the 3 h grazing period, tubes were inverted every 15–20 min and briefly uncapped after 1.5 h to allow air exchange. Host size (length, L_β) was measured at the end of the grazing period. We used a Trilogy fluorometer (*in vivo* module, Turner Designs, Sunnyvale, CA, USA) to quantify the food remaining in each tube, based on carbon–fluorescence regressions for both resource species.

Second experiment: Infection assay

In a follow-up experiment, we tested whether effects of food quality were caused by protease inhibitors in the low quality cyanobacterium. To do this, we performed an infection assay similar to that in the first experiment. Prior to parasite exposure, hosts

were fed the high quality green alga coated with solvent only ("control"), or with solvent plus organic compounds extracted from the cyanobacterium ("extract"; see Appendix A for details). On the day of spore exposure, half of the hosts from the control group were permanently switched to food coated with extract. This "control-to-extract" treatment allowed us to test whether effects of cyanobacterial compounds on transmission rate were due to effects on body size. The experiment began with 68 individuals per treatment, and an average of 44 (range: 39–52) individuals per treatment survived to the end.

Statistical analysis

Statistical analyses were performed in R (R Core Team 2012) and Matlab. Body sizes of hosts on the day of parasite exposure and at the end of the experiment were analyzed with one- and two-way ANOVAs, respectively. We used a generalized linear model (GLM) with a binomial error distribution to analyze proportion infected among beakers. Parasite spore load per infected host was analyzed using a glm with a quasipoisson error distribution (for overdispersed count data). When there were significant effects in omnibus tests, we performed post-hoc pairwise comparisons using Tukey's honestly significant difference (HSD) tests.

Details of parameter estimation for the transmission model are provided in Appendix A. Briefly, we estimated components of transmission rate (β) by simultaneously fitting the transmission model (equ. 3.1) to infection data, and the feeding model (equ. A.4) to the feeding rate data (Sarnelle and Wilson 2008, Bertram et al. 2013). To estimate the parameters, we simply added the log-likelihood values produced from the transmission and feeding model. We estimated 95% confidence intervals around them using 10,000 bootstraps, and we used randomization tests to compare differences in point estimates among treatments (with Holm–Bonferroni adjusted significance levels) (Gotelli and Ellison 2004).

Details of parameter estimation for the transmission model are provided in the SI.

Briefly, we estimated the size-corrected components ($\hat{u}$ and $\hat{f}$) of transmission rate (β) by simultaneously fitting the transmission model (equ. 3.1) to infection data (i.e., body size and binary infection status), and a foraging model (equ. A.4) to the feeding rate data (i.e., body size and initial and final concentrations of food) (Sarnelle and Wilson 2008, Bertram et al. 2013). Best-fit estimates of $\hat{u}$ and $\hat{f}$ were obtained by minimizing the sum of the negative log-likelihood values produced from fitting the transmission and foraging models. We estimated 95% confidence intervals around these point estimates using 10,000 bootstraps, and we used randomization tests for comparisons between treatments (with Holm–Bonferroni adjusted significance levels) (Gotelli and Ellison 2004).

Results

Infection risk depended on food quality (proportion infected: χ^2 = 33·75, d.f. = 2, $P < 0{\cdot}0001$, Fig. 3.1A; transmission rate, β: Fig. 3.1B). Hosts that ate high quality food during parasite exposure had higher infection risk than those that ate low quality food during exposure (comparison of "high" vs. "high-to-low" and "low"; Figs 3.1A,B), and infection risk was similar for hosts in the high-to-low and low quality treatments. The greater infection risk of hosts fed exclusively high quality compared to exclusively low quality food was due to differences in body size as well as foraging behavior (i.e., size-corrected exposure rate). Hosts in the high quality treatment were larger (L_β; $F_{2,57}$ = 92·34, P < 0·0001; Fig. 3.1C) and had higher size-corrected exposure rate ($\hat{f}$, Fig. 3.2A) than those in the low quality treatment. Therefore, they had higher exposure to spores (*f*, Fig. 3.2B). Though food quality did not affect size-corrected per spore susceptibility ($\hat{u}$, Fig. 3.2C), the larger body size of hosts in the high quality treatment boosted their per

spore susceptibility relative to hosts reared on low quality food (*u*, Fig. 3.2D). Hosts that were switched from high to low quality food at exposure also had lower infection risk than those in the high quality treatment (Figs 3.1A,B), despite being just as large (Fig. 3.1C), because they had low size-corrected exposure rate (Fig. 3.2A). The negative effect of this diet shift on size-corrected feeding rate outweighed the positive effect of body size on feeding rate, such that hosts in the high-to-low quality group had the lowest spore exposure overall (Fig. 3.2B). Their per spore susceptibility, however, was similar to that of hosts in the other two treatments (Fig. 3.2D). Thus, low infection risk in the low quality treatment was due to effects of poor quality food on growth and foraging behavior, while low infection risk in the high-to-low quality treatment stemmed entirely from an effect on foraging behavior.

The quality of food eaten early in life (i.e., before spore exposure) determined body size at the end of the experiment (L_e). Regardless of infection status, hosts in the high-to-low quality treatment were as large as those that always ate high quality food, and hosts in the low quality treatment were significantly smaller (Food: $F_{2,106} = 291{\cdot}95$, $P < 0{\cdot}0001$; Infection: $F_{1,106} = 0{\cdot}98$, $P = 0{\cdot}33$; Food*Infection: $F_{2,106} = 0{\cdot}53$, $P = 0{\cdot}59$; Fig. 3.3A). Despite their larger sizes, infected animals from the high quality and high-to-low quality treatments did not yield significantly more spores (σ) than hosts that were exclusively fed low quality food (though this test had low sample size in the low quality group [n = 3] due to low infection risk; $F_{2,29} = 1{\cdot}53$, $P = 0{\cdot}23$; Fig. 3.3B). However, those three infected hosts from low quality treatment fell along a significant positive relationship between body size (volume, L_e^3) and spore load (σ) across food treatments ($R^2 = 0.26$, $P = 0{\cdot}002$; Fig. 3.3C). When we pulled the components together, we found that transmission potential (βσ) was greatest for hosts in the high quality treatment, and

did not differ significantly between the other two groups (Fig. 3.3D). Thus, for hosts in the high-to-low quality treatment, the steep drop in transmission rate (β; Fig. 3.1B) outweighed positive effects of their size on spore production (σ; Fig. 3.3C), resulting in low overall transmission potential.

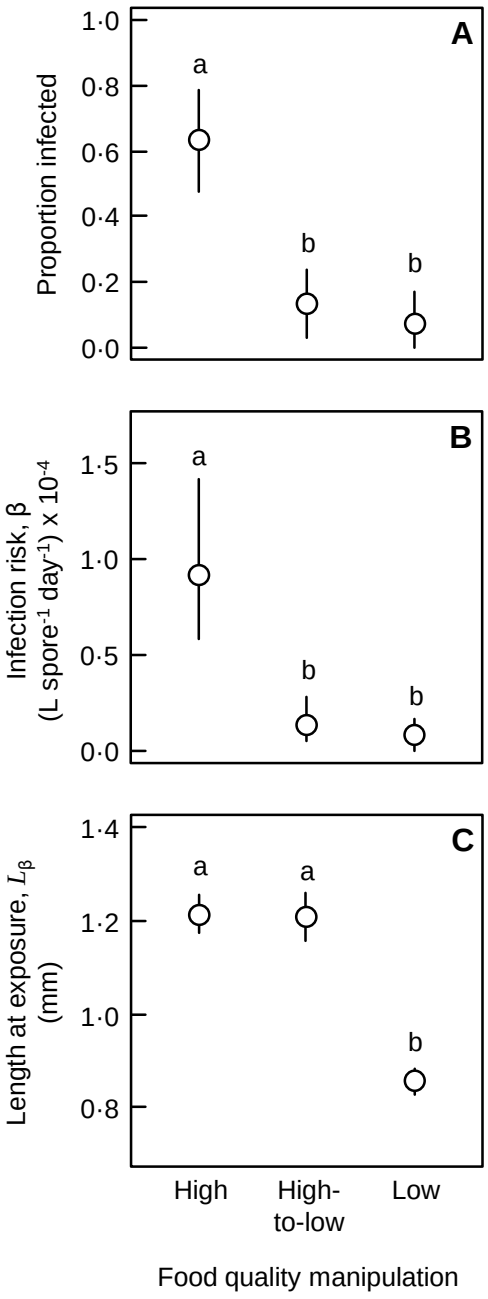

Figure 3.1. Infection risk and body size at spore exposure in the first experiment. Compared to hosts fed "high" quality food, those in the "low" quality or "high-to-low" quality treatment groups had lower infection risk, quantified as either (A) infection prevalence or (B) transmission rate (β). (C) Hosts reared on high quality food were larger at exposure (length, L_β) than those reared on low quality food. Error bars are bootstrapped 95% confidence intervals and letters denote significant differences between treatments after correcting for multiple comparisons.

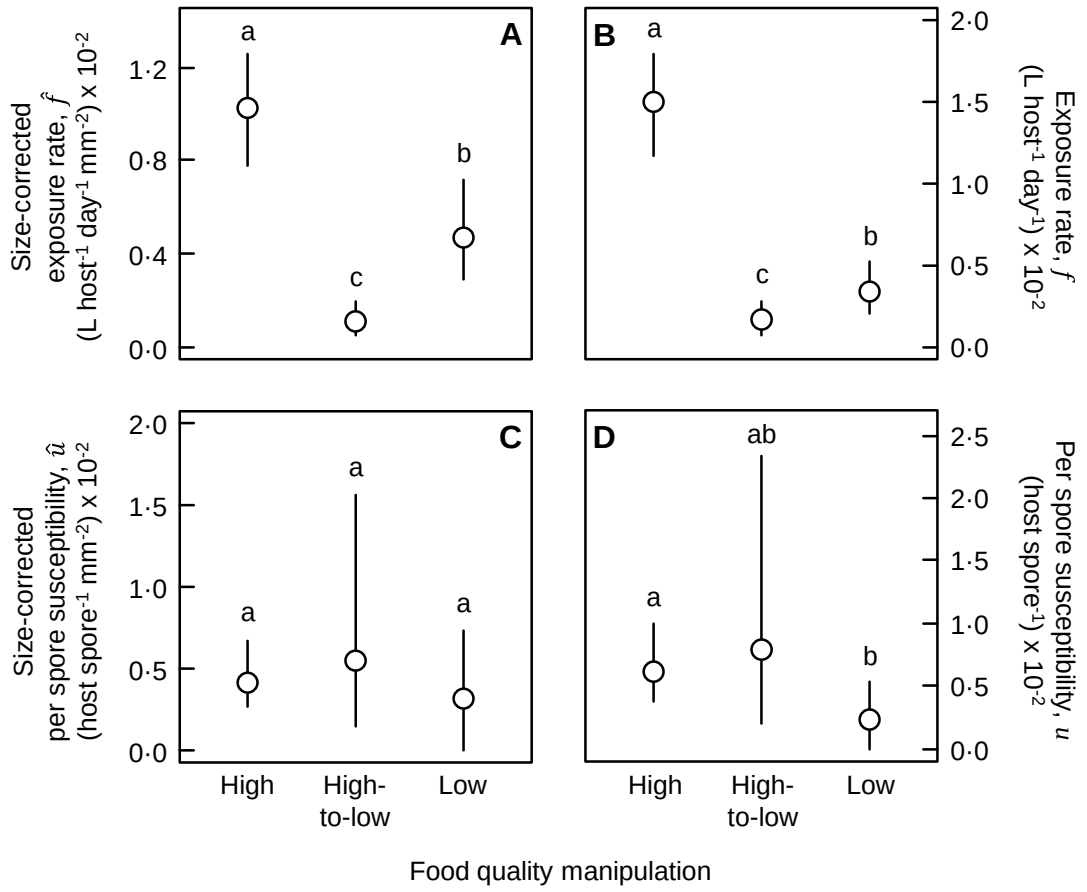

Figure 3.2. Components of transmission rate in the first experiment (see equ. 3.2). Both (A) size-corrected feeding rate ($\hat{f}$) and (B) feeding rate (f) were highest for hosts in the high quality treatment, lowest in the high-to-low quality group, and at an intermediate level in the low quality group. (C) Food quality did not affect size-corrected per spore susceptibility ($\hat{u}$). However, (D) with the influence of body size, hosts in the high quality treatment had greater susceptibility (u) than those in the low quality treatment, while the high-to-low quality group had highly variable susceptibility.

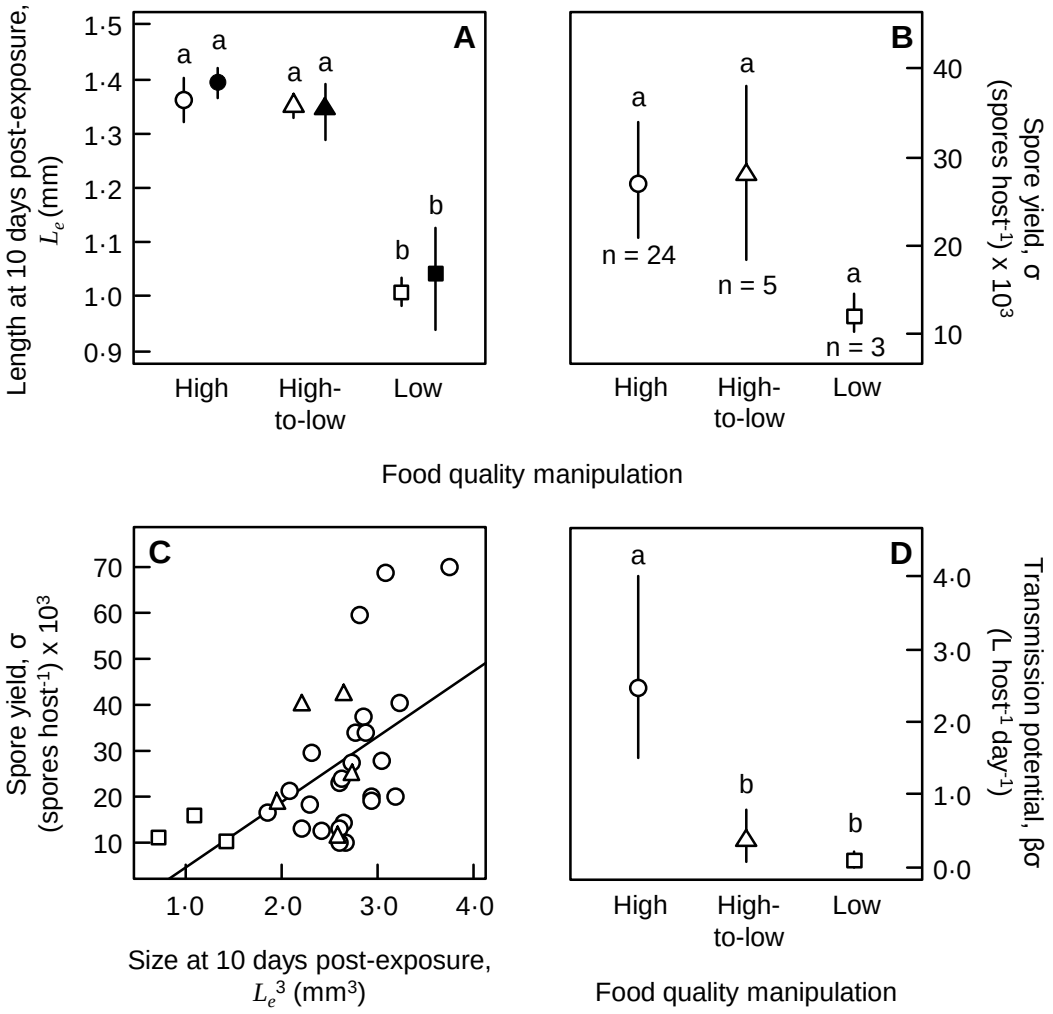

Figure 3.3. Host size and spore load at the end of the first experiment (i.e., at 10 days post-exposure to spores). (A) Hosts in the low quality treatment (squares) were smaller (length, L_e) than those in the high-to-low quality (triangles) or high quality (circles) treatments. Within food treatments, there was no difference in size between infected (filled circles) and uninfected (open circles) hosts. (B) Food quality did not significantly affect spore load within infected hosts (σ). Sample size, n, is indicated for each treatment. (C) Across all three treatments, infected hosts with larger bodies (volume, L_e^3) yielded more spores at 10 days post-exposure. (D) Transmission potential ($\beta\sigma$) was greater for hosts fed high quality compared to high-to-low quality or low quality food.

The second experiment revealed that protease inhibitors in the cyanobacterium were likely not responsible for the effects of this low quality resource. High quality green algal cells coated with cyanobacterial extract (containing protease inhibitors; see Appendix A for details) did not decrease infection risk relative to the green algal "control", regardless of whether hosts were fed the extract-coated food from exposure onward ("control-to-extract"), or throughout the experiment ("extract") (proportion infected: χ^2 = 2·25, d.f. = 2, P = 0·33, Fig. 3.4A; transmission rate, β: Fig. 3.4B). Body size at exposure (L_β) did not differ between hosts from the two initial food treatments (i.e., fed control versus extract from birth until exposure) ($F_{1,23}$ = 1·10, P = 0·30; Fig. 3.4C). Neither diet nor infection status affected size at the end of the experiment (L_e; Food: $F_{2,123}$ = 1·59, P = 0·21; Infection: $F_{1,123}$ = 0·48, P = 0·49; Food*Infection: $F_{2,123}$ = 0·74, P = 0·48; Fig. 3.4D). At 10 days post-exposure, spore yield from infected hosts (σ) was similar across the three food treatments ($F_{2,44}$ = 0·39, P = 0·68; Fig. 3.4E). Overall, the cyanobacterial extract did not significantly influence transmission potential (βσ; Fig. 3.4F).

Discussion

Our study illustrates mechanistic connections between resource quality and components of transmission potential. In the first experiment, hosts in the "high quality" treatment (i.e., those that always ate high quality food) had the highest rate of spore exposure because they were large and foraged quickly for their size. In addition, their large body size boosted per spore susceptibility. Thus, exposure rate and susceptibility worked together to enhance transmission rate in the high quality treatment. Furthermore, larger hosts yielded more parasite propagules, likely because their greater volume could contain more spores, and because they provided more fuel for parasite reproduction (Hall et al. 2009c). This combination of high transmission rate and spore yield meant that hosts

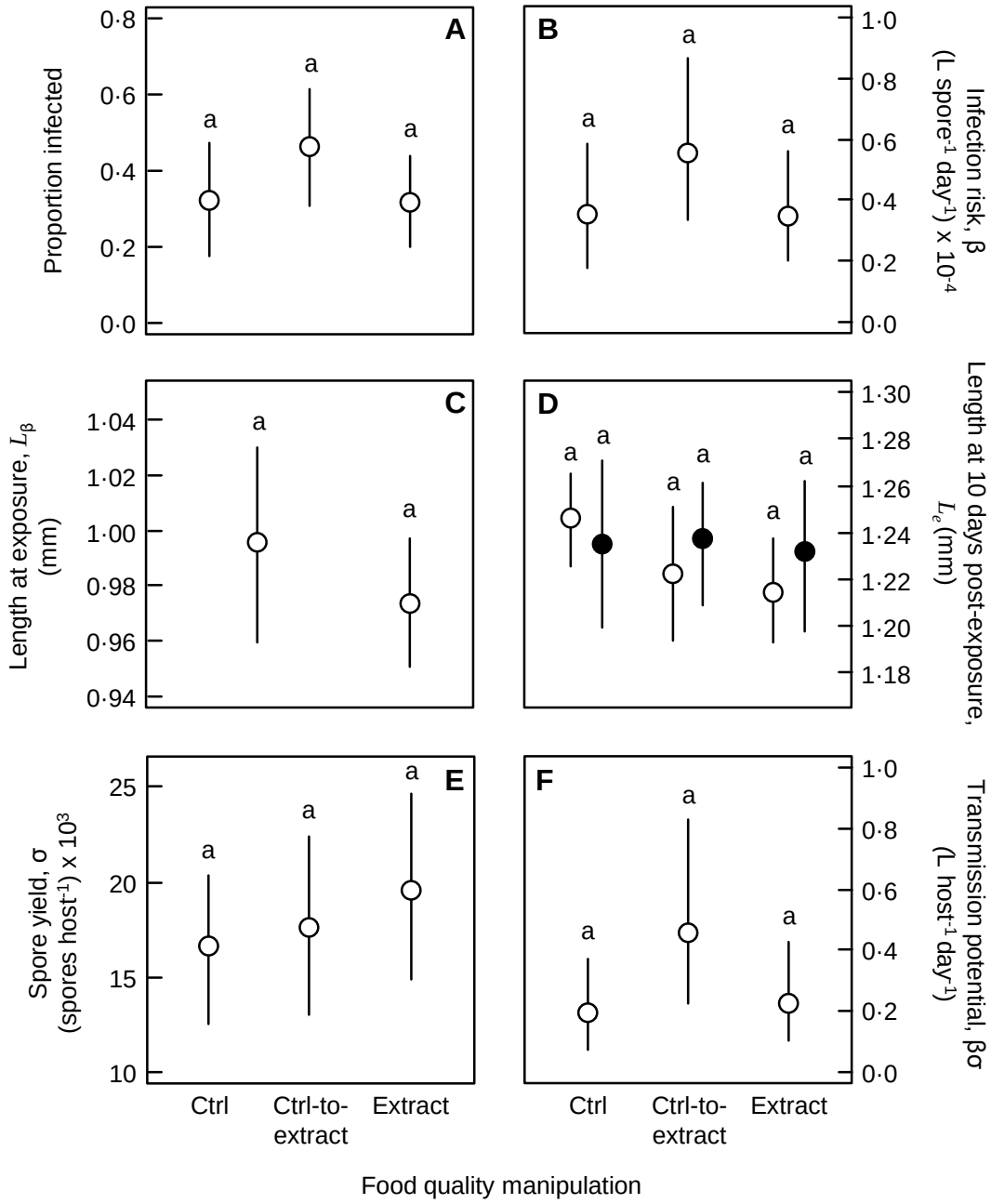

Figure 3.4. Infection risk, body size, and components of transmission potential in the second experiment. Whether quantified as (A) proportion infected or (B) transmission rate (β), infection risk did not differ among hosts fed the green alga coated with plain solvent (control ["ctrl"]) or solvent plus cyanobacterial compounds ("extract" and control-to-extract ["ctrl-to-extract"] treatments). Food treatment did not significantly affect either (C) body size at exposure (length, L_β) or (D) size at 10 days post-exposure (length, L_e). There were also no significant differences across treatments in (E) spore yield per infected host (σ) or (F) overall transmission potential (βσ).

in the high quality treatment had the greatest transmission potential. By contrast, hosts in the "low quality" treatment (i.e., those that always ate low quality food) were small and foraged slowly for their size. As a result, both exposure rate and susceptibility were low, which translated into low transmission rate for the low quality group. Because these small hosts also yielded few spores when infected, their transmission potential was low. Transmission potential was just as low for hosts in the "high-to-low quality" treatment (i.e., those that were switched from high to low quality food at exposure), even though they were as large as hosts in the high quality treatment. In the high-to-low quality group, the positive influence of body size on exposure, susceptibility, and spore yield was overwhelmed by effects of poor food quality on foraging behavior (i.e., lower size-corrected exposure rate).

Though our experiments did not reveal which traits of the cyanobacterium decreased host growth and feeding rate, we can rule out some features of this low quality resource. We can dismiss inedible morphology as a driver because both food species had single, small cells. We can also eliminate phosphorus (P) deficiency, since both food species contained non-limiting ratios of P to carbon (Sterner and Hessen 1994, Urabe et al. 1997) (see Appendix A and Table A.1). In addition, the low quality food lacked a common class of cyanobacterial compounds – microcystins – that can be toxic to *Daphnia* (Demott et al. 1991, Lürling and van der Grinten 2003, Wilson et al. 2006). It did contain the compounds nostopeptin BN920 (Ploutno and Carmeli 2002) and cyanopeptolin CP954 (von Elert et al. 2005), which can inhibit digestive proteases and stunt somatic growth of a different *Daphnia* species (von Elert et al. 2012). However, our second experiment showed that these compounds likely did not underlie the results of the first experiment; that is, green algal cells coated with cyanobacterial extract containing these two compounds at realistic concentrations did not reduce either transmission rate or

spore yield. Compared to green algae, cyanobacteria tend to be deficient in sterols and polyunsaturated fatty acids required for *Daphnia* growth and development (DeMott and Muller-Navarra 1997, Ravet et al. 2003, Martin-Creuzburg et al. 2008). Such lipid deficiency could explain the small size of hosts in the low quality treatment. By contrast, hosts in the high-to-low quality treatment were not smaller than those in the high quality group at the end of the experiment. This could indicate that a critical period of somatic growth was complete before the switch to nutritionally poor food. Hosts in the high-to-low quality group may also have assimilated the low quality resource more efficiently because food spent more time in their longer guts (DeMott et al. 2010). However, nutritional inadequacy probably did not drive reductions in size-corrected feeding rate (Lürling and van der Grinten 2003). Thus, future studies should test other traits (e.g., surface chemicals) of this cyanobacterium that could deter or inhibit grazing by *Daphnia* hosts (Rohrlack et al. 1999, Lürling and van der Grinten 2003).

How general are these effects of resources on the components of transmission potential? The positive relationship between host size and spore yield is consistent with other studies in this host–parasite system, including experimental manipulations of food quantity (Hall et al. 2009c) or quality (Hall et al. 2009b), nutrient availability (Civitello et al. 2013b), chemical contaminants (Civitello et al. 2012), or predator cues (Duffy et al. 2011, Bertram et al. 2013). The increase in parasite reproduction with host size is also consistent with studies of many other invertebrate hosts (Johnson et al. 2007, Seppälä et al. 2008, Daniels et al. 2013). Relationships between resources and transmission rate are more idiosyncratic, even in this *Daphnia*–fungus system. For example, transmission rate can depend on food density (Hall et al. 2007b), can increase with poor quality resources from lakes (Hall et al. 2009b) or certain pollutants (Civitello et al. 2012), and may not change in response to other nutrients (Civitello et al. 2013b). Thus, manipulations of resources could pull transmission rate and spore yield in opposite directions. However, in this study, low food quality depressed both parts of transmission potential.

All else being equal, these results suggest that poor resource quality could dampen epidemics in natural systems. However, to assess implications of these results for epidemics in nature, we need to consider additional factors including drivers of food quality in lakes, variation among host genotypes in use of poor quality food, and the potential for food quality to determine host density. Nutrient enrichment is a major driver of resource quality in lakes, and eutrophication may promote growth of cyanobacteria over higher quality phytoplankton (Schindler et al. 2008, Schindler and Vallentyne 2008, O'Neil et al. 2012). However, nutrient enrichment may correlate with other factors that shape disease spread, such as fish predation (Duffy and Hall 2008) or chemical contamination (Lafferty and Holt 2003, Coors and De Meester 2011, Civitello et al. 2012). Thus, correlated factors may influence whether poor food quality suppresses epidemics in eutrophic lakes. Additionally, host genotypes in a natural population will vary in their ability to ingest and assimilate poor quality resources (Hall et al. 2010a, 2012). Therefore, future studies should test whether the observed effects of food quality on growth and foraging behavior depend on host genotype. If some genotypes respond less sensitively, resource quality could have variable effects on transmission potential among lakes, or within populations over time. Finally, disease spread may also depend on how resources affect host birth rates. Poor food quality tends to reduce *Daphnia* fecundity (Lürling and van der Grinten 2003, Ravet et al. 2003, Hall et al. 2009b), and a resulting decrease in host density could work with low transmission potential to quell epidemics. Further investigation of these factors will advance our understanding of how resources shape epidemics in nature.

This study offers an approach for delineating mechanisms by which resource quality affects the spread of disease. Such an approach is valuable for two general reasons. First, it can help us anticipate how disease epidemics in a key grazer will respond to climate change and eutrophication, which typically favor cyanobacteria over other phytoplankton (Schindler et al. 2008, Carey et al. 2012, O'Neil et al. 2012). Our

results suggest that shifts to cyanobacterial dominance may inhibit transmission potential of some aquatic pathogens. Second, this mechanistic approach could disentangle roles of resource quality in disease spread in other systems. Climate and other human-driven changes are altering resource quality in aquatic and terrestrial ecosystems worldwide (MEA 2005, McKenzie and Townsend 2007, Schindler et al. 2008, Elser et al. 2010). Will these changes alter disease outbreaks in other wildlife populations? To answer this question, we need to understand how resource quality influences key epidemiological traits of hosts and parasites.

CHAPTER 4

NUTRIENT ENRICHMENT, HABITAT STRUCTURE, AND DISEASE IN THE PLANKTON

Abstract

In order to better predict ecosystem responses to changing climate and nutrient regimes, we need to understand how such environmental changes drive disease. In addition, we need to assess whether disease influences how ecosystems respond to environmental forcing. Here, we investigated interactions among nutrient (nitrogen and phosphorus) enrichment, alteration of thermal habitat structure, and disease in the plankton of freshwater lakes. Specifically, we studied how nutrient levels and the frequency of water column mixing affected a zooplankton (*Daphnia*) host, its fungal parasite, and algal resources. By manipulating nutrients, mixing, and parasite exposure in whole water column enclosures in a lake, we were able to test for interactive effects of these variables on epidemiology and consumer–resource dynamics. We found that nutrient enrichment and mixing together promoted disease spread, likely due to positive effects on host density and resuspension of parasite spores, respectively. The high nutrient manipulation yielded greater densities of both infected and uninfected hosts over the course of the experiment. Greater densities of infected hosts might reflect greater total parasite production during epidemics, and could seed larger epidemics in the future. In a survey of natural lakes, correlations between infected host density and epidemic size across years were consistent with this hypothesis. The nutrient and parasite exposure manipulations also had broader ecosystem consequences. We found that disease reduced host density and allowed the abundance of algal resources to increase, particularly in the low nutrient treatment. This pattern of greater algal density under low nutrient conditions

was not evident in the absence of disease. Epidemics also drove a reduction in the carbon-to-phosphorus ratio in algae. Through such mechanisms, interplay between environmental variables (e.g., nutrients levels and habitat structure) and disease could shape how ecosystems respond to environmental change.

Introduction

Eutrophication and climate change are altering aquatic ecosystems worldwide (Smith 2003, van de Waal et al. 2010, Winder and Sommer 2012). There is concern that these types of ecosystem changes will lead to larger or more frequent outbreaks of infectious diseases (Johnson et al. 2010b). For example, nutrient enrichment might influence the spread of disease through mechanisms involving the quantity or quality of resources available to hosts (Johnson et al. 2007, Frost et al. 2008b). Climate change may also affect disease patterns, not only due to thermal scaling of host and parasite physiology, but also by modifying the thermal structure of aquatic habitats (Marcogliese 2001). Alteration of habitat structure could affect densities and spatial distributions of hosts, parasites, and other community members that influence the spread of disease (Ostfeld et al. 2005, Hall et al. 2010b, Penczykowski et al. in press). Because nutrient levels and habitat structure are changing simultaneously in many bodies of water – and are predicted to change further – these potential disease drivers may interact. Thus, we need to understand the independent and joint effects of nutrient enrichment and habitat alteration on disease in order to better predict their consequences in nature.

Nutrient enrichment and habitat structure could affect the spread of disease through a variety of mechanisms. For diseases that spread through density-dependent transmission, we might expect that higher nutrient levels should lead to larger epidemics, due to increased host density with ecosystem productivity (Anderson and May 1992). Hosts with more abundant or nutrient-rich resources may produce more parasite propagules when infected, which should also promote transmission (Smith et al. 2005,

Frost et al. 2008b, Seppälä et al. 2008). On the other hand, nutrient enrichment might limit the spread of disease by allowing other species to out-compete hosts, or by fueling the growth of poor quality resources (Penczykowski et al. in review). Changes to habitat structure could also either enhance or depress disease spread. For example, larger habitat patches might support greater host densities and larger epidemics. Alternatively, an increase in patch size could lead to smaller outbreaks by supporting greater densities of non-host species that impede transmission (e.g., through a 'dilution effect'; Allan et al. 2003, Hall et al. 2010b, Penczykowski et al. in press). Fragmentation of habitat might increase parasite transmission at habitat edges (Sullivan et al. 2011), or may inhibit the spread of disease by segregating hosts from parasites (Smith et al. 2002). Given these possibilities, nutrient enrichment and habitat alteration may interact synergistically, or in opposition, to shape disease.

Here, we studied how nutrient enrichment and alteration of habitat structure affected disease in freshwater lakes. Our study system features a zooplankton (*Daphnia*) host that encounters infective spores of a fungal parasite while grazing on small phytoplankton in the water column (Ebert 2005, Hall et al. 2007b). We expected both nutrient enrichment and thermal habitat structure to be relevant to disease spread in this system. There is wide variation in nutrient levels among lakes, and over seasons (Fee 1979, Tessier and Woodruff 2002). Enrichment with nutrients such as nitrogen (N) and phosphorus (P) can stimulate growth of phytoplankton, and can also influence stoichiometry of carbon (C), N, and P in algal cells. Greater quantity or nutritional quality (e.g., high P:C) of algae should boost host density (Sterner and Hessen 1994, Anderson and Hessen 2005). This increased host density could enhance the spread of disease, as predicted by density-dependent models of transmission (Anderson and May 1992). Better fed hosts also yield more parasite spores, which can further promote transmission (Hall et al. 2009b, Hall et al. 2009c). Host habitat is structured by thermal stratification of the water column, and the strength of stratification varies among lakes and through time

(Tessier and Welser 1991, Snucins and Gunn 2000, Penczykowski et al. in press). In lakes with a strong gradient in water temperature (and thus water density) with depth, material settled at the bottom does not easily mix with surface layers (MacIntyre and Melack 1995). The corpses of infected hosts – including parasite spores contained within – likely sink to the sediment (Kirillin et al. 2012). Therefore, during times of strong stratification, these spores should be inhibited from mixing into host habitat (Brookes et al. 2004, Johnson et al. 2007, Johnson et al. 2009b). Disruption of stratification might promote the spread of disease by resuspending spores from the sediment. In addition, mixing of the water column could enhance disease spread by resuspending nutrients (i.e., through the nutrient enrichment mechanisms discussed above) (Soranno et al. 1997). In this system, there is also the potential for disease to indirectly affect the algal community. That is, epidemics that affect host densities (or traits; Penczykowski et al. in prep.-b) could indirectly alter the abundance or nutrient stoichiometry of algae (Elser and Urabe 1999, Duffy 2007).

We performed a mesocosm experiment to test for effects of nutrient enrichment and water column mixing (i.e., habitat structure) on resources, host populations, and disease. In this experiment, we factorially manipulated levels of nutrients, mixing, and parasite exposure in thermally stratified water column enclosures in a lake. We predicted that raising levels of N and P would stimulate growth of algal resources, yielding greater host densities and infection prevalence. Periodic mixing of the water column was expected to enhance disease through spore resuspension. Because we tracked nutrient levels over time, we could evaluate whether mixing also bolstered disease by resuspending nutrients. The results supported our hypothesis that nutrient enrichment should fuel a greater density of infected hosts, and the results were consistent with a contribution of spore resuspension to larger epidemics under high nutrient conditions. Epidemics, in turn, affected the plankton community. Specifically, disease reduced host densities and indirectly increased the abundance and P:C content of algae. We also

surveyed 15 lakes over three years, and found that the density of infected hosts in a given year predicted epidemic size the following year. Infection prevalence was not as strong of a predictor across years. These results are consistent with a hypothesis that a greater density of infected hosts produces a greater total number of parasite spores during an epidemic, thereby seeding larger epidemics in the future.

Methods

Host–parasite system

Daphnia dentifera is a dominant zooplankton grazer in small, thermally stratified lakes in temperate North America (Tessier and Woodruff 2002). This host species ingests free-living spores of the fungal parasite *Metschnikowia bicuspidata* while non-selectively foraging in the water column (Ebert 2005, Hall et al. 2007b). In a successful infection, the parasite penetrates the gut wall of its host and reproduces in the hemolymph (Ebert 2005). The proliferation of spores throughout the host's body can cause large reductions in host fecundity and survivorship (Hall et al. 2009c). Infective spores are released into the water only after the host dies (Ebert 2005). In the Midwestern USA, epidemics typically occur between July and December (Hall et al. 2011, Overholt et al. 2012).

Mesocosm experiment: methods

We manipulated nutrient concentrations, the frequency of water column mixing, and parasite exposure in 32 mesocosms in University Lake (Monroe County, Indiana, USA) from 8 September (day 1) to 23 October 2011 (day 46). We created whole water column enclosures by suspending polyethylene bags (N = 32, depth = 6 m, diameter = 1 m) from rafts (N = 4) in a randomized block design (Hall et al. 2011, Civitello et al. 2013b). We filled the bags with ambient lake water (sieved through an 80 μm mesh) on 23 August. The lake was strongly stratified during this time, and the epilimnion was 4 m deep. We collected zooplankton from the lake and added them to the bags on 6

September, at initial *D. dentifera* densities of ~5000 m^{-2} (samples collected on day 1). We began the nutrient and mixing treatments on 8 September (day 1). Initial nutrient concentrations were approximately 400 µg N L^{-1} and 10 µg P L^{-1} inside the bags. We used these initial conditions as target levels for the "low nutrient" treatment. To bags in the "high nutrient" treatment, we added pulses of K_2HPO_4 and $NaNO_3$ aimed at a target level of 750 µg N L^{-1} and 30 µg P L^{-1}. This high nutrient pulse was effective at creating an initial difference in nutrient conditions (see Appendix Fig. B.1). We assumed that nutrients would be lost from the water column (e.g., due to settling) at a rate of 5% per day (Civitello et al. 2013b). To replenish nutrients that may have been lost between sampling visits, we added twice weekly supplements of N and P at 13% of the target concentrations for the low and high nutrient treatments. To manipulate habitat structure, we disrupted stratification of the water column. In the "mixed" treatment, we vigorously mixed the bags on each sampling visit with three bottom-to-surface pulls of a Secchi disk, after the nutrient additions. Bags in the "unmixed" treatment were allowed to remain stratified throughout the experiment. On 13 September (day 6), we inoculated bags in the "+spores" treatment with 3.6 spores mL^{-1} of the parasite, *M. bicuspidata*.

We sampled all bags twice weekly. Before adding nutrients or mixing the bags, we collected integrated water samples from the top 3 m (i.e., the epilimnion). We next collected a zooplankton sample using a Wisconsin net (13 cm diameter, 153 µm mesh), towed once from the bottom of the bag to the surface. Using a dissecting microscope at 25–50X magnification, we counted the number of infected and uninfected *D. dentifera* (juveniles and adults) to quantify host density and infection prevalence.

We analyzed the integrated epilimnetic water samples for concentrations of nutrients and chlorophyll *a* (a proxy for algal biomass). We measured total nitrogen (TN) on a UV-1700 spectrophotometer (Shimadzu Scientific Instruments, Columbia, MD, USA), using second derivative UV-spectrophotometry following persulfate digestion and acidification (Crumpton et al. 1992, Bachmann and Canfield 1996). Total phosphorus

(TP) was measured on the same spectrophotometer, using the ascorbic acid method following persulfate digestion (APHA 1995). We measured chlorophyll *a* in both the total and edible (< 80 µm) size fractions of seston, using narrow band filters on a Trilogy fluorometer (Turner Designs, Sunnyvale, CA) following chilled ethanol extraction (Webb et al. 1992, Welschmeyer 1994). On 8 October and 23 October (days 31 and 46) we also analyzed the elemental nutrient stoichiometry of edible seston. We collected samples onto precombusted filters (GF/F, 0.7 µm pore size, Whatman, Piscataway, NJ, USA). C content was measured on a 2400 series CHN analyzer (Perkin Elmer, Waltham, MA, USA). We measured P content as in the TP analysis described above.

On 8 October (day 31), we estimated extinction of photosynthetically active radiation (PAR) using irradiance data collected at 0 m and 4 m with a LI-250A light meter (LI-COR, Lincoln, NE). We regressed natural log-transformed irradiance $I(z)$ against depth (z):

$$\ln(I[z]) = a - kz + \varepsilon, \tag{4.1}$$

with intercept a and residual errors ε. The slope is the coefficient of light extinction, k (µmol quanta cm^{-2} s^{-1} m^{-1}), where larger values of k indicate shallower light penetration.

The experiment began with 4 replicates in each of the 8 treatments. We excluded a total of 5 replicates from analyses, each from a different treatment, for the following reasons. One bag (low nutrients, unmixed, +spores) was contaminated with high levels of nutrients in the first week of the experiment. In one bag (high nutrients, mixed, +spores) the host population crashed before epidemics began. Two bags (low nutrients, one mixed, one unmixed, -spores) were infested with high densities of *Chaoborus* midge larvae, which are predators of the host (>10x more *Chaoborus* than the mean of the other bags). Finally, one bag (high nutrients, unmixed, –spores) was entangled and destroyed by an anchor line that broke loose from a raft on 7 October.

Field survey: methods

We surveyed 15 lakes (Greene and Sullivan Counties, Indiana, USA) weekly from August to the first week of December in 2009, 2010, and 2011. On each sampling visit, we collected two replicate zooplankton samples (each with 3 pooled tows of a Wisconsin net, towed bottom to surface). One sample was used to estimate infection prevalence, as in the mesocosm experiment. The other sample was preserved in 60–75% ethanol and later used to enumerate host density.

Statistical analysis

All analyses were performed in R. We tested for effects of the nutrient and mixing manipulations on infection prevalence over time using a generalized linear mixed model (GLMM) with binomially distributed error and the logit link function, and bag fitted as a random effect. Host densities and concentrations of nutrients and chlorophyll *a* were log-transformed prior to analysis to meet assumptions of normality and homoscedasticity. To test for effects of the nutrient, mixing, and spore manipulations on host density and C:P ratios (as well as TP and chlorophyll *a*; see Appendix B), we performed linear mixed effect models with autoregressive (AR[1]) error structures. In these models, bag was a random effect term, and date was nested within bag. We also calculated indices of overall epidemic size and overall densities of hosts and their algal resources by integrating under each time series using the trapezoid rule. ANOVAs were used to test for effects on these integrated metrics. There were no significant effects of block (i.e., the four rafts) in any models; therefore, we reran the analyses without block. In all models, we performed stepwise removal of non-significant interaction terms.

We used Pearson correlations to test for linear relationships between the density of hosts and density of algae (measured as chlorophyll *a*), and between carbon concentration, light extinction, and C:P. In the field survey, we tested for correlations

between the density of infected hosts in a given year (integrated over all sampling dates) and the size of epidemics the next year (indexed as integrated infection prevalence).

Results

Mesocosm experiment: results

Epidemics began approximately 9 days after the addition of parasite spores (Fig. 4.1A). An initial wave of infections peaked at ~10% prevalence in all nutrient and mixing treatments. After these infected hosts died, spores released from their carcasses fueled larger second waves of infections, which we detected 11 days after the start of the first wave. These second epidemics peaked at ~30–35% prevalence (~60–75% prevalence among adults; not shown), and began to wane 9 days after they began. There was a significant interactive effect of nutrients and mixing on infection prevalence over time (GLMM with vs. without this interaction term: $X^2 = 79.78$, d.f. = 4, $p < 0.0001$; Fig. 4.1A). The overall size of epidemics (i.e., prevalence integrated over time) tended to be greater in high nutrient, mixed bags, compared to low nutrient bags. However, integrated prevalence was highly variable among high nutrient, unmixed bags, and there were no significant main or interactive effects of nutrients or mixing on this measure of epidemic size (Nutrients: $F_{1,11} = 1.65$, $p = 0.22$; Mixing: $F_{1,11} = 0.55$, $p = 0.47$; Fig. 4.1B). The results were qualitatively the same when we analyzed prevalence among adults only, or integrated prevalence over just the second wave of the epidemics. The density of infected hosts followed the trajectory of infection prevalence over time, and was significantly increased by nutrient enrichment (Nutrients: $F_{1,11} = 5.99$, $p = 0.032$; Mixing: $F_{1,11} = 2.36$, $p = 0.15$; Date: $F_{1,125} = 9.76$, $p = 0.0022$; Fig. 4.1C). Integrated over time, there were greater densities of infected hosts in the high nutrient treatments, and mixing the water column did not significantly enhance the overall abundance of infected hosts (Nutrients: $F_{1,11} = 11.21$, $p = 0.0065$; Mixing: $F_{1,11} = 4.26$, $p = 0.064$; Fig. 4.1D).

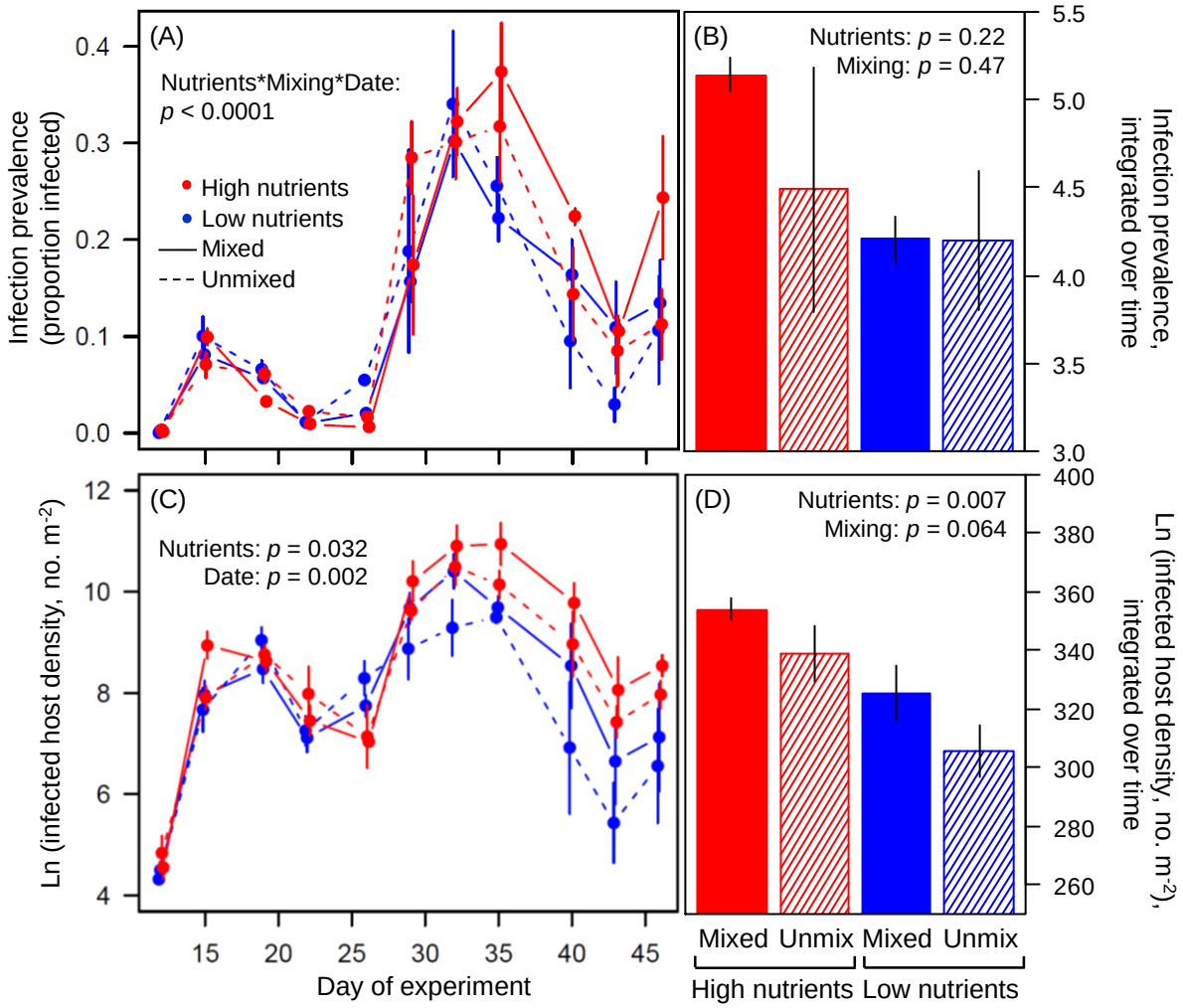

Figure 4.1. Infection prevalence and infected host density results (mean ± SE) in the +spores treatments, which were inoculated with parasite spores on the 6th day of the experiment. (A) There were small epidemics that began 9 days after spore addition. Spores produced during these initial epidemics fueled larger second epidemics in all treatments. There was a significant interactive effect of nutrients and mixing over time. (B) The total size of epidemics (integrated prevalence) tended to be greater in the high nutrient, mixed treatment compared to either of the low nutrient treatments, but was highly variable among high nutrient, unmixed bags. Overall, there were no significant effects of the nutrient and mixing treatments on this index of disease. (C) The density of infected hosts followed the trajectory of infection prevalence through time. Nutrient enrichment boosted the density of infected hosts throughout the epidemics. (D) Infected host density, integrated over the course of the experiment, was greater in the high nutrient treatments, but was not significantly enhanced by mixing the water column.

Total (infected and uninfected) host densities diverged over time due to manipulation of nutrient levels and parasite exposure (Nutrients: $F_{1,23} = 5.16$, $p = 0.033$; Mixing: $F_{1,23} = 0.35$, $p = 0.56$; Spores: $F_{1,23} = 4.00$, $p = 0.058$; Date: $F_{1,322} = 21.6$, $p < 0.0001$; Nutrients*Date: $F_{1,322} = 11.37$, $p = 0.0008$; Spores*Date: $F_{1,322} = 8.49$, $p = 0.0038$; Fig. 4.2A,C). In particular, the density of hosts in the low nutrient treatment tended to decrease during the second wave of the epidemic (Fig. 4.2C). Total host density, integrated over time, was significantly increased by nutrient enrichment, and significantly reduced by epidemics (Nutrients: $F_{1,23} = 7.17$, $p = 0.013$; Mixing: $F_{1,23} = 1.27$, $p = 0.27$; Spores: $F_{1,23} = 4.66$, $p = 0.041$; Fig. 4.2B,D). These changes in host density likely drove changes in algal abundance over time (see also Appendix B; Fig. B.2). Beginning at the peak of the second epidemic, bags with fewer hosts had more algae in both the edible ($r = -0.63$, $p = 0.0004$; Fig. 4.3A) and inedible ($r = -0.57$, $p = 0.002$; Fig. 4.3B) size fractions. There was no relationship between host density and the ratio of edible to inedible algae during this time ($r = -0.06$, $p = 0.86$; not shown). However, nutrient additions and epidemics significantly decreased C:P of edible resources (Nutrients: $F_{1,24} = 37.89$, $p < 0.0001$; Mixing: $F_{1,24} = 0.30$, $p = 0.59$; Spores: $F_{1,24} = 11.67$, $p = 0.0023$; Date: $F_{1,26} = 9.09$, $p = 0.0057$; Fig. 4.4A,B). These reductions in C:P were not explained by light limitation of algae. In bags with a greater total concentration of chlorophyll *a* (i.e., a proxy for algal density), light did not penetrate as deeply ($r = 0.69$, $p = 0.0002$; Fig. 4.4C). Light-limited algae would then be expected to have lower C:P, but C:P was not significantly correlated with either algal abundance ($r = 0.34$, $p = 0.10$; Fig. 4.4D) or light extinction ($r = 0.10$, $p = 0.64$; not shown).

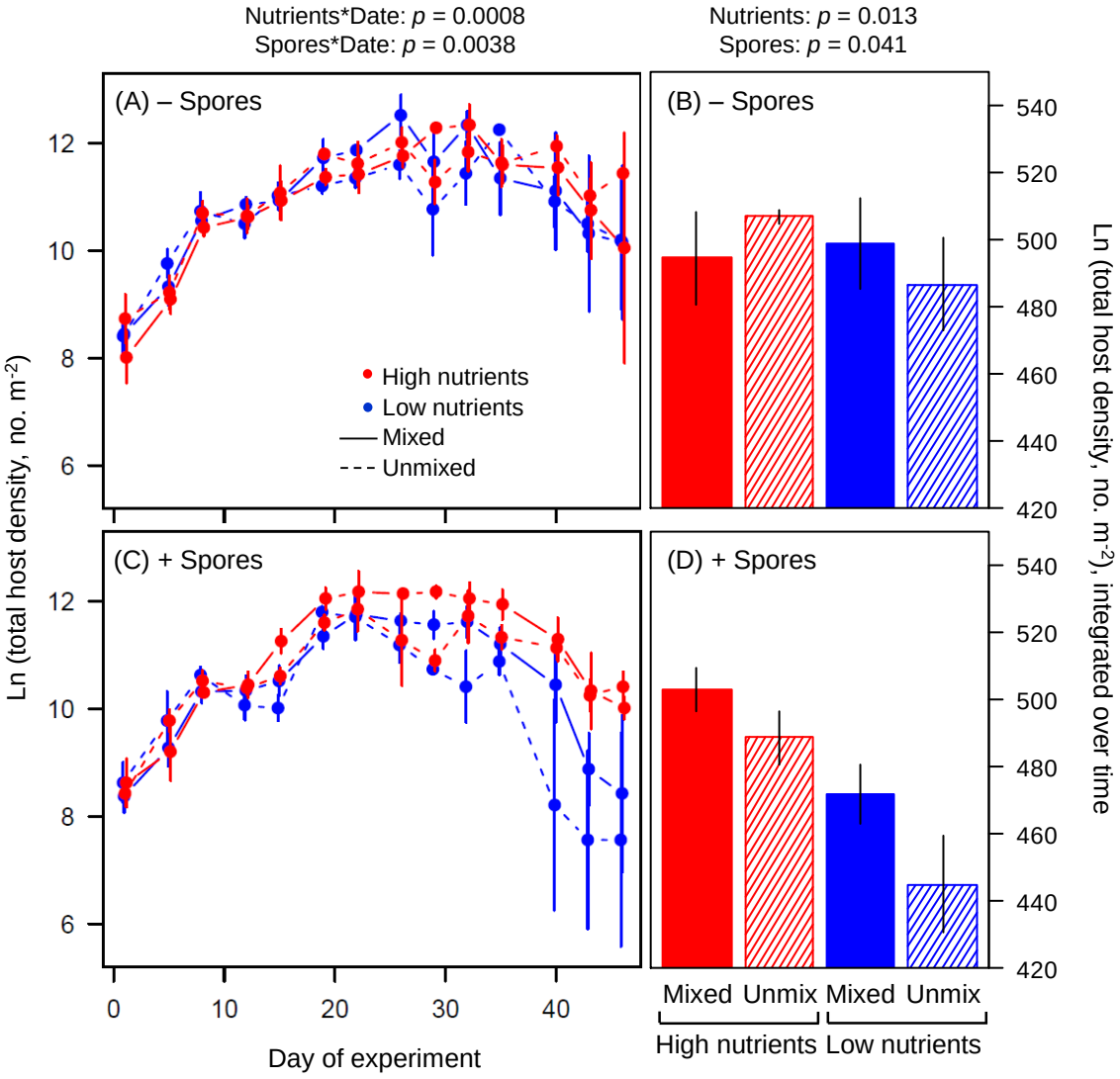

Figure 4.2. Total (infected + uninfected) host density (mean ± SE) in the (A,B) –spores and the (C,D) +spores treatments. (A,C) The density of hosts in all treatments generally increased until the end of September (day 22), then plateaued or waned over the remainder of the experiment. Host density differed over time between the high and low nutrient treatments, and between the +spores and –spores treatments, but did not depend on whether the water column was mixed. Over time, high nutrients boosted host density, and epidemics caused reductions in total host density. (B,D) There were more hosts overall in high nutrients and –spores treatments.

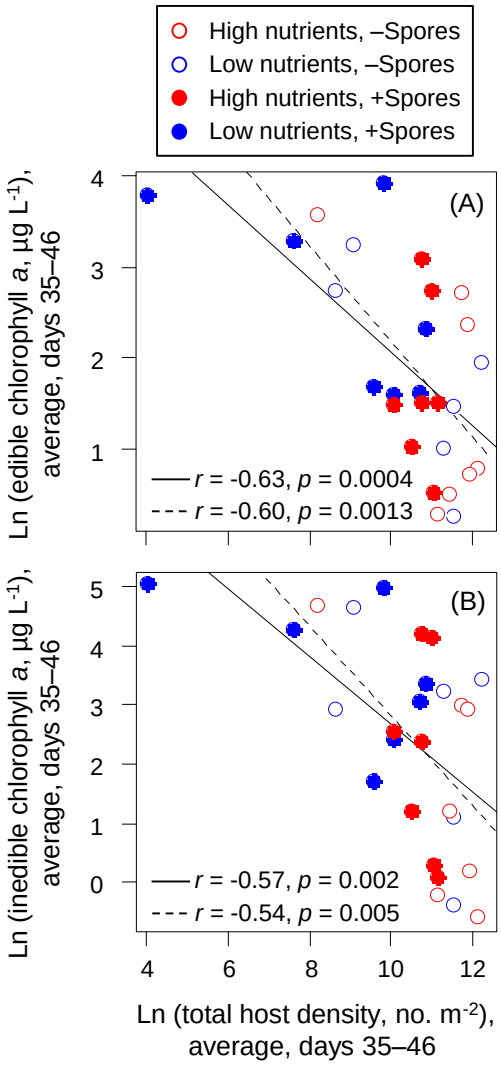

Figure 4.3. Chlorophyll *a* (an index of algal biomass) and total host density among bags in all treatments, averaged from just the peak of the second epidemic (day 35) until the end of the experiment (day 46). When there was a greater total (infected and uninfected) density of hosts, there was a lower abundance of algae in both the (A) edible and (B) inedible size fractions. The solid line is the fit of linear regression through all data points; the dashed line is the regression excluding the low nutrient, +spores bag with very low host density (in upper left of both panels).

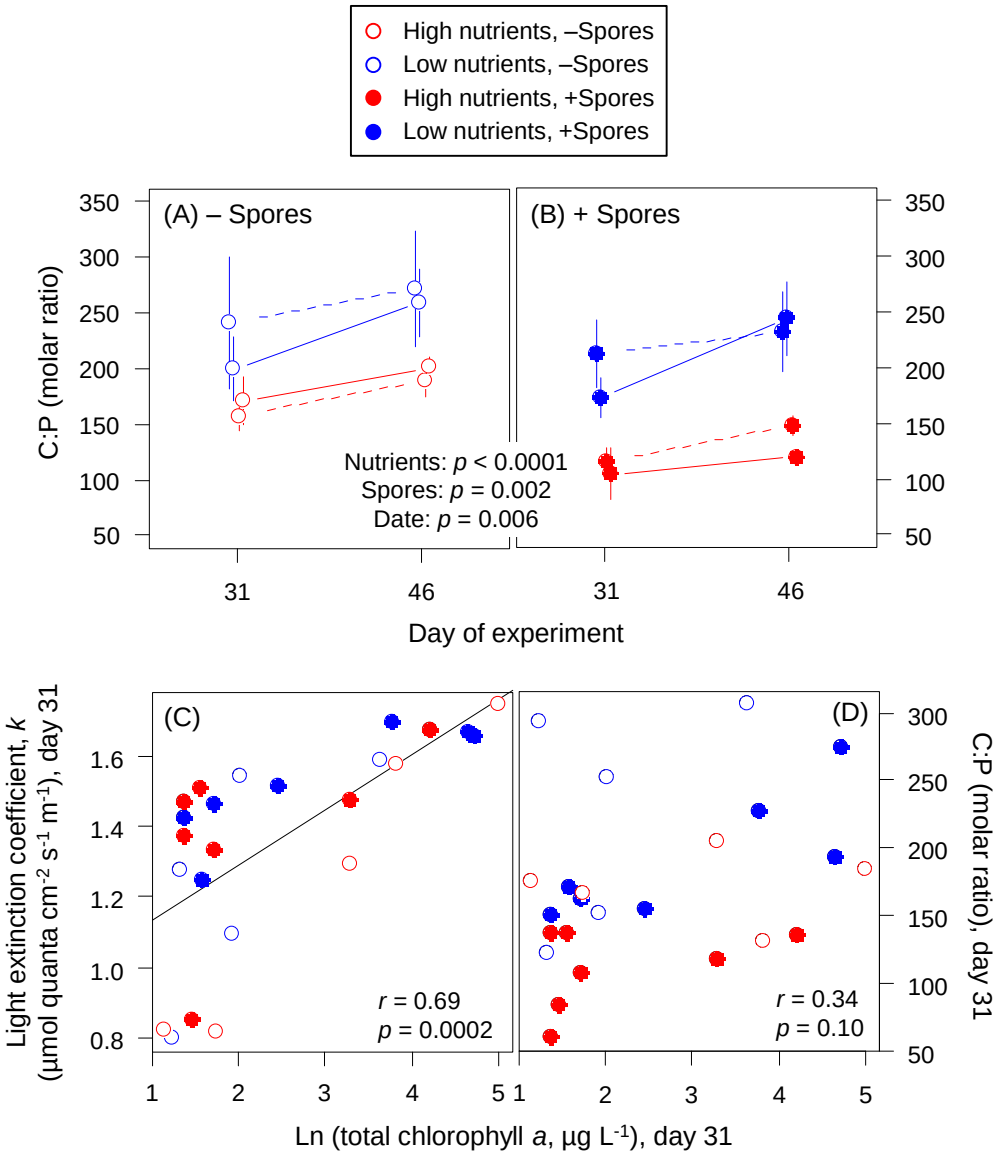

Figure 4.4. Nutrient stoichiometry (molar ratios; mean ± SE) of the edible size fraction of seston (i.e., potential host resources), measured at the peak of the second epidemic (day 31) and on the final day of the experiment (day 46). (A,B) Within each treatment, the C:P ratio of edible resources increased slightly over time. C:P did not differ between mixed (solid lines) and unmixed (dashed lines) treatments. However, C:P was significantly lower (P-enriched) in the high nutrients treatments, and in bags that had epidemics (+spores). These reductions in C:P were likely not driven by light limitation. (C) Bags with greater concentrations of total chlorophyll *a* (i.e., a proxy for algal density) had shallower light penetration (i.e., larger values of *k*). In contrast to the pattern expected for light limitation (i.e., more algae, larger *k*, and lower C:P), (D) algal density was not significantly correlated with C:P.

Field survey: results

Based on metrics of host density and infection prevalence integrated over the course of each sampling season, lakes that had a greater density of infected hosts in 2009 had larger epidemics in 2010 ($r = 0.60$, $p = 0.018$; Fig. 4.5A). The relationship between infected host density and epidemic size was even stronger between 2010 and 2011 ($r = 0.75$, $p = 0.001$; Fig. 4.5B). By contrast, integrated infection prevalence did not significantly correlate between 2009 and 2010 ($r = 0.43$, $p = 0.11$; Fig. 4.5C). Integrated infection prevalence was correlated between 2010 and 2011 ($r = 0.73$, $p = 0.002$; Fig. 4.5D), but this relationship was no stronger than the correlation with infected host density (Fig. 4.5B). That is, over two between-year comparisons, infected host density was better than infection prevalence at predicting the size of the next year's epidemic.

Discussion

Ecosystem characteristics can both affect, and be affected by, host-parasite interactions (Tompkins et al. 2011, Hatcher et al. 2012). In this study, we showed that nutrient enrichment fueled greater densities of *Daphnia* infected with a fungal parasite. Epidemics then reduced *Daphnia* densities, and affected both the abundance and nutrient composition of algae. We hypothesized that nutrient additions and water column mixing would boost infection prevalence, through stimulation of algal resources and resuspension of parasite spores, respectively (Johnson et al. 2007, Smyth 2010). The nutrient and mixing manipulations did jointly influence infection prevalence over time. Specifically, mixing tended to promote disease in the high nutrient bags during the second wave of infections. However, there were no significant effects of either nutrients or mixing on overall epidemic size (i.e., integrated infection prevalence).

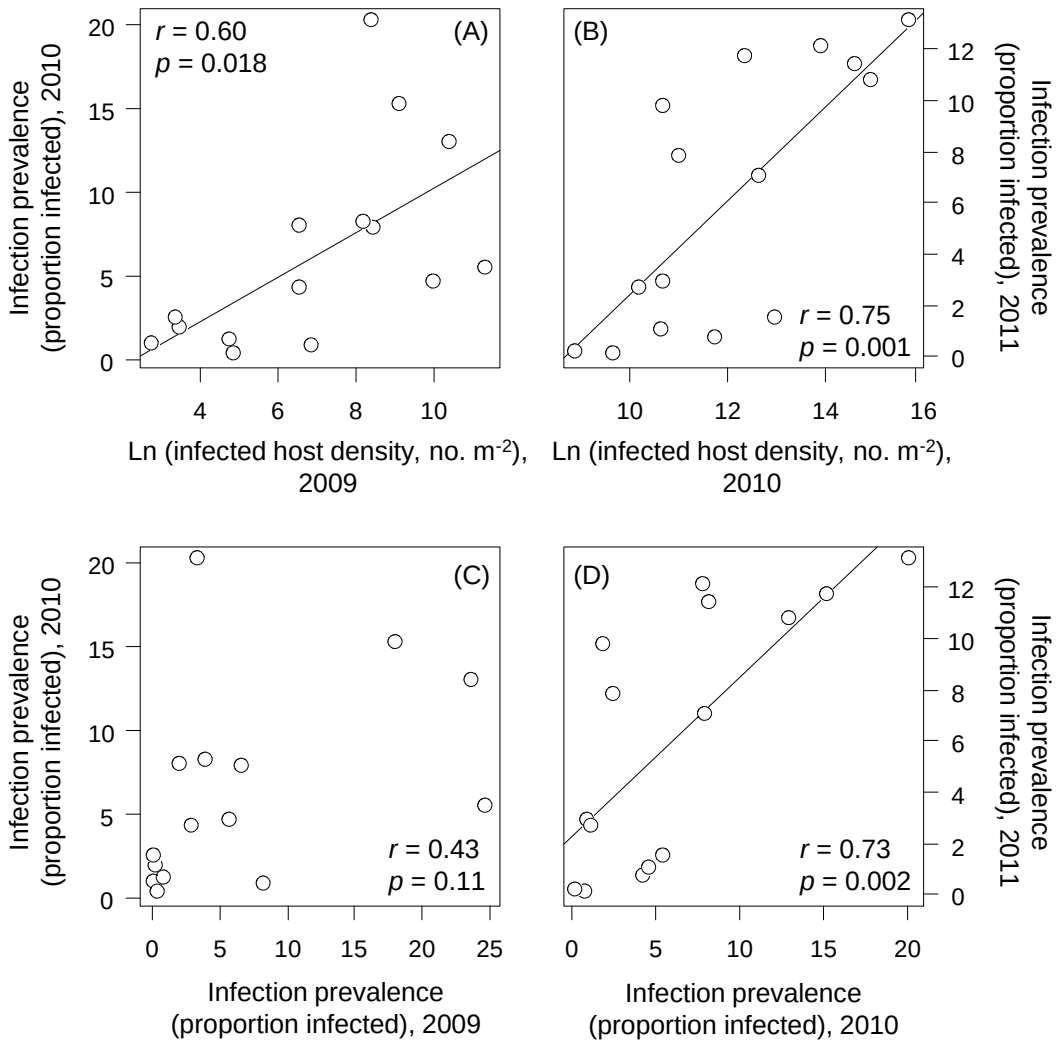

Figure 4.5. The density of infected hosts in natural populations correlates positively with the size of epidemics the following year. (A) Lakes that had a greater density of infected hosts (integrated over time) in 2009 had larger epidemics (integrated prevalence) in 2010. (B) There was an even stronger correlation between integrated density of infected hosts in 2010 and integrated prevalence in 2011. (C) Epidemic size (integrated prevalence, not accounting for host density) in 2009 does not significantly correlate with the size of epidemics in 2010. (D) However, epidemic size on its own did correlate between 2010 and 2011.

Nutrient enrichment has been shown to promote the spread of disease in a variety of aquatic systems (e.g., Bruno et al. 2003, Johnson et al. 2007, Hall et al. 2009b, Civitello et al. 2013b). On the other hand, there are many reasons why this does not always occur. Even in our focal *Daphnia*–fungus system, host density and infection prevalence do not necessarily correlate across lakes (Cáceres et al. 2006, Penczykowski et al. in press). One possible explanation is that host foraging rate, and thus the rate of spore exposure, may saturate or decrease when the density of resources or hosts is very high (Hall et al. 2007b, Civitello et al. 2013a). That is, due to handling time constraints or foraging interference by conspecifics, infection prevalence might be lower than expected for parasites with density-dependent transmission (Civitello et al. 2013a). Nutrient enrichment may also fuel the growth of low quality resources (e.g., cyanobacteria; Schindler and Vallentyne 2008) that inhibit foraging and parasite ingestion by hosts (Penczykowski et al. in review). Because such low quality resources might be morphologically edible and replete in nutrients (Penczykowski et al. in review), we cannot tell from our chlorophyll *a* and C:P data whether this shift in resource composition occurred. However, this mechanism is unlikely, given that low quality resources should not have fueled high densities of hosts (Martin-Creuzburg et al. 2008).

The high nutrient manipulation boosted the density of infected and uninfected hosts. This could have both epidemiological and ecological consequences. First, the total density of infected hosts in a given epidemic may reflect the total potential parasite production during that time. By contrast, infection prevalence on its own does not indicate the magnitude of spore production in the system (i.e., a small population could have a high proportion of infected individuals, yet produce few spores overall). If more hosts release spores into the environment, this could fuel larger epidemics in the future (Ebert et al. 2000). The results of our field survey are consistent with this hypothesis. The density of infected hosts in a given year correlated with the size of the next year's epidemic, over two pairs of consecutive years, while infection prevalence was less

predictive of future epidemic size. Second, grazer density is important in a food web context. Towards the end of the mesocosm experiment, lower host density allowed for greater abundance of algal resources, particularly in bags that received low nutrient inputs and had epidemics (see Appendix B). Thus, nutrient conditions may modulate indirect effects of disease on resources (Penczykowski et al. in prep.-b).

Disease influenced not just the quantity, but also the elemental nutrient content of algae. Algal resources in the edible size range were more P-enriched in treatments that had epidemics, even in bags that received lower nutrient additions. One way that disease could have decreased algal C:P is by driving light limitation (Sterner et al. 1997). Through this mechanism, an indirect increase in algal density due to disease could lead to self-shading of algae, resulting in less incorporation of C relative to P in algal tissue. However, this mechanism was not supported by our data. While bags with more algae had shallower light penetration, neither algal abundance nor light extinction correlated with C:P. Another hypothesis is that disease may have reduced C:P by increasing rates of algal turnover, since algae with higher per capita growth rates should have lower C:P (Droop 1968, Hall et al. 2007a). This possibility warrants further study. We should also explore the potential for disease-mediated *Daphnia* mortality to speed up the recycling of nutrients from P-rich host carcasses (Andersen and Hessen 1991). Finally, it is possible that stoichiometry of the parasite itself affects nutrient availability for algae. Given that the parasite uses energy and nutrients to fill its host with spores, this may represent a significant diversion of resources into parasite biomass (Kuris et al. 2008). Therefore, quantification of parasite C:N:P could be an important step in determining how disease alters algal stoichiometry.

To understand how alteration of climate and nutrient regimes might affect ecosystems, we need to understand how such environmental changes drive disease. This study illustrates that we also need to consider how disease may influence the response of ecosystems to environmental forcing. We found that eutrophication and alteration of

thermal habitat structure can interact to promote disease spread, and that nutrient enrichment may boost the density of infected hosts. These epidemiological results are important not only for host populations, but also for ecosystems. In our experiment, disease caused reductions in host density that allowed for greater resource abundance. This effect was most pronounced under low nutrient conditions. Thus, instead of the expected pattern of lower algal biomass in lower nutrient systems, disease led to greater algal density in the low nutrient manipulations. In addition, epidemics drove a reduction in the C:P content of algae. Through such mechanisms, interplay between environmental variables (e.g., nutrients levels and habitat structure) and disease could shape how ecosystems respond to environmental change.

CHAPTER 5

DISEASE REDUCES HOST FORAGING RATE: TRAIT-MEDIATED INDIRECT EFFECTS OF DISEASE ON RESOURCES

Abstract

Parasites can indirectly affect communities and ecosystems through effects on host densities or traits. In many systems, there may be both density- and trait-mediated indirect effects of disease (DMIEs and TMIEs, respectively). Therefore, to understand how effects of disease might extend beyond host populations, we need to elucidate the mechanisms for indirect effects. Here, we investigated the potential for TMIEs in a freshwater zooplankton (host)–fungus (parasite)–algae (resource) system. We focused on effects of disease on host foraging rate. In this system, foraging rate governs exposure to parasite spores; thus, it is a key ecological as well as epidemiological trait. In a laboratory experiment, we established that infection can reduce host feeding rate, and we developed models to describe the mechanism behind this trait change. The model that best fit the empirical data featured an increase in host feeding rate with body size, but a reduction in feeding rate due to infection. The reduction in feeding rate became more pronounced as hosts filled with parasite spores. Then we parameterized the foraging model with field-collected body size and spore load data to show that the average feeding rate of adult hosts might be substantially reduced by epidemics in nature. Finally, we used a dynamic epidemiological model to explore the potential for parasite-mediated foraging inhibition to have TMIEs on resources. The results of our model suggest that disease could indirectly increase densities of both resources and hosts. That is, the increase in birth rate due to more abundant resources could offset the negative effects of disease on host fecundity and survivorship. In addition, reduced spore consumption by infected hosts

could promote transmission to susceptible hosts, leading to larger epidemics. Overall, our study shows that non-lethal trait changes due to disease could have major implications for host populations and food webs.

Introduction

Ecologists increasingly recognize that effects of diseases on host populations can propagate through communities and ecosystems (Hudson et al. 2006, Tompkins et al. 2011, Dunn et al. 2012). One way that parasites extend their influence beyond host populations is through density-mediated indirect effects (DMIEs). That is, by impacting host density, parasites can indirectly affect other members of the community and ultimately drive changes in the flow of energy and nutrients through ecosystems (Lafferty et al. 2008, Holdo et al. 2009, Hatcher et al. 2012). Another way that parasites affect communities and ecosystems is through trait-mediated indirect effects (TMIEs). Infection can alter a variety of host traits (i.e., in addition to fecundity and mortality), including size, morphology, behavior, and habitat use (Moore 1995). Such trait changes include attempts by hosts to resist or compensate for infection (Hart 1990), symptoms of within-host parasite growth (Forshay et al. 2008), and parasite manipulation of hosts to increase the probability of transmission (Lafferty and Morris 1996, Lefèvre et al. 2009, Sato et al. 2012). Both DMIEs and TMIEs of parasites likely occur in many systems; therefore, we need to disentangle the two in order to understand the role of parasites in food webs. This will require a combination of observations of natural systems, experimental characterization of parasite effects on host traits, and mathematical models that incorporate those trait changes.

Here, we focus on parasite-driven changes in host foraging rate. Foraging rate is a key ecological trait, influencing host–resource dynamics and the transfer of energy and matter through food webs. Foraging rate is also a core epidemiological trait in many disease systems. For the diverse array of hosts that encounter parasites while foraging

(e.g., Hutchings et al. 2001, Dwyer et al. 2005, de Roode et al. 2008), feeding rate may govern the probability of host–parasite contact. In addition, feeding rate can affect the spread of disease by determining the supply of energy and nutrients available to the parasite and its host (Seppälä et al. 2008, Hall et al. 2010a). Thus, parasite modification of foraging rate could have consequences for food webs (Hernandez and Sukhdeo 2008a), and also for the spread of disease through populations. There are several mechanisms through which parasites may alter foraging rate. For instance, infected hosts might forage less to limit diversion of energy from immune function to locomotion or digestion (Hart 1990, Adamo et al. 2010). Parasites may also damage or mechanically inhibit the physical structures involved in acquiring or assimilating food (Wood et al. 2007, Peñalva-Arana et al. 2011). In addition, ingestion rates scale with body size (specifically, surface area) for many taxa (Kooijman 2010); therefore, parasites that stunt growth (e.g., Booth et al. 1993, Thomas et al. 1998) or cause gigantism (e.g., Ebert et al. 2004, Lafferty and Kuris 2009b) might decrease or increase feeding rate, respectively. Finally, increased food intake may yield more fuel for parasite growth, or may allow the host to partially offset the energetic cost of infection (Bernot and Lamberti 2008). These various modifications of foraging rate could have very different implications for host populations, food webs, and disease dynamics. Thus, to assess the potential for TMIEs to influence populations, communities, and ecosystems, it is essential to elucidate the mechanism underlying the trait change.

In this study, we quantified foraging-mediated indirect effects of disease in a freshwater food web. Specifically, we investigated how effects of a fungal parasite on feeding rate of a zooplankton (*Daphnia*) host could indirectly impact algal resources, and how this change in resource availability might influence host density and disease dynamics. This is an ideal system in which to investigate foraging-mediated indirect effects of disease, for several reasons. First, *Daphnia* are dominant grazers in many lakes, and function as important links between their algal resources and higher trophic levels

(Tessier and Welser 1991, Lampert 2006). Therefore, a change in *Daphnia* foraging behavior could substantially affect the abundance of algae and transfer of energy and nutrients through the food web. Second, the focal parasite decreases host fecundity and survivorship, sometimes reducing host density and indirectly increasing resource density (Duffy 2007, Hall et al. 2011, Penczykowski et al. in prep.-a). Thus, we can study the potential for both DMIEs and TMIEs in this system. Third, we know that feeding rate is central to transmission of the parasite (Hall et al. 2007b, Hall et al. 2010a, 2012). *Daphnia* become infected after ingesting fungal spores while non-selectively grazing (Ebert 2005). This means faster feeding hosts are more likely to encounter spores (Hall et al. 2007b, Penczykowski et al. in review). In addition, hosts that feed faster may provide more fuel for within-host parasite replication (Hall et al. 2009c, Hall et al. 2010a). Feeding rate of uninfected *Daphnia* generally increases with body length squared, likely due to scaling of feeding appendages with surface area (Hall et al. 2007b, Kooijman 2010). However, effects of infection on foraging were not previously characterized in this host–parasite system. We predicted that infection would reduce feeding rate, especially as spores proliferated throughout the body of the host.

To test this prediction, we built mechanistic models of foraging rate, which we fit to data from hosts of a range of sizes and infection stages. The candidate models included effects of host size (surface area) and/or parameters that allowed feeding rates of infected and uninfected hosts to vary with spore load or other factors. In the best fitting model, feeding rate increased with body size but decreased with spore load. We parameterized this model with field-collected host size and spore load data to assess the potential effect of disease on average feeding rates of natural host populations. Then we used a dynamic epidemiological model to explore the potential for TMIEs due to parasite-altered foraging rate. Our results suggest that a parasite-mediated reduction in feeding rate could boost resource density, host density, and infection prevalence.

Methods and Results

Disease system

Daphnia dentifera is a common zooplankton grazer in small, thermally stratified lakes throughout the Midwestern USA (Tessier and Woodruff 2002). This host species ingests spores of the parasitic fungus *Metschnikowia bicuspidata* while non-selectively foraging on small (< 60 μm) phytoplankton (Hall et al. 2007b). In a successful infection, the fungus penetrates the gut wall of its host and replicates in the hemolymph (Green 1974, Ebert 2005). As the parasite fills its host with spores, it reduces host growth, fecundity, and survivorship (Hall et al. 2009c). Upon death of the host, infectious fungal spores are released into the water.

Foraging models

We built a set of models to describe how infection influences per capita feeding rate (f) of hosts. These models were competed by comparing their fit to feeding rate data collected from infected and uninfected hosts of three genotypes, where individuals of each genotype spanned a range of body sizes and infection stages. The best fitting (hereafter, "winning") model was then used to estimate the average feeding rate of adult hosts in natural populations (see the *Field survey* section below). Key features of the winning model were also used to parameterize a dynamic epidemiological model, which allowed us to explore the potential food web implications of parasite-modified feeding rate (see the *Dynamic epidemiological model* section below).

Foraging model formulation

We present the six candidate foraging models in Table 5.1. In model 1 (*null*), per capita feeding rate (f) is represented as a single parameter (the feeding coefficient, $\hat{f}$). We estimated parameters separately for infected and uninfected hosts; thus, f could depend on infection status even in the *null* model. In model 2 (*size only*), the feeding coefficient ($\hat{f}$)

is multiplied by observed body length squared (L^2); this model is known to fit well to feeding rate data for uninfected hosts (Hall et al. 2007b, Kooijman 2010). The next two formulations (model 3: *spores only, linear* and model 4: *spores only, power*) lack the size (L^2) component, but feature a term that reduces *f* as either a linear or a power function of the number of spores (σ) per host volume (L^3). That is, we hypothesized that feeding rate would depend on the volumetric density of spores. In the two most complex models (model 5: *size and spores, linear* and model 6: *size and spores, power*), *f* increases in proportion to L^2 but decreases through a linear or power function of spore density (σL^{-3}). The coefficients related to spore load (parameters *b* and *c*; Table 5.1) were not estimated (i.e., they were fixed at zero) for uninfected hosts.

Feeding rate experiment: methods

We measured feeding rates, body sizes, and spore yields to parameterize the foraging models for uninfected and infected *D. dentifera* hosts of three genotypes. The A4-4 and Standard (STD) genotypes, as well as the parasite (*M. bicuspidata*) were originally collected from lakes in Barry County, Michigan, USA. The Beaver Dam 30 (BD-30) genotype was from a lake in Greene County, Indiana, USA. To standardize maternal effects, *D. dentifera* of each genotype were reared in groups of six in 150-mL beakers containing a mixture of Artificial *Daphnia* Medium (ADaM; Klüttgen *et al.* 1994) and filtered water from Lake Lanier (Georgia, USA), and fed 0.9 µg C mL^{-1} day^{-1} (a standard, non-limiting level) of the nutritious green alga *Ankistrodesmus falcatus*. We generated cohorts of each host genotype that were 8, 10, 12, 14, 16, 20, and 24 days old during the feeding rate assay. For each cohort, neonate hosts born within a 24 h period were placed in groups of 10 in 150-mL beakers and kept at 20 °C in a 16:8 h light:dark cycle. When a cohort was 6 days old, hosts were distributed into new groups of six per beaker, and beakers were haphazardly assigned to be either unexposed to the parasite, or exposed to 900 parasite spores mL^{-1} for 24 h. After spore exposure, we transferred all

Table 5.1. Results of the foraging model competition.

Model	Foraging rate (f)[1]	Parameters[2]	AIC	ΔAIC[3]	Akaike weight (w_i)[4]
(6) *size and spores, power*	$\hat{f}L^2\left(1-b\left(\frac{\sigma}{L^3}\right)^c\right)$	12	-225.5	0	0.59
(5) *size and spores, linear*	$\hat{f}L^2\left(1-b\left(\frac{\sigma}{L^3}\right)\right)$	9	-224.5	0.9	0.41
(3) *spores only, linear*	$\hat{f}\left(1-b\left(\frac{\sigma}{L^3}\right)\right)$	9	-108.3	117.2	2.3×10^{-26}
(4) *spores only, power*	$\hat{f}\left(1-b\left(\frac{\sigma}{L^3}\right)^c\right)$	12	-106.3	119.2	7.8×10^{-27}
(2) *size only*	$\hat{f}L^2$	6	-86.2	139.3	4.1×10^{-31}
(1) *null*	$\hat{f}$	6	-18.1	207.4	6.7×10^{-46}

[1]Per capita rates.

[2]Number of estimated parameters for infected and uninfected hosts of three genotypes.

[3]The winning model has ΔAIC = 0. Models with ΔAIC > 10 have essentially no support.

[4]Akaike weights represent the probability that the model is the best among those under consideration.

hosts (both exposed and unexposed) to fresh medium. Hosts were transferred to fresh medium again every 4 days until the feeding rate assay.

On the day of the feeding rate assay, hosts were placed singly into 15-mL centrifuge tubes ($n \geq 12$ for each age x infection x genotype combination, but $n = 3$ for 24-day-old infected STD hosts, as most STDs of that age had already died of infection). Hosts were fed 0.45 µg C mL^{-1} of *A. falcatus* and allowed to graze for 4 h. The assay was run in two overlapping time blocks, with half of the replicates in each treatment in each block. We also set up ungrazed controls at seven levels of algal density ($n = 8$ in each block), following Sarnelle and Wilson (2008). Tubes were inverted every 20 min and briefly uncapped after 2 h to allow air exchange. At the end of the grazing period, hosts were measured (length, *L*) from the middle of the eye to the base of the tail at 40X magnification using DP2-BSW software (Olympus America, Center Valley, PA, USA). We measured the fluorescence of food remaining in each tube using a Trilogy fluorometer (*in vivo* module, Turner Designs, Sunnyvale, CA, USA).

Of the hosts that were exposed to parasite spores, we only used data from those later confirmed to be infected. Spores were visually apparent in infected hosts that were at least 16 days old (i.e., 10 days post-exposure). Therefore, the infection status of hosts in the oldest three cohorts could be confirmed immediately after the feeding rate assay, and these hosts could be killed to measure their spore yields. We transferred them to microcentrifuge tubes, gently smashed each individual using a pestle, and counted the released spores using a hemocytometer at 200X magnification. However, we could not be certain whether hosts younger than 16 days old were infected. Thus, the younger cohorts of exposed hosts were placed singly in beakers of fresh medium immediately after the feeding rate assay. We examined them for infection at 25–50X magnification when they reached 10 days post-exposure. For these younger cohorts, we measured feeding rates of a surplus of exposed hosts. In the end, each treatment had at least 9 replicates.

We tested whether body size and feeding rate differed between infection classes within age cohorts. First, we tested for a significant random effect of genotype, using the package 'MixMod' in R. After establishing significant age x infection x genotype effects on both body size (X^2 = 246, d.f. = 1, $p < 0.0001$) and feeding rate (X^2 = 86.3, d.f. = 1, $p < 0.001$), we used ANOVAs to test for effects of age and infection (and their interaction) within each genotype. When there were significant omnibus effects, we performed post-hoc contrasts using Tukey's honestly significant difference (HSD) tests. For A4-4 and BD-30, there were significant age x block interactions. Fig. 5.1 shows results for pooled blocks, but asterisks denote only the differences between infected and uninfected hosts that were significant in both time blocks. For infected hosts in age 16, 20, and 24 day cohorts, we tested for a significant effect of age on spore yield. Because the spore yields were overdispersed count data, we used a generalized linear model with quasipoisson error distribution.

Parameterization and model selection: methods

Full details for the parameterization and model selection are presented in Appendix C. Briefly, we used maximum likelihood methods to parameterize and compete the foraging models in their fit to data from the feeding rate experiment (i.e., initial and final algal densities, host size, and spore load, depending on the model) in Matlab. For each genotype, foraging models were fit separately to data from infected and uninfected hosts. Then we summed the negative log-likelihoods across infection status and genotype to compute a single value of the Akaike information criterion (AIC, Burnham and Anderson 2002) for each model. Models were ranked in their relative performance based on ΔAIC and Akaike weights (Burnham and Anderson 2002) (see Table 5.1 and Appendix C). We estimated 95% confidence intervals around parameter estimates using 10,000 bootstraps, and we used permutation tests (9999 randomizations per contrast) to compare point estimates between genotypes or infection classes (with Holm–Bonferroni

adjusted significance levels) (Gotelli and Ellison 2004). All results presented here were generated after pooling data from the two time blocks (see Table C.2 and Fig. C.2 for comparisons between blocks).

Feeding rate experiment and model selection: results

Body size (length, L) of both infected and uninfected hosts tended to increase with age, but infected hosts did not grow as large (infection x age; A4-4: $F_{6,187} = 2.42$, $p = 0.028$; BD-30: $F_{6,157} = 19.99$, $p < 0.0001$; STD: $F_{6,179} = 7.26$, $p < 0.0001$; Fig. 5.1A–C). For the A4-4 and BD-30 genotypes, infected and uninfected hosts were similarly sized until late stages of infection (Fig. 5.1A,B). However, by 4 days post-exposure to parasite spores, STD hosts were already smaller than their uninfected counterparts (Fig. 5.1C). The extent to which spore yield increased over the oldest three age cohorts also depended on host genotype (Fig. 5.1D–F). The number of spores per infected individual increased from age 16 to 24 days for A4-4 hosts ($F_{2,32} = 20.16$, $p < 0.0001$; Fig. 5.1D), plateaued at age 20 days for BD-30 hosts ($F_{2,29} = 9.74$, $p = 0.0006$; Fig. 5.1E), and did not consistently increase with age for STD hosts ($F_{2,23} = 3.13$, $p = 0.063$; Fig. 5.1F).

Feeding rate (f) generally increased with age for uninfected hosts and those at early stages of infection, but decreased over later stages of infection (infection x age; A4-4: $F_{6,187} = 18.09$, $p < 0.0001$; BD-30: $F_{6,157} = 11.93$, $p < 0.0001$; STD: $F_{6,179} = 9.57$, $p < 0.0001$; Fig. 5.1G–I). These trends with age were driven by changes in size of uninfected hosts; for infected hosts, they were driven by changes in size and spore load. Models 5 and 6, which included effects of surface area (L^2) and within-host spore density (σL^{-3}), best fit the feeding rate data from all three genotypes, and these two models perform equally well (ΔAIC < 1; Table 5.1). Because model 5 (*size and spores, linear*) is simpler, we refer to it as the "winning model" in the remainder of the text. We show best-fit predictions of this model in Fig. 5.1G–I (see Fig. C.1 for fits of all six models to data and Fig. C.3 for a regression of observed and predicted values from model 5).

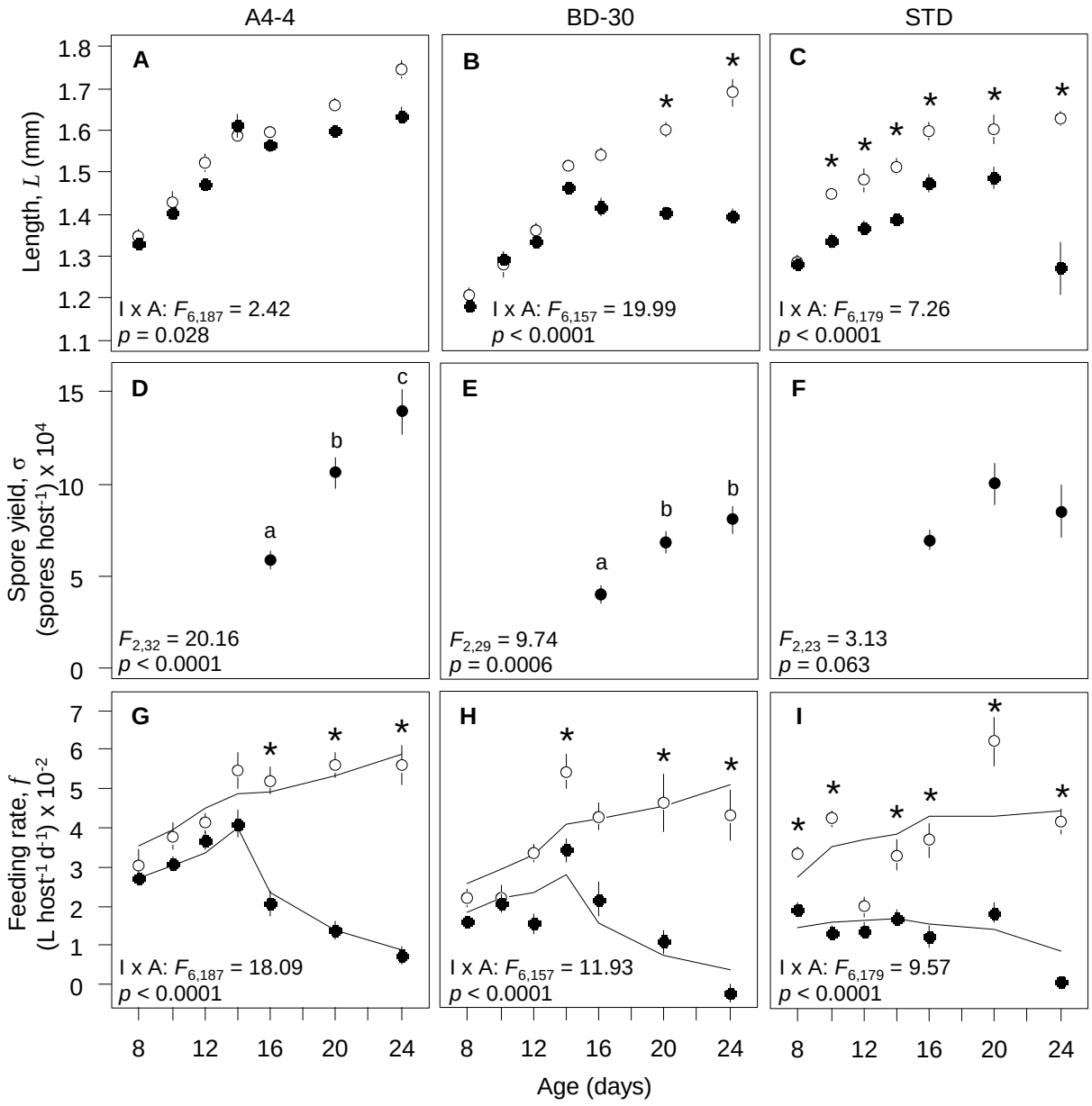

Figure 5.1. Body size, spore yield, and feeding rate results (mean ± SE) for infected (filled circles) and uninfected (open circles) hosts of three genotypes. Asterisks denote significant differences between infected and uninfected hosts. (A–C) Host size (length, *L*) generally increased with age, but infection stunted growth. (A,B) *A4-4 and BD-30*: Hosts at late stages of infection were smaller than same-aged uninfected hosts. (C) *STD*: Infected hosts were already smaller than their uninfected counterparts 2 days after spore exposure (i.e., at age 8 days). Infected hosts that survived to age 24 days (n = 3) were very small. (D–F) For the oldest three infected cohorts, spore yield (σ) either (D) increased with age (*A4-4*), (E) leveled off after age 20 days (*BD-30*), or (F) did not differ significantly with age (*STD*). (G–I) The winning foraging model (*size and spores, linear*) fit to observed feeding rates, *f*. (G,H) *A4-4 and BD-30*: The model correctly predicts the

increase in *f* with age for uninfected hosts and those at early stages of infection, as well as the decrease in *f* over later infection stages. (I) *STD*: The model captures the earlier divergence in *f* between infection classes in this genotype.

To illustrate the opposing effects of host size and spore yield on feeding rate, we parameterized the winning model with the best estimates of $\hat{f}_S$, $\hat{f}_I$, and b for each genotype, and predicted feeding rates over a realistic range of host lengths (L) and spore yields (σ) (Fig. 5.2). In the winning model, feeding rate of uninfected hosts (f_S) increases as simply the product of the feeding coefficient ($\hat{f}_S$) and size, L^2, because uninfected individuals contain no spores ($\sigma = 0$). This was the expected relationship for uninfected hosts. At early stages of infection (i.e., before spore growth is apparent), feeding rate of infected hosts (f_I) also increases in proportion to just L^2. However, for all three genotypes in our experiment, the best estimates of $\hat{f}_I$ were significantly lower than $\hat{f}_S$ (Fig. 5.3A, Table C.2). Thus, even when they contain few spores, infected hosts are predicted to have lower feeding rates than same-sized uninfected hosts. The difference between estimates of $\hat{f}_I$ and $\hat{f}_S$ was greatest for STD hosts (Fig. 5.3A); this reflects the earlier divergence in observed feeding rates of infected and uninfected STD hosts, compared to the other genotypes (Fig. 5.1I). Then, as the within-host density of spores (σL^{-3}) increases, feeding rates of infected hosts are further reduced; this describes the observed decrease in feeding rate over the oldest infection stages (Fig. 5.1G–I). The more gradual decrease in feeding rate with age for STD hosts, compared to the other genotypes, is captured by the lower estimate of the spore load coefficient (b) for STD hosts (Fig. 5.3B, Table C.1).

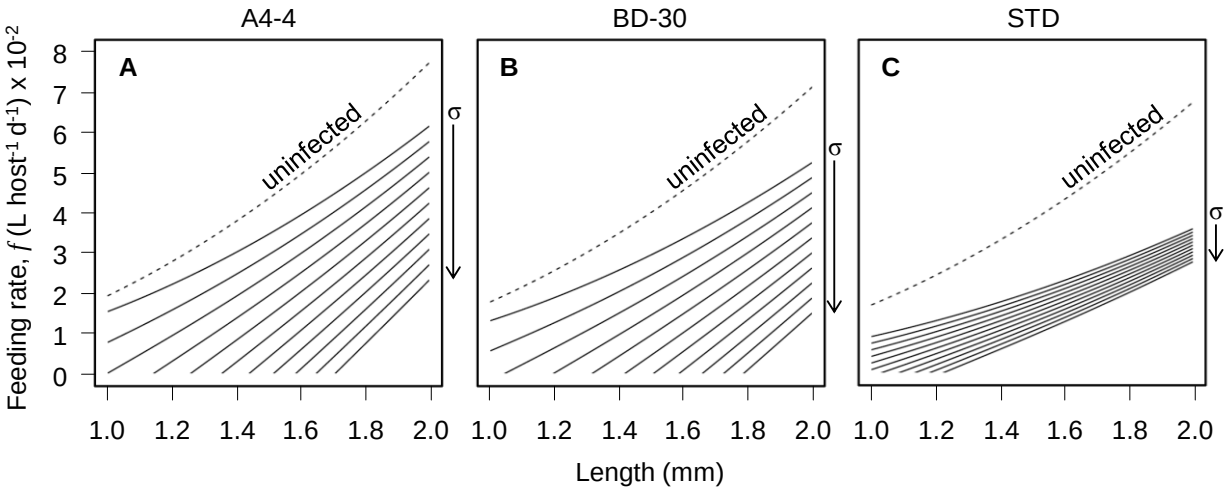

Figure 5.2. Illustration of how body size (length, L) and spore load (σ) influence feeding rate (f) in the winning foraging model (*size and spores, linear*), using best-fit parameter estimates for each genotype. Feeding rate (f) increases with L^2 for both uninfected (dashed curve) and infected (solid curves) hosts. Infected hosts have smaller values of the feeding rate coefficient ($\hat{f}$; Fig. 5.3A); thus, they have lower f than uninfected hosts of the same size, even before spore growth is apparent (top-most solid curve). Feeding rate is further reduced as a linear function of spores per host volume (σL^{-3}). The arrow indicates σ increasing from 0 to 200,000 spores host^{-1}.

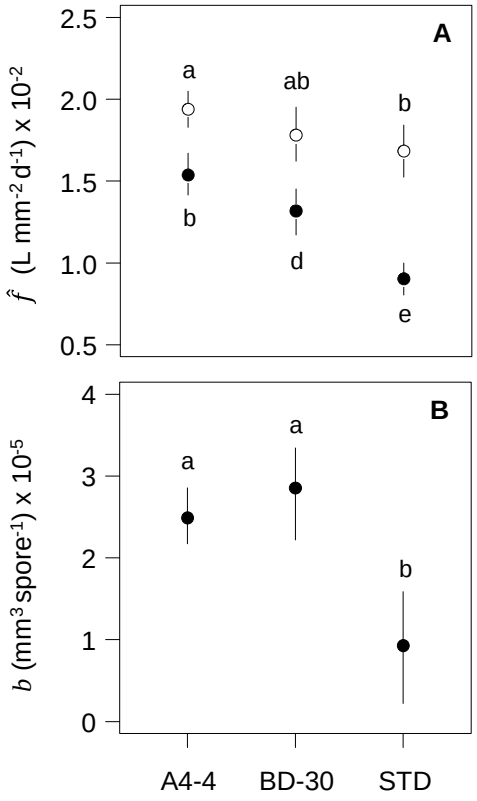

Figure 5.3. Best-fit parameter estimates for the winning foraging model (*size and spores, linear*), with bootstrapped 95% confidence intervals. Different letters indicate significant pairwise contrasts after Holm–Bonferroni correction. (A) Within each genotype, the feeding rate coefficient ($\hat{f}$) was lower for infected (filled circles) compared to uninfected (open circles) hosts. Within infection classes, $\hat{f}$ varied across genotypes. (B) There was a smaller reduction in feeding rate with spore load (i.e., a lower value of b) for STD hosts compared to the other genotypes.

Field survey

Field survey methods

We assessed the potential for disease to depress the average grazing rate of adults in natural populations during epidemics. To do this, we parameterized foraging models with best estimates of $\hat{f}$ and b for the three lab-reared genotypes (Fig. 5.3) and field-collected size and spore load data. We sampled 13 lakes in southern Indiana (Greene and Sullivan Counties, USA) weekly from August until the first week of December 2010. On each sampling visit, we collected a plankton sample containing three pooled tows of a Wisconsin net (13 cm diameter, 153 µm mesh, towed bottom to surface). From this sample, we estimated infection prevalence by diagnosing infection status of at least 400 live *D. dentifera* under a dissecting scope at 20–50X magnification, following Ebert (2005). We measured body length (L) of subsets of uninfected and infected adult hosts, as well as the average spore yield (σ) of a subset of infected hosts.

In particular, we wanted to estimate the potential disease-mediated reduction in average feeding rate from mechanisms other than a reduction in average host length. First, we estimated the average adult feeding rate for each lake-date assuming that infected and uninfected hosts differed only in body size. That is, we used model 2 (*size only*; Table 5.1), but we assumed $\hat{f}_I = \hat{f}_S$. Feeding rates of infected and uninfected hosts (f_I and f_S, respectively) were calculated using best estimates of $\hat{f}_S$ from the three genotypes in the feeding rate experiment (Fig. 5.3A) and lengths (L) of infected and uninfected hosts from the field survey. We averaged the estimates of f_I and f_S, weighted by the relative proportion of infected and uninfected hosts in the plankton sample. Second, we estimated average adult feeding rates using the winning foraging model (*size and spores, linear*). We parameterized this model using values of $\hat{f}_I$, $\hat{f}_S$, and b estimated for the three lab-reared genotypes (Fig. 5.3A,B) and field-collected length (L) and spore yield (σ) data. Then we calculated the difference between the first and second estimates

of average adult feeding rate, as a percentage of the estimate from the first model (i.e., *size only*, $\hat{f}_I = \hat{f}_S$).

Field survey results

As infection prevalence increased, the estimates of average adult feeding rate from the first model (*size only*, $\hat{f}_I = \hat{f}_S$; Fig. 5.4A–C) and the second model (*size and spores, linear*; Fig. 5.4D–F) increasingly diverged (Fig. 5.4G–I). On lake-dates with the highest levels of infection prevalence among adults (approximately 80% infected), our winning foraging model predicted that the average feeding rate of adult hosts could have been reduced by more than 0.01 L host^{-1} day^{-1} compared to an uninfected population with the same weighted average body size. That is, when epidemics were at their peak, average adult feeding rates may have been 30–40% lower than predicted by a model that assumed no effect of infection on $\hat{f}$ and no reduction in feeding rate with spore load. When adult infection prevalence was more moderate (approximately 40% infected), average feeding rates predicted by the winning foraging model were still 10–30% lower than expected from the *size only* model.

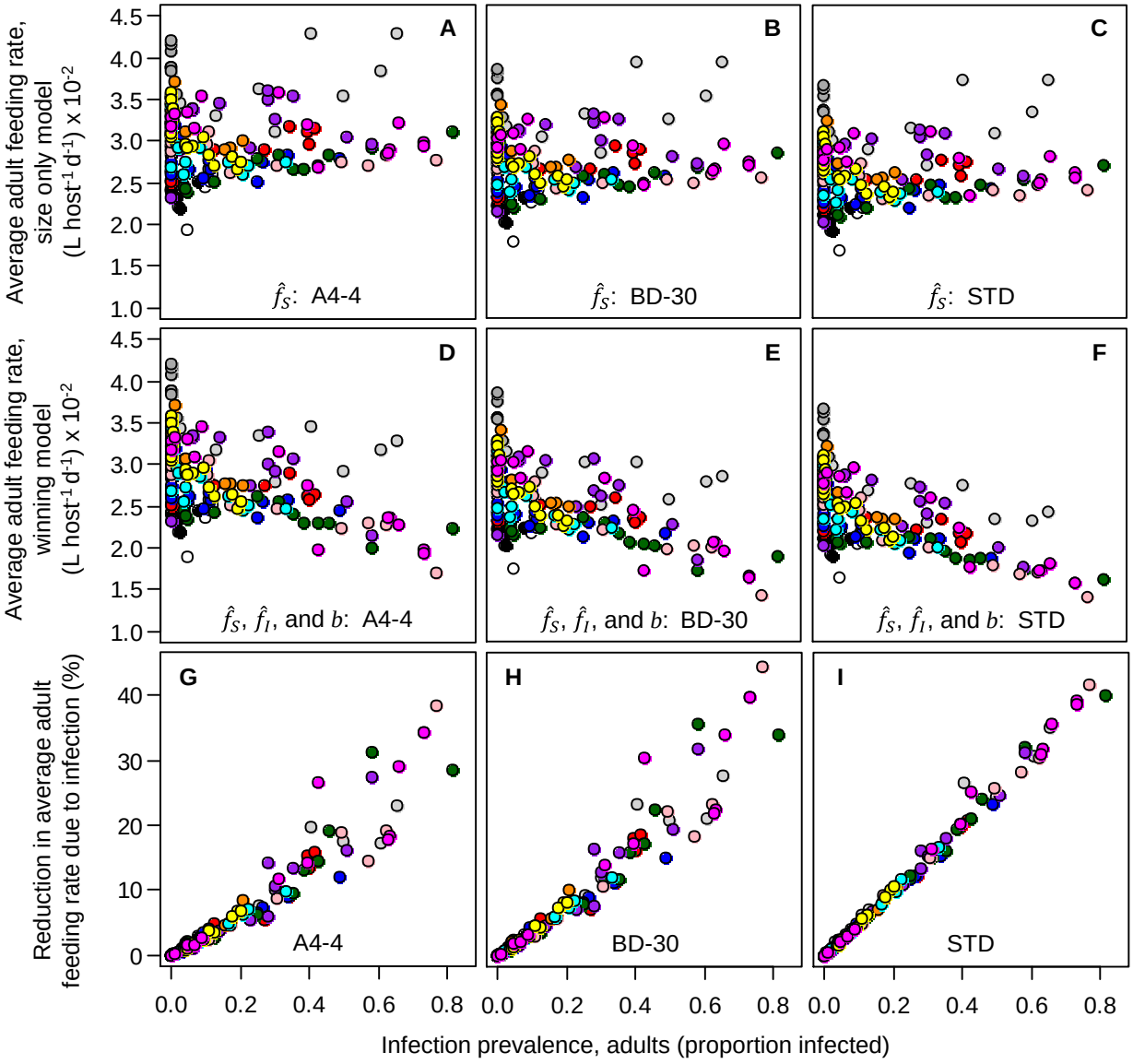

Figure 5.4. Estimates of average adult feeding rate (*f*) during epidemics in 13 lakes (grouped by color), calculated using field-collected infection prevalence, size, and spore load data, and values of $\hat{f}$ and *b* estimated for the three genotypes in the lab experiment. For each lake-date, average adult *f* was estimated using (A–C) a *size only* model that assumes no effect of infection on $\hat{f}$ (i.e., $\hat{f}_I = \hat{f}_S$), and (D–F) the winning foraging model (*size and spores, linear*), in which $\hat{f}_I < \hat{f}_S$. (G–I) On lake-dates with greater infection prevalence, the estimate from the winning model is increasingly reduced compared to the estimate from the *size only* model.

Dynamic epidemiological model

Model formulation

We investigated the potential for density- and trait-mediated indirect effects of disease using a dynamic model that tracks changes in densities of susceptible (*S*) and infected (*I*) hosts, free-living parasite spores (*Z*), and algal resources (*A*):

$$dS/dt = ef_S AS + \rho ef_I AI - dS - uf_S SZ \quad (5.1.a)$$

$$dI/dt = uf_S SZ - (d + v)I \quad (5.1.b)$$

$$dZ/dt = \sigma(d + v)I - mZ - f_S SZ - f_I IZ \quad (5.1.c)$$

$$dA/dt = rA(1 - A/K) - f_S SA - f_I IA \quad (5.1.d)$$

In the model, susceptible hosts (equ. 5.1.a) increase through births as susceptible and infected hosts consume algal resources at rates f_S and f_I, respectively, assuming a linear (type I) functional response, and convert algal carbon into new individuals at efficiency *e*. Infected hosts reproduce at a lower rate ($0 \leq \rho < 1$). Susceptible hosts are lost as they die at rate *d* or become infected through a density-dependent transmission process in which hosts are exposed to parasite spores at rate f_S (feeding rate), and subsequently become infected at rate *u* (per spore susceptibility). Infected hosts (equ. 5.1.b) increase as susceptible hosts become infected, and are lost at a higher than background death rate due to infection ($d + v$). Spores (equ. 5.1.c) are released into the environment at spore yield σ when infected hosts die, and are lost at background rate *m* and from consumption by susceptible hosts (at rate f_S) and infected hosts (at rate f_I). Algal resources (equ. 5.1.d) grow logistically, with maximal rate *r* and carrying capacity *K*, and decrease through consumption by susceptible and infected hosts (at rates f_S and f_I, respectively). We note that, though host body size is a key determinant of feeding rate for both infected and uninfected hosts (Figs 5.1 and 5.3, Table 5.1), size is implicit in this model. The model was parameterized using reasonable values for our system (Table 5.2).

Table 5.2. Variables and parameters used in simulations of the dynamic epidemiological model (equ. 5.1).

Symbol	**Units**	**Meaning**	**Value/range**
A	mg C · L^{-1}	Density of resource, in carbon (C) units	–
I	host · L^{-1}	Density of infected hosts	–
S	host · L^{-1}	Density of susceptible hosts	–
Z	sp. · L^{-1}	Density of spores (sp.)	–
t	day	Time	–
d	day^{-1}	Background mortality rate of susceptible hosts	0.05[a]
e	host · $(mg\ C)^{-1}$	Conversion efficiency of resource into hosts	25[b]
f_I	L · $host^{-1}$ · day^{-1}	Exposure (feeding) rate of susceptible hosts	range[c]: $0.74 – 1.5 \times 10^2$
f_S	L · $host^{-1}$ · day^{-1}	Exposure (feeding) rate of susceptible hosts	1.5×10^2
K	mg C · L^{-1}	Carrying capacity of resources; an index of productivity	5
m	day^{-1}	Loss rate of spores	0.8[d]
r	day^{-1}	Maximal growth rate of resource	1.0[e]
u	host · $spore^{-1}$	Per spore susceptibility of hosts (post exposure)	range[f]: $5 – 9 \times 10^{-4}$
v	day^{-1}	Elevated mortality due to infection	0.05[a]
ρ	–	Birth rate of infected relative to susceptible hosts	0.8[a]
σ	sp. · $host^{-1}$	Spores produced per host	range[c]: $0 – 1.5 \times 10^5$

[a] Typical values for a host genotype (Hall et al. 2010a).

[b] This value of e yields an instantaneous birth rate, b, of 0.375 day^{-1} for uninfected hosts at 1.0 mg C L^{-1} (where $b = ef_S A$); this is a reasonable value for a high quality resource for this host (Hall et al. 2010a).

[c] In Scenario 1 (Fig. 5.5A –C), $f_I = f_S = 0.0150$ L host^{-1} day^{-1} for all values of spore yield (σ). In Scenario 2 (Fig. 5.5D–F), f_I decreases linearly with σ according to the winning foraging model (model 5: s*ize and spores, linear*), using values of $\hat{f}_I$ and b estimated for the A4-4 genotype (scaled relative to $f_S = 0.015$ L host^{-1} day^{-1}), and assuming a body length of 1.5 mm. See Appendix C for a formulation of the model with resource-dependent spore production (equ. C.2.c and Fig. C.4).

[d] Assumes a high daily loss rate due to solar radiation (Overholt et al. 2012) and other sources (e.g., consumption by non-focal hosts: Hall et al. 2009a).

[e] A reasonable value for a fast-multiplying algal resource.

[f] These values of u yield infection risk (transmission rate, β) values in the range of 7.5 x 10^{-6} – 1.35 x 10^{-5} L · spore^{-1} · day^{-1} (where $\beta = uf_S$).

We studied the model using a simulation approach, using Matlab. We simulated the model for 1000 days, then used the average values of the state variables from t = 1000–2000 days (i.e., after an initial transient period) as 'equilibrium' values. In the first scenario, we assumed that feeding rates of susceptible and infected hosts were equal ($f_I = f_S$). This allowed us to investigate the potential for density-mediated indirect effects of disease on resources. In the second scenario, we assumed that feeding rate of infected hosts (f_I) decreased linearly with spore yield (σ) as in the winning foraging model (model 5: s*ize and spores, linear*), using values of $\hat{f}_I$ and b estimated for the A4-4 genotype (Table 5.2). This second scenario allowed us to explore whether disease could have trait-mediated indirect effects on resources, through a reduction in feeding rate of infected hosts. In both scenarios, we simulated the model over a range of values of spore yield (σ) and per spore susceptibility (u). By increasing either σ or u, we were able to elevate the transmission potential of the parasite. In Appendix C, we study a version of the model (scenarios 1 and 2) in which spore production is resource-dependent (see equ. C.2.c). Results of that model (see Fig. C.4) were consistent with those presented here.

Model results

When feeding rates of infected and uninfected hosts were the same ($f_I = f_S$; scenario 1), increasing transmission potential by increasing either spore production (σ) or per spore susceptibility (u) caused a density-mediated indirect effect (DMIE) on resources (Fig. 5.5A–C). Infection prevalence increased with increasing values of either σ or u (Fig. 5.5A). Because infected hosts had higher mortality and lower birth rates than their uninfected counterparts, the increase in prevalence caused a decrease in host density (Fig. 5.5B). This reduction in host density, in turn, allowed resource density to increase (Fig. 5.5C).

When we assumed that feeding rate (f_I) decreased as a linear function of spore load (σ; scenario 2), disease could indirectly increase resource density through a trait-mediated indirect effect (TMIE; Fig. 5.5D–F). Infection prevalence increased with transmission potential, but the proportion infected at a given value of σ and u was slightly higher than in the first scenario (Fig. 5.5D compared to Fig. 5.5A). This amplification of disease occurred because infected hosts consumed and removed fewer spores from the water, leaving more spores to infect susceptible hosts. In the second scenario, host density increased with transmission potential (Fig. 5.5E). This result is explained by a TMIE of disease on resources. With a greater proportion of infected hosts in the population, the average grazing rate was lower, so there were more resources available per host (Fig. 5.5F). This greater resource abundance then fuelled higher birth rates. Thus, by altering a key host trait (feeding rate), the parasite indirectly boosted its own transmission rate, as well as densities of both resources and hosts.

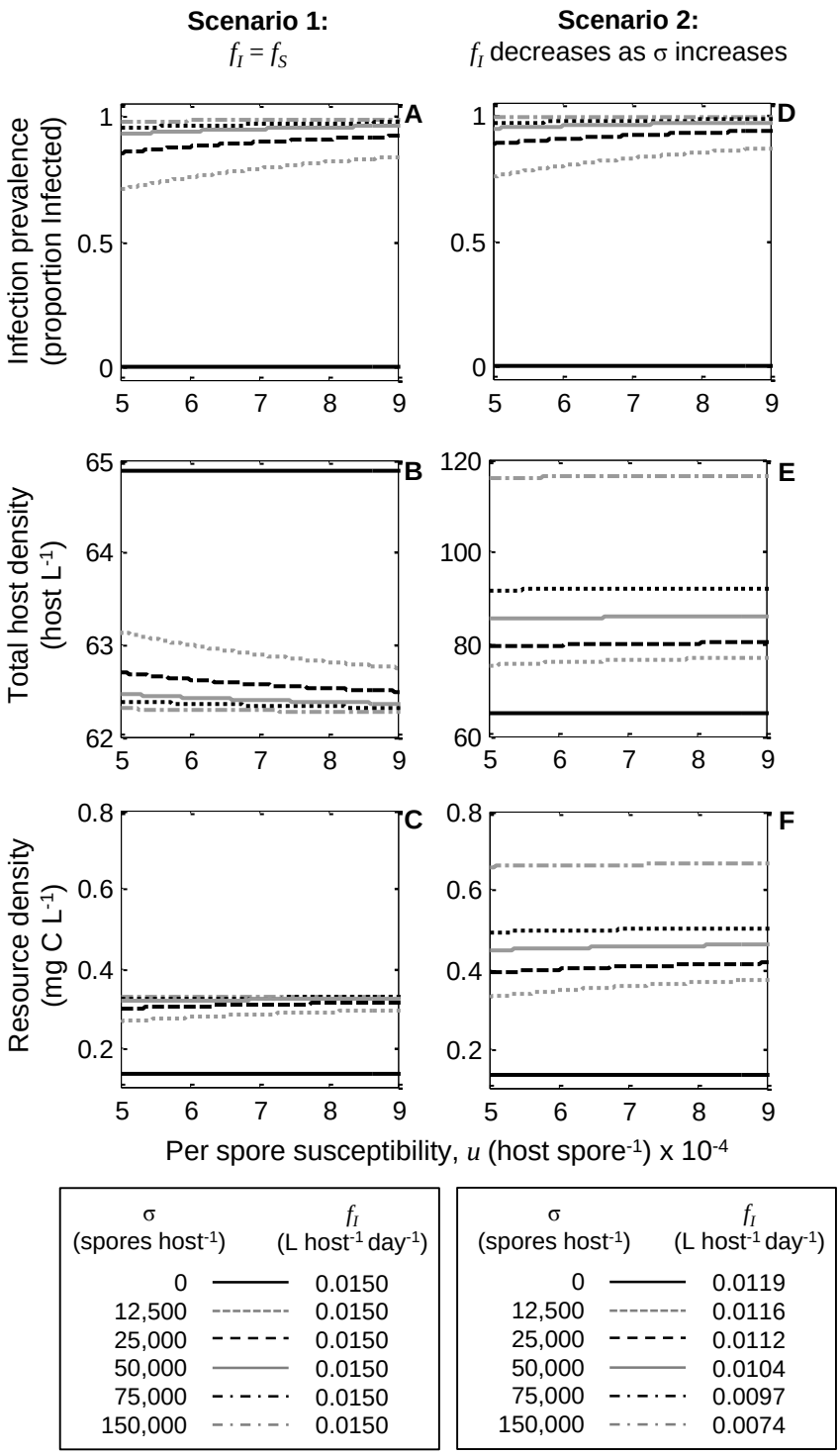

Figure 5.5. Equilibrium results of the dynamic epidemiological model over a range of values of per spore susceptibility, u (x-axis) and spore yield, σ (contours). (A–C) *Scenario 1, DMIE:* infection does not alter feeding rate ($f_I = f_S$). As u or σ increases, (A) infection prevalence increases, (B) host density decreases, and (C) resource density

increases. (D–F) *Scenario 2, TMIE:* feeding rate of infected hosts (f_I) decreases linearly with spore yield (σ). As u increases, or as f_I decreases with increasing σ, (D) infection prevalence increases to higher levels than in Scenario 1 because infected hosts remove fewer spores from the water. In contrast to Scenario 1, (E) host density increases with infection prevalence because the average grazing rate of the population decreases, (F) allowing resource density to increase.

Discussion

Parasites can indirectly affect populations, communities, and ecosystems by altering host traits (Hernandez and Sukhdeo 2008a, Lefèvre et al. 2009). In this study, we showed that a fungal parasite of *Daphnia* can strongly decrease host foraging rate, which is a key ecological and epidemiological trait. The model of foraging rate that best fit our experimental results included effects of body size and spore load. Specifically, feeding rate increased with body size more gradually for infected compared to uninfected hosts, and feeding rate was further reduced as parasite reproduction filled infected hosts with spores. By informing this winning foraging model with field-collected body size and spore load data, we showed that the average per capita feeding rate of adult hosts in natural populations might decrease substantially during epidemics. Simulations of a dynamic epidemiological model revealed that, if the parasite has no effect on host feeding rate, disease should decrease host density through negative effects on fecundity and survivorship, resulting in greater resource density (i.e., a DMIE). However, when the parasite reduces host foraging rate as observed in the lab experiment, the model predicts that disease should increase densities of both resources and hosts (i.e., a TMIE). Host density can increase with disease because the positive TMIE on resources increases the per capita birth rate of hosts. The increase in birth rate due to relaxed competition for food exceeds the direct negative effects of the parasite on host fecundity and mortality, so epidemics can increase the density of hosts (Washburn et al. 1991). This mechanism may

be considered a type of 'hydra effect', in which an increase in per capita mortality rate drives an increase in population density (Abrams 2009). In addition, because infected hosts remove spores from the water at a lower rate, transmission to susceptible hosts can increase when the average feeding rate of hosts decreases. That is, infected hosts are less likely to reduce disease through a dilution effect (Hall et al. 2009a, Keesing et al. 2010).

Given that foraging rate is central to both ecology and epidemiology, we need to know what drives variation in this trait to understand how energy and nutrients flow through food webs, and to better predict diseases in nature. What drives infection-related declines in host feeding rate? One possible explanation is that feeding appendages may be mechanically inhibited when within-host spore density is high. However, for one of the host genotypes in our lab experiment, feeding rate was significantly reduced many days before spore growth was apparent. Plausible reasons for this early reduction in feeding rate include diversion of energy from foraging to other functions of the host (e.g., fighting or tolerating infection) or to functions of the parasite (e.g., replication; Hall et al. 2009c). The rate at which *Daphnia* forage also depends on factors including resource density (Hall et al. 2007b, Sarnelle and Wilson 2008) resource quality (Demott et al. 1991, Rohrlack et al. 1999, Darchambeau and Thys 2005, Penczykowski et al. in review), and concentrations of pollutants in the environment (Civitello et al. 2012). Future studies could assess whether feeding rates of infected and uninfected hosts converge or diverge over gradients of these environmental variables. In addition, when host density is high, per capita feeding rate can be inhibited through foraging interference (Civitello et al. 2013a). Because our dynamic epidemiological model predicts that host density could increase with epidemic size in the TMIE scenario, future work should explore the potential effects of foraging interference under those conditions.

Variation in feeding rate could have implications at the level of individual hosts and parasites, as well as for communities and ecosystems. It is possible that some of the negative consequences of infection for individual hosts could be the result of reduced

feeding rate. For example, we know that body size partly determines feeding rate, and that infected hosts generally do not grow as large as uninfected hosts (Hall et al. 2007b, Hall et al. 2009b). Perhaps a reduction in feeding rate at early stages of infection, and thus a reduction in energy intake, helps explain the stunted growth of infected hosts (Hall et al. 2009c). Future studies using dynamic energy budget models will address this possibility, as well as the potential for low rates of energy intake to contribute to reductions in fecundity and survivorship of hosts. At the level of communities and ecosystems, we need to assess whether the large increases in resource and host densities predicted by our model could occur in nature. For instance, our model does not take into account the potential for nutrient limitation of algal resources. In a large population of *Daphnia* with high infection prevalence (as predicted by our model), a large biomass of nutrients might be in host and parasite tissue, and thus, unavailable to algae. In particular, high densities of phosphorus (P)-rich *Daphnia* could lead to P-limitation of algae (Elser and Urabe 1999). Parasites can account for a substantial proportion of total biomass in ecosystems (Kuris et al. 2008); thus, depending on the nutrient content of parasite tissue, sequestration of nutrients by parasites could contribute to nutrient limitation of algae.

To understand the impacts of parasites on populations, communities, and ecosystems, we need to uncover effects of disease on host traits as well as densities. In the focal *Daphnia*–fungus system, we showed that disease could lead to large reductions in the average feeding rate of adult hosts. This might lead to greater densities of resources and hosts, and could also diminish the ability of infected hosts to remove infectious propagules from the environment. These trait-mediated indirect effects of disease could have major implications for the flow of energy and nutrients through food webs, as well as for the spread of disease.

CHAPTER 6

CONCLUSIONS AND FUTURE DIRECTIONS

Conclusions

In light of ongoing and predicted global changes to climate and land use, there is much interest in determining how these changes impact the distribution and severity of infectious diseases (e.g., Patz et al. 2004, Lafferty 2009), as well as how they impact ecosystem functioning (e.g., Smith 2003, van de Waal et al. 2010). The consequences for diseases and ecosystems are typically considered separately. Here, I argue that in order to better predict the response of ecosystems to 'global change' (including, but not limited to, altered climate and land use; MEA 2005), we need to understand both 1) how diseases are affected by environmental alteration, and 2) how diseases may modulate the response of ecosystems to drivers of change. Below, I address the contributions of my dissertation to these two areas of research. I also discuss other themes that resonate throughout my dissertation.

My dissertation research uncovered multiple mechanisms by which modification of ecosystems – in particular, alterations to habitat structure or nutrient availability – can influence the spread of disease. In Chapter 2, I illustrated indirect links from two different aspects of habitat structure to disease, mediated by densities of two different non-host species. Deeper lakes had larger refuges from predation for a 'diluter' species that removes parasite spores from the environment (Hall et al. 2009a); this pathway correlated with later, smaller epidemics. In a second pathway, lakes with stronger stratification had greater densities of a 'sloppy predator' that spreads disease by releasing spores into the environment (Cáceres et al. 2009); this pathway correlated with larger epidemics. The results of this field study are also consistent with direct links from stratification strength and its physical driver (light penetration) to disease. In Chapter 3, I showed how

environmental changes that lead to the growth of poor quality resources might diminish the transmission potential of certain parasites. In the focal study system, this occurred because lower quality resources inhibited host foraging rates, and thus the rate of exposure to parasite spores. Finally, environmental changes may interact to affect the spread of disease. In the mesocosm experiment featured in Chapter 4, nutrient enrichment and disruption of habitat structure (i.e., water column mixing) interacted to enhance the spread of disease. The high nutrient manipulation also fueled greater densities of infected hosts.

These effects of environmental change on disease matter not only for host populations, but also for food webs and ecosystems. In Chapter 4, epidemics led to reductions in host density which had indirect positive effects on resource abundance. This parasite-mediated trophic cascade was most apparent in the low nutrient manipulation; in high nutrient enclosures, hosts remained abundant enough to suppress algae. Due to the greater reductions in host density in the low nutrient treatment, epidemics caused total phosphorus concentrations to converge over time between enclosures in the high and low nutrient treatments. Moreover, the nutritional quality of algae (measured as P:C) improved during epidemics. These results suggest that disease might influence how ecosystem productivity and stoichiometry respond to nutrient enrichment. In addition to the parasite-mediated decrease in host density that I observed in this mesocosm experiment, it is possible that infection altered other host traits, such as foraging rate. In Chapter 5, I measured strong reductions in feeding rates of infected hosts in a laboratory experiment. Then I developed a mechanistic mathematical model that captured these observed effects. By building this model of foraging reduction into a dynamic epidemiological model, I showed that disease could have large trait-mediated indirect effects on resources, and these positive effects on resources could then fuel greater host densities. Given the evidence for density- and trait-mediated indirect effects of disease on

resources in this system, it is possible that disease influences how lake ecosystems respond to changes in climate and the surrounding landscape.

The importance of host foraging rate was a recurring theme in my dissertation. Foraging rate is central to both the ecology and epidemiology of the focal *Daphnia*-fungus-algae system, and I showed that this trait was influenced by resources (Chapter 3) as well as by infection (Chapter 5). As discussed above, this parasite could indirectly increase abundances of resources and hosts by reducing host feeding rate (i.e., an ecological role of foraging). Additionally, host feeding rate determines the rate of parasite exposure and may ultimately govern the supply of energy for both host and parasite (Hall et al. 2007b, Hall et al. 2009c). Hence, it is a key epidemiological trait, as demonstrated experimentally in Chapter 3. Modeling results in Chapter 5 also showed how a reduction in feeding rate of infected hosts could lead to enhanced transmission to susceptible hosts, since infected hosts are less able to 'dilute' disease by removing spores from the water (Keesing et al. 2006, Hall et al. 2009a).

Another theme in my dissertation was that host density did not drive infection prevalence as expected for parasites with density-dependent transmission (Anderson and May 1992). In Chapter 2, there was no correlation between average host density and epidemic size across lakes. In Chapter 4, there was also no significant overall correspondence between host density and epidemic size. These results are consistent with other studies in this *Daphnia*-fungus system (Cáceres et al. 2006, Civitello et al. 2013a), and highlight the importance of studying details of the transmission process (e.g., Hall et al. 2007b, Civitello et al. 2013a) as well as community-level drivers of disease. In addition, the between-year field patterns in Chapter 4 hint that, for certain epidemiological questions, infected host density may be a better index of 'epidemic size' than metrics based solely on infection prevalence.

Future directions

We are only beginning to understand the roles of parasites in ecosystems. Few studies have attempted to quantify energy or nutrient fluxes through parasites (Bailey 1975, Sato et al. 2011), and a comprehensive study of how parasites alter the movement of both energy and nutrients through multiple levels of biological organization (i.e., from individuals to ecosystems) has not been published to date. However, recent advances in three areas of biology have paved the way for further investigations of how parasites affect flows of energy and nutrients through ecosystems: 1) the inclusion of parasites in food webs (Lafferty et al. 2006, Hernandez and Sukhdeo 2008b, Lafferty et al. 2008, Hechinger et al. 2011, Preston et al. 2012), 2) progress in linking the biochemical basis and food web consequences of ecological stoichiometry (Sterner and Elser 2002, Allen and Gillooly 2009, Hall 2009), and 3) developments in the theory and interpretation of dynamic energy budget models (Kooijman 2010, Nisbet et al. 2012).

The few published food webs that include parasites reveal that parasites can feature in a substantial percentage of all trophic links (Lafferty et al. 2006, Preston et al. 2012). Parasites obtain energy and nutrients from their hosts, and are consumed by both host and non-host consumers (Duffy et al. 2005, Lagrue et al. 2007, Johnson et al. 2010a). Including parasites in food webs affects metrics including connectance, trophic chain length, average interaction strength, and consumer-resource body size relationships, and these effects on food web structure have consequences for ecosystem stability, resilience, and robustness (Thompson et al. 2005, Arias-Gonzalez and Morand 2006, Hernandez and Sukhdeo 2008b, Lafferty et al. 2008, Lafferty and Kuris 2009a, Warren et al. 2010, Niquil et al. 2011). In addition to elucidating trophic links to parasites, recent studies have documented that parasites comprise a significant, and historically overlooked, proportion of total biomass in some ecosystems (Kuris et al. 2008). Because parasites are abundant and alter food web topology, it is reasonable to assume that they affect the flow of both energy and nutrients through ecosystems. However, we know little

about the magnitude of energy or nutrient fluxes through parasites (Tompkins et al. 2011).

Parasites can alter host energy and nutrient content by consuming internal host resources and by causing hosts to allocate resources to immunity or repair (Careau et al. 2010). By replacing host tissue with parasite tissue or altering allocation of host energy and nutrients, parasites can alter within-host nutrient stoichiometry (Forshay et al. 2008, Frost et al. 2008a). Ecological stoichiometry theory tells us that mismatches in nutrient ratios between consumers and resources affect consumer growth rates as well as rates at which nutrients are assimilated, egested, and excreted (Elser and Urabe 1999, Sterner and Elser 2002, Frost et al. 2004, Anderson et al. 2005). Therefore, effects of parasites on host stoichiometry may affect the quality of hosts as prey items, host feeding and assimilation rates, and rates and ratios at which nutrients are returned to the environment in waste products. The stoichiometry of organisms depends on their nutrient needs for structure and growth, which vary across species and life stages. For example, the "growth rate hypothesis" predicts that organisms with faster growth rates should have higher phosphorus contents, because their fast growth requires more phosphorus-rich ribosomal RNA (rRNA) for protein synthesis (Hessen and Lyche 1991, Elser et al. 1996). Thus, we might expect that variation in parasite life history strategy could entail differences in allocation to rRNA, with implications for parasite stoichiometry and nutrient fluxes.

To investigate the potential for parasites to alter energy and nutrient flows at the ecosystem level, we must first determine how energy and matter flux through individual hosts and their parasites. Dynamic energy budget (DEB) models are powerful tools for modeling flows of energy and nutrients through organisms over time (Kooijman 2010). DEB theory is built on thermodynamic and stoichiometric principles that underlie the physiology of all organisms (Vrede et al. 2004). Within the general DEB framework, models can be parameterized to investigate energy and nutrient allocation to physiological processes in specific organisms (Hall et al. 2006a, van der Meer 2006,

Kooijman et al. 2008, Saraiva et al. 2011). These models can be used to relate biochemical stoichiometry to physiological processes that, when scaled up from individuals to populations, influence energy transfer and nutrient cycling at the ecosystem level (Nisbet et al. 2000, Vrede et al. 2004).

In future research, I intend to use an approach integrating ecological stoichiometry, host-parasite DEB models, and empirical food webs to mechanistically model the fate of energy and nutrients ingested by infected hosts, from the level of individual hosts and parasites to entire ecosystems. Key questions include for future studies include:

1) How does stoichiometry of parasite tissue differ from that of hosts? Is variation in parasite stoichiometry across species and life stages consistent with theoretical predictions from ecological stoichiometry and DEB theory (Elser et al. 1996, Sterner and Elser 2002, Vrede et al. 2004)?
2) How do parasites affect feeding rates and ratios of nutrients recycled from hosts? What are the consequences of these altered host traits for primary producers?
3) At the ecosystem level, do parasites affect long-term averages of energy or nutrients at different trophic levels, or the availability of nutrients to primary producers?

These questions could guide a comprehensive study of how energy and nutrients flow through food webs with parasites. This would be an important step in assessing how parasites might modulate the response of ecosystems to global change.

APPENDIX A

SUPPLEMENT TO CHAPTER 3

Here, we provide methods used to determine the nutrient content of the two resource species, and a table of their carbon:nitrogen:phosphorus (C:N:P) ratios (Table A.1). We also give methods for the preparation of food treatments used in the second experiment. In addition, we describe statistical methods used to estimate components of transmission potential, and provide a table of *P*-values for pairwise contrasts of those parameters between food treatments (Table A.2).

Additional methods

Nutrient content of food

We assessed whether elemental nutrient stoichiometry (i.e., C:N:P) drove differences in food quality in the first experiment. To determine C:N:P of the two food species, we collected stationary phase samples of the high quality (*Ankistrodesmus falcatus*) and low quality (*Microcystis aeruginosa*) phytoplankton onto precombusted filters (GF/F, 0·7 µm pore size, Whatman, Piscataway, NJ, USA). C and N content (five replicates each) were measured on a 2400 series CHN analyzer (Perkin Elmer, Waltham, MA, USA). P content (three replicates) was measured on a UV-1800 spectrophotometer (Shimadzu Scientific Instruments, Columbia, MD, USA) using the ascorbic acid method following persulfate digestion (APHA 1995). We compared nutrient ratios between the two food species using one-tailed two sample t-tests with equal variances (Table A.1). In both experiments, food levels were standardized to C content based on absorbance (750 nm)–C regressions for each species.

Microcystis extraction, fractionation, and coating of food

In the second experiment, we tested whether protease inhibitors (or other chemical compounds) in the low quality food (*M. aeruginosa* strain NIVA-Cya 43) could have driven its effects on transmission potential in the earlier experiment. To do this, we extracted material from *M. aeruginosa* cells (using methods adapted from von Elert et al. [2012]), and verified that it contained nostopeptin BN920 (Ploutno and Carmeli 2002) and cyanopeptolin CP954 (von Elert et al. 2005). These two compounds inhibit digestive proteases (chymotrypsins) of a related zooplankter, *Daphnia magna* (von Elert et al. 2012). We created food treatments by coating the extracted material onto high quality *A. falcatus*, as described below. By using *A. falcatus* as a substrate, we could isolate effects of the focal compounds while controlling for other factors, such as cell morphology or nutritional content.

Lyophilised *M. aeruginosa* (0·87 g dry mass) was exhaustively extracted in methanol (MeOH). We separated this crude extract on a reversed-phase C_{18} silica gel column (10 g Supelclean ENVI-18 SPE, Supelco, Bellefonte, PA, USA) using a stepwise MeOH/H_2O mobile phase (20%, 40%, 60%, 80%, and 100% aqueous MeOH, ending with a 100% ethyl acetate wash). This yielded six fractions that differed in polarity. To determine which fraction(s) contained the compounds of interest, we used liquid chromatography–mass spectrometry. We analysed each fraction at 1 mg mL^{-1} with a Waters 2695 high performance liquid chromatograph coupled to a Waters 2996 photodiode array UV detector and a Waters Micromass ZQ 2000 mass spectrometer (Waters Corporation, Milford, MA, USA). A Grace Alltima C_{18} silica gel column (Grace Alltech, Deerfield, IL, USA) was employed with a gradient of 30% to 100% aqueous acetonitrile (with 0.1% acetic acid), and the focal compounds were detected via positive and negative electrospray ionisation modes (mass-to-charge ratios: BN920: m/z = 921.5; CP954: m/z = 955.4). We estimated the relative abundance of the focal compounds across the six fractions by comparing integrated mass peak areas for each molecular ion.

Approximately 90% of both compounds was contained in the fractions eluted with 60% and 80% MeOH, and the remaining 10% was in the fractions eluted with 20% and 40% MeOH.

We pooled the 60% and 80% MeOH fractions and coated them onto lyophilised *A. falcatus* cells using dimethyl sulfoxide (DMSO) as a carrier solvent; this became our "extract" food treatment. The amount of material extracted from 1 mg C of *M. aeruginosa* was coated onto each 1 mg C of *A. falcatus*. The "control" diet consisted of *A. falcatus* coated only with DMSO. We also coated *A. falcatus* with the pooled 20% and 40% MeOH or pooled 100% MeOH and 100% ethyl acetate fractions; these two treatments did not affect any of the components of transmission potential (R.M. Penczykowski, unpublished data). To minimize degradation of the food treatments over the course of the experiment, we prepared aliquots for each day. The aliquots were lyophilised to remove the DMSO, stored at -20 °C, and rehydrated in Artificial *Daphnia* Medium (ADaM; Klüttgen *et al.* 1994) immediately before being fed to hosts.

Statistical methods for estimating parameters

In the first experiment, we estimated components of infection risk (transmission rate, β) by simultaneously fitting models to our infection data and feeding rate data (Bertram et al. 2013). The two model fits had separate likelihood values, which we added together to estimate parameters, as described below. To the infection data, we fitted the dynamical transmission model (equ. 3.1), where β was broken down into its constituent parts (per spore infectivity, *u*, and feeding rate, *f*, both of which increase with surface area, $L_\beta^{\,2}$; equ. 3.2):

$$dS/dt = -\hat{u}\hat{f}L_\beta^4 SZ \qquad \text{(A.1.a)}$$

$$dI/dt = \hat{u}\hat{f}L_\beta^4 SZ \qquad \text{(A.1.b)}$$

$$dZ/dt = -\hat{f}L_\beta^2 (S+I)Z. \qquad \text{(A.1.c)}$$

This model (equ. A.1) can be solved analytically to give the predicted proportion of hosts infected, *p*, at the end of the spore exposure period of duration t_β :

$$p = \frac{I(t_\beta)}{N} = 1 - exp\left(\hat{u}L_\beta^2\left(\frac{Z(0)}{N}\right)\left(exp\left(-\hat{f}L_\beta^2 N t_\beta\right) - 1\right)\right), \quad \text{(A.2)}$$

where *N* and *Z*(0) are initial densities of hosts and spores, respectively, in the infection assays, and $N = S + I$ is fixed. The binomial-based likelihood function for the infection process is:

$$\ell_\beta = \binom{N}{I} p^I (1-p)^{N-I}, \quad \text{(A.3)}$$

where *I* is the density of infected hosts at the end of the experiment.

We simultaneously estimated size-corrected feeding rate, $\hat{f}$, by fitting a natural log-transformed version of a standard formula for calculating foraging-based "clearance rate" (Sarnelle and Wilson 2008):

$$\log(C_t) = \log(C_0) - ft/V + \varepsilon, \quad \text{(A.4)}$$

where C_t is the concentration of algae remaining at the end of the grazing period of length *t*, C_0 is the concentration of algae in ungrazed reference tubes at the end of the grazing period, $f = \hat{f}L_\beta^{\,2}$ (with size-corrected feeding rate $\hat{f}$ and body length L_β during the feeding assay), *V* is the volume of medium in the tube, and errors (ε) were assumed to be normally distributed. Fitting this model (equ. A.4) produced likelihood values for feeding rate, ℓ_f . Then we estimated the parameters $\hat{u}$ and $\hat{f}$ by minimizing the sum of the two negative log-transformed likelihoods, ℓ_β and ℓ_f .

To summarize, we simultaneously fit two datasets (infection and "clearance rate") to obtain point estimates (with bootstrapped 95% confidence intervals) for size-corrected per spore susceptibility, $\hat{u}$, and size-corrected feeding rate, $\hat{f}$. Using these estimates, we could then calculate (with bootstrapped 95% confidence intervals) the effective per spore

susceptibility, *u*, as the product of $\hat{u}$ and mean length at infection squared ($L_\beta{}^2$); the rate of spore exposure, *f* as the product of $\hat{f}$ and $L_\beta{}^2$; and total infection risk, β, as the product of *u* and *f*. In Figure 3.2, we show how these constituent parameters combine to form infection risk (β). Finally, we calculated transmission potential as the product of β and spore yield (σ), and bootstrapped over the infection and spore yield data to generate 95% confidence intervals (Fig. 3.3).

In the second experiment, we tested whether the cyanobacterial extract affected overall transmission potential ($\beta\sigma$), but we did not tease apart the two components of infection risk (*u* and *f*). Thus, we estimated β by fitting only the transmission model to the infection data, and bootstrapped over the infection and spore yield data to generate 95% confidence intervals for transmission potential ($\beta\sigma$; Fig. 3.4).

In Tables A.2 and A.3, we present *P*-values for pairwise contrasts of these parameters between food treatments in the first (Figs 3.1, 3.2, and 3.3) and second experiments (Fig. 3.4), respectively. We performed 9999 randomizations of the datasets in each contrast (Gotelli and Ellison 2004).

Table A.1. Molar ratios (mean ± 1 SD) of carbon (C), nitrogen (N), and phosphorus (P) in the two food species. High quality *A. falcatus* had significantly higher C:N, C:P, and N:P compared to low quality *M. aeruginosa* (two sample *t*-test for each ratio, all $P <$ 0·0001). These results mean that nutrient (N and P) content of the two phytoplankton resources was high; thus, stoichiometric composition of the two resources did not explain differences in their nutritional quality (Sterner and Hessen 1994, Urabe et al. 1997).

Quality: Food species	**C:N**	**C:P**	**N:P**
High quality: *Ankistrodesmus falcatus*	7·85 ± 0·13	46·08 ± 0.83	5·87 ± 0·13
Low quality: *Microcystis aeruginosa*	6·22 ± 0·05	23·21 ± 0·45	3·73 ± 0·07

Table A.2. *P*-values for comparisons of parameter estimates between food quality manipulations in the first experiment (Figs 3.1, 3.2, and 3.3). Bolding denotes significant pairwise differences after Holm–Bonferroni correction.

		Food quality manipulation		
Parameter	**Symbol**	**High vs. High-to-low**	**High-to-low vs. Low**	**High vs. Low**
Infection risk (Fig. 3.1B)	β	**0·0005**	0·30	**< 0·0001**
Size at exposure (Fig. 3.1C)	L_β	1·0	**< 0·0001**	**< 0·0001**
Size-corrected exposure rate (Fig. 3.2A)	$\hat{f}$	**0·0001**	**< 0·0001**	**< 0·0001**
Exposure rate (Fig. 3.2B)	f	**< 0·0001**	**0·0027**	**< 0·0001**
Size-corrected per spore susceptibility (Fig. 3.2C)	$\hat{u}$	1·0	0·44	0·50
Per spore susceptibility (Fig. 3.2D)	u	1·0	0·099	**0·015**
Transmission potential (Fig. 3.3D)	$\beta\sigma$	**< 0·0001**	0·061	**0·0001**

Table A.3. *P*-values for comparisons of parameter estimates between food quality manipulations in the second experiment (Fig. 3.4). There were no significant pairwise differences after Holm–Bonferroni correction.

		Food quality manipulation		
Parameter	**Symbol**	**Control vs. Control-to-extract**	**Extract vs. Control-to-extract**	**Control vs. Extract**
Infection risk (Fig. 3.4B)	β	0·087	0·058	0·97
Size at exposure (Fig. 3.4C)	L_β	N/A[†]	N/A	0·18
Transmission potential (Fig. 3.4F)	$\beta\sigma$	0·020	0·040	0·65

[†]N/A indicates that there is no associated pairwise comparison

APPENDIX B

SUPPLEMENT TO CHAPTER 4

In this Appendix, we show results for total phosphorus (TP) and the edible size fraction of chlorophyll *a* over the course of the mesocosm experiment. The change in TP over time depended on the nutrient and spore exposure manipulations (Nutrients: $F_{1,21}$ = 16.48, p = 0.0006; Mixing: $F_{1,21}$ = 0.33, p = 0.57; Spores: $F_{1,21}$ = 0.21, p = 0.65; Date: $F_{1,355}$ = 275.4, p < 0.0001; Nutrients*Spores*Date: $F_{1,355}$ = 4.14, p = 0.043; Fig. B.1). In bags without disease, adding larger pulses of nitrogen and phosphorus (i.e., the high nutrient treatment) increased TP relative to the low nutrient treatment, as anticipated (Fig. B.1A). However, in bags that had epidemics, there was less of a difference between TP in the high and low nutrient manipulations (Fig. B.1B). This result suggests that disease may affect how systems respond to nutrient enrichment.

The abundance of algae (indexed as chlorophyll *a*) in the edible size fraction varied over time through interactions between the nutrients, mixing, and parasite treatments (Nutrients: $F_{1,21}$ = 0.046, p = 0.83; Mixing: $F_{1,21}$ = 0.067, p = 0.80; Spores: $F_{1,21}$ = 0.30, p = 0.59; Date: $F_{1,352}$ = 75.95, p < 0.0001; Nutrients*Date: $F_{1,352}$ = 12.85, p = 0.0004; Nutrients*Mixing*Date: $F_{1,352}$ = 5.24, p = 0.023; Nutrients*Spores*Date: $F_{1,352}$ = 7.01, p = 0.0085; Mixing*Spores*Date: $F_{1,352}$ = 5.28, p = 0.022; Fig. B.2A,C). During the second wave of infections (i.e., beginning day ~26) the density of edible algae generally increased in the low nutrient, unmixed, +spores treatment (Fig. B.2C). This occurred as the density of hosts was decreasing in that treatment (Figs 4.1C and 4.2C). However, there were no significant main or interactive effects of the nutrient, mixing, or spore manipulations on the abundance of edible algae, integrated over time (Nutrients: $F_{1,23}$ = 0.007, p = 0.93, Mixing: $F_{1,23}$ = 0.08, p = 0.77, Spores: $F_{1,23}$ = 0.31, p = 0.58; Fig. B.2B,D).

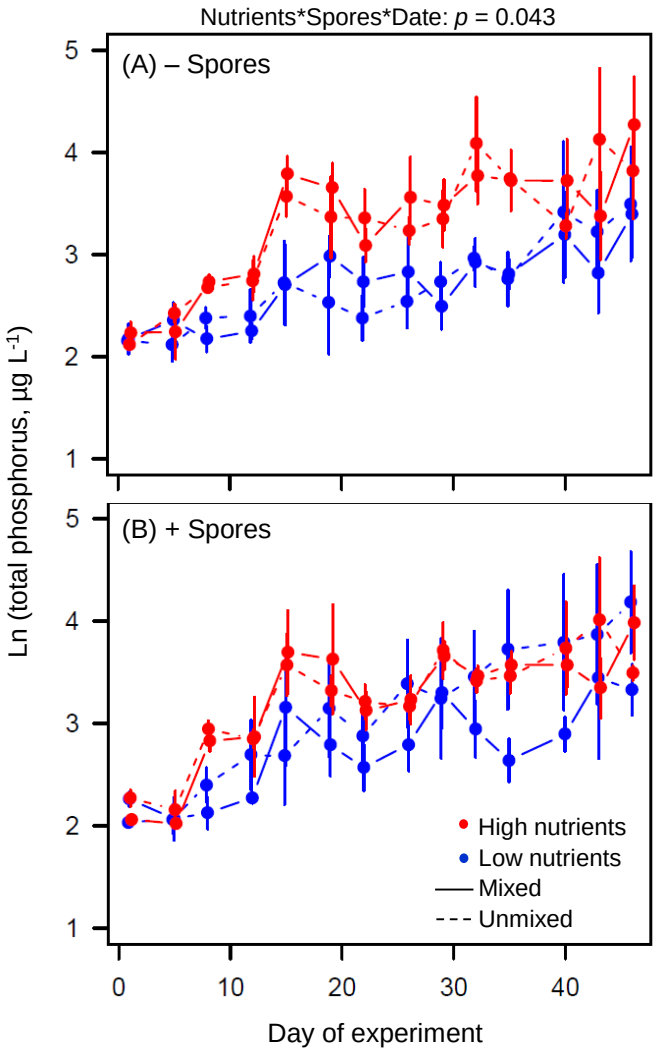

Figure B.1. Total phosphorus (TP) concentrations (mean ± SE) over the course of the experiment. (A) In –spores bags, the high nutrient manipulation generally increased TP, relative to the low nutrient manipulation. (B) In the +spores bags, there was not a clear difference in TP between the high and low nutrient manipulations.

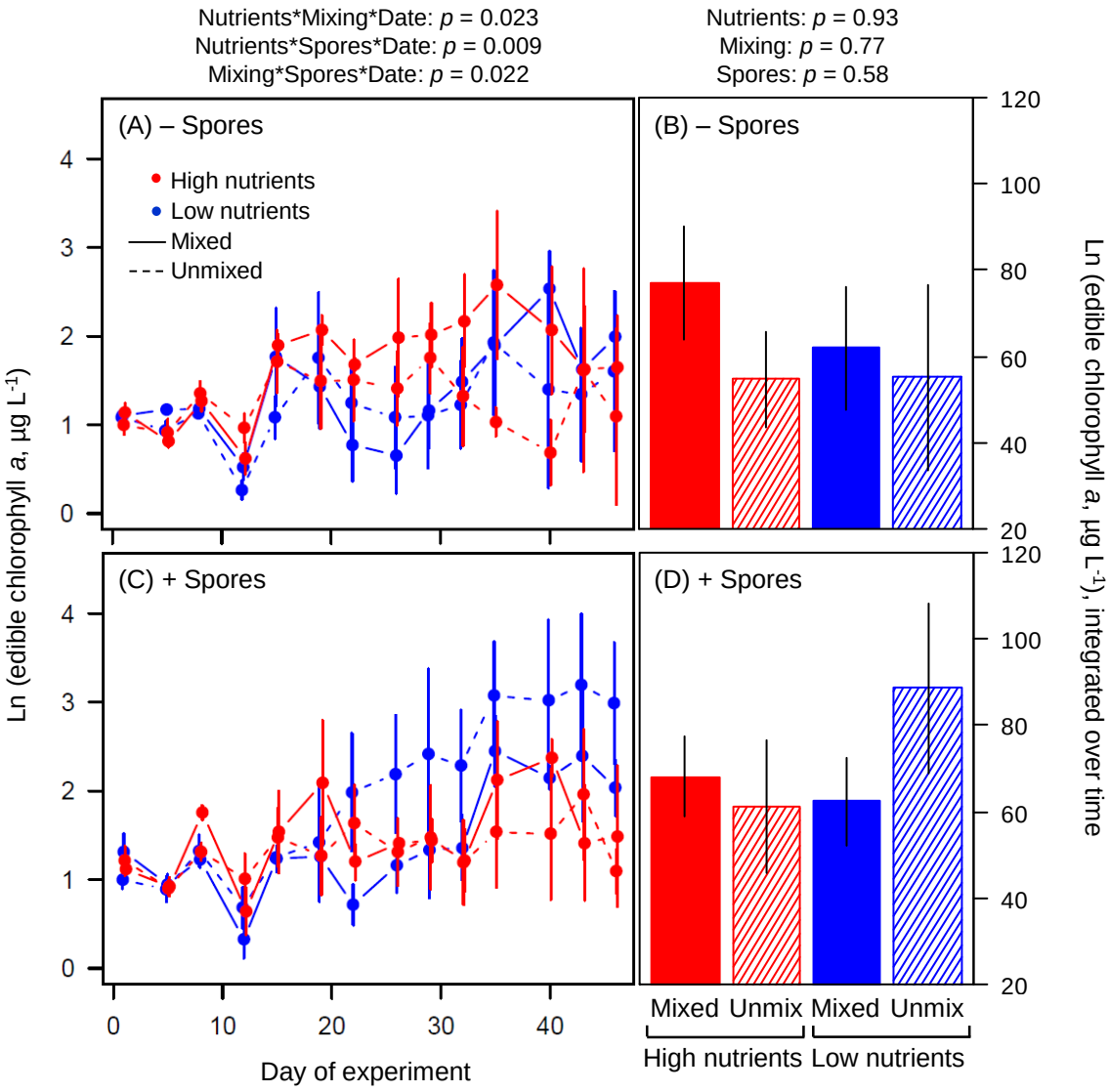

Figure B.2. Concentrations of chlorophyll *a* in the < 80 µm size fraction (mean ± SE), a proxy for the biomass of algae that was edible to hosts. (A,C) There were complex interactions among nutrients, mixing, and spores on algal dynamics. Edible algae tended to increase over time in the low nutrient, unmixed, +spores treatment. (B,D) Overall, the nutrient, mixing, and spore manipulations did not significantly alter the abundance of edible algae, integrated over time.

APPENDIX C

SUPPLEMENT TO CHAPTER 5

Here, we provide additional methods used in fitting the foraging models to data, and we show the fits of each candidate model to observed feeding rates. For the winning foraging model, we test for significant differences in parameter estimates between the two time blocks of the experiment, and we show a linear regression between and observed and predicted values of algal concentration for each host individual in the feeding rate assay. In addition, we present results from a version of the dynamic epidemiological model in which the reduction in feeding rate of infected hosts is linked to resource-dependent spore production.

Additional methods

Fitting the foraging models

We estimated parameters in the foraging models by fitting a natural log-transformed version of a standard formula for calculating foraging-based "clearance rate" (Sarnelle and Wilson 2008):

$$\log(C_t) = \log(C_0) - ft/V + \varepsilon, \quad \text{(C.1)}$$

where C_t is the concentration of algae remaining at the end of the grazing period of length t, C_0 is the concentration of algae in ungrazed reference tubes at the end of the grazing period, f is one of the foraging models specified in Table 5.1, V is the volume of medium in the tube, and errors (ε) were assumed to be normally distributed. We assumed that uninfected hosts and infected hosts younger than 16 days old contained no spores. Fitting this model (equ. C.1) produced likelihood values for feeding rate, ℓ_f. We estimated the parameters $\hat{f}$ (in all models), b (in models 3–6), and c (in models 4 and 6) by

minimizing the negative log-transformed likelihood ℓ_f. In Fig. C.1, we show the best fit of each candidate foraging model to the feeding rate data.

To compare parameter estimates in the winning model (model 5: *size and spores, linear*) between time blocks of the experiment, we used permutation tests (9999 randomizations per contrast) with Holm–Bonferroni adjusted significance levels (Gotelli and Ellison 2004). We used a linear regression to check for concordance between log-transformed final concentrations of algae observed in the experiment and predicted by the winning model for each individual host in the feeding rate experiment. The slope and intercept of this regression were very close to 1 and 0, respectively, indicating that the model performed well over the full range of data (*Observed* = 1.007 * *Predicted* – 0.056 + ε; $R^2 = 0.55$, $p < 0.0001$; Fig. C.3) (Piñeiro et al. 2008).

Table C.1. *P*-values for comparisons of parameter estimates for the winning model (model 5: *size and spores, linear*) between host genotypes. Asterisks indicate significant pairwise differences after Holm–Bonferroni correction.

		Host genotype comparison		
Parameter	**Symbol**	**A4-4 vs. BD-30**	**BD-30 vs. STD**	**STD vs. A4-4**
Feeding rate coefficient, uninfected	$\hat{f}_S$	0.028	0.26	0.0002 *
Feeding rate coefficient, infected	$\hat{f}_I$	0.0017 *	< 0.0001 *	< 0.0001 *
Spore load coefficient[1]	b	0.095	< 0.0001 *	< 0.0001 *

[1]We did not estimate *b* for uninfected hosts because they contained no spores.

Table C.2. *P*-values for comparisons of parameter estimates for the winning model (model 5: *size and spores, linear*) between infected and uninfected hosts (pooled blocks), and between blocks of the feeding rate experiment for each genotype. Asterisks indicate significant pairwise differences after Holm–Bonferroni correction.

		Host genotype		
		A4-4	**BD-30**	**STD**
Parameter	**Symbol**	**Infected vs. uninfected**	**Infected vs. uninfected**	**Infected vs. uninfected**
Feeding rate coefficient	$\hat{f}$	< 0.0001 *	< 0.0001 *	< 0.0001 *
Parameter	**Symbol**	**Block 1 vs. 2**	**Block 1 vs. 2**	**Block 1 vs. 2**
Feeding rate coefficient, uninfected	$\hat{f}_S$	0.78	< 0.0001 *	0.34
Feeding rate coefficient, infected	$\hat{f}_I$	0.17	0.018	0.039
Spore load coefficient[1]	b	0.86	0.032	0.006 *

[1]We did not estimate b for uninfected hosts because they contained no spores.

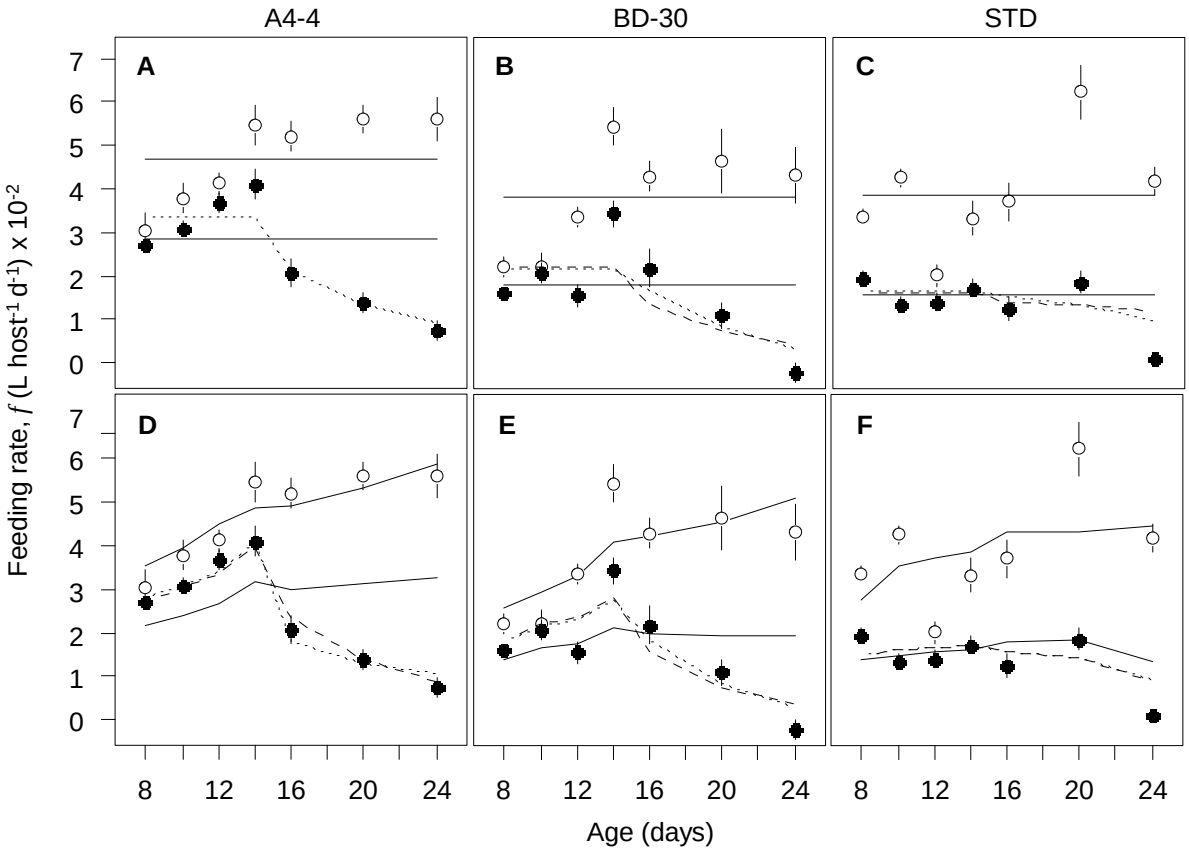

Figure C.1. The six candidate models fit to observed (mean ± SE) feeding rate, *f*, for infected (filled circles) and uninfected (open circles) hosts from three genotypes. (A–C) Models in which feeding rate does not depend on host size performed poorly: *null* (solid line); *spores only, linear* (dashed line); *spores only, power* (dotted line). (D–E) Models in which feeding rate depends on host size (surface area, L^2). The *size only* model (solid line) performed poorly. The two best models feature effects of both size and spore load (σ). The *size and spores, linear* (dashed line) and *size and spores, power* (dotted line) models performed equally well.

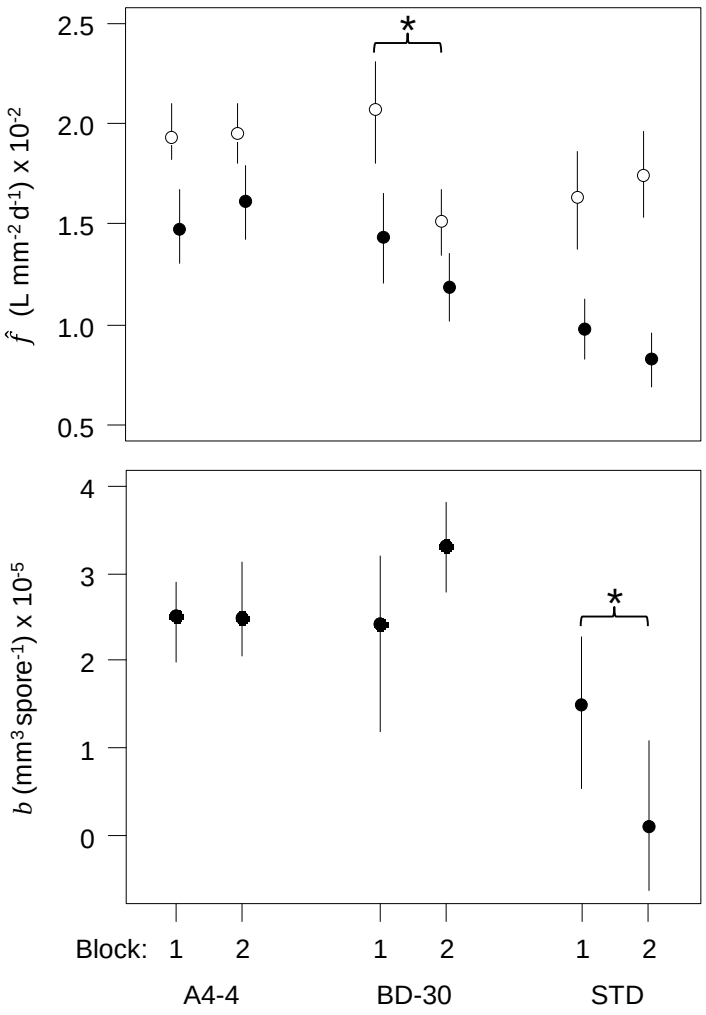

Figure C.2. Parameter estimates (with bootstrapped 95% confidence intervals) for the winning model (*size and spores, linear*), estimated separately for each time block for infected (filled circles) and uninfected (open circles) hosts of each genotype. Brackets indicate significant differences between time blocks.

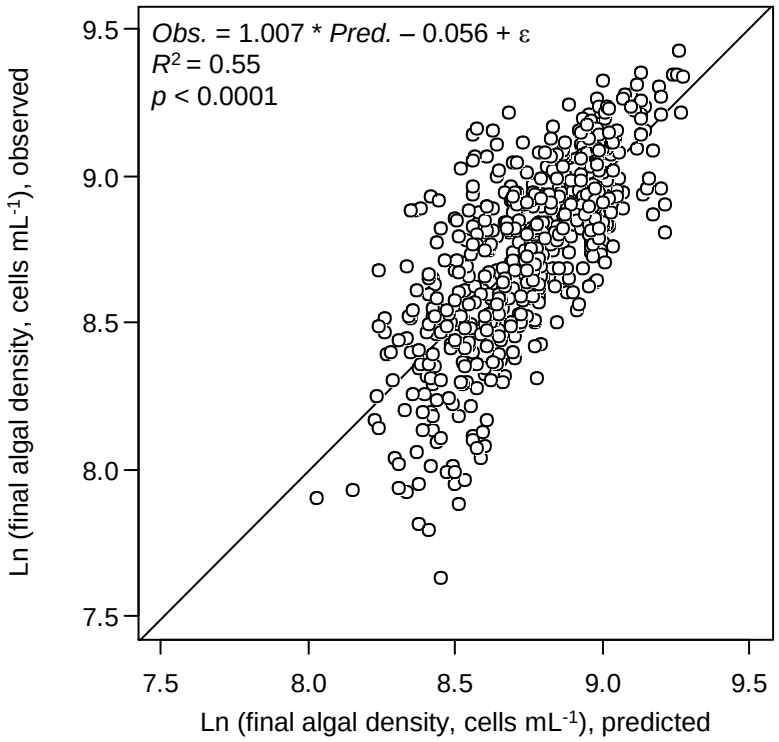

Figure C.3. Density of algae observed at the end of the grazing period and predicted by the winning foraging model (*size and spores, linear*) for each host in the feeding rate experiment (i.e., infected and uninfected individuals from all seven age groups of three genotypes).

Resource-dependent spore production in dynamic epidemiological model

In this version of the model, we assume that the yield of spores per infected host increases with resource density:

$$dS/dt = ef_S AS + \rho ef_I AI - dS - uf_S SZ \quad \text{(C.2.a)}$$

$$dI/dt = uf_S SZ - (d + v)I \quad \text{(C.2.b)}$$

$$dZ/dt = (\sigma_0 + \sigma_1 A)(d + v)I - mZ - f_S SZ - f_I IZ \quad \text{(C.2.c)}$$

$$dA/dt = rA(1 - A/K) - f_S SA - f_I IA \quad \text{(C.2.d)}$$

As in the previous version of the model (equ. 1), free-living parasite spores (Z) increase over time as infected hosts (I) die and release spores into the water. Here, the number of spores released per infected host (σ) is a linear function of algal density (A), with slope, σ_1, and intercept, σ_0. We first simulated this model assuming feeding rates were the same for infected and uninfected hosts (scenario 1; Fig. C.4). Next, we explored the potential for TMIEs when feeding rate of infected hosts (f_I) is linked to the slope of spore production with resources (σ_1) (scenario 2; Fig. C.4). That is, we assumed hosts producing more spores per unit resource incur a greater reduction in feeding rate. In this second scenario, we linked f_I and σ_1 through the linear relationship used in the previous version of the model (i.e., an abstraction of the winning foraging model; Table 5.2). All other parameters were the same as in the earlier version of the model (Table 5.2).

Additional results

Simulation results with resource-dependent spore production

As in the resource-independent model (Fig. 5.5), this version can produce both DMIEs (scenario 1) and TMIEs (scenario 2) of disease (Fig. C.4). In both scenarios, epidemics are inhibited at low values of σ_1 (Fig. C.4A,D). This occurs because, using the parameters in Table 5.2, resource density is low when σ_1 is low, and not enough spores are produced to maintain epidemics. When σ_1 is high enough for epidemics to persist, a DMIE of disease on resources occurs in scenario 1 (Fig. C.4A-C). When epidemics can occur in scenario 2 (Fig. C.4D-F), the TMIE of disease is exacerbated compared to the earlier version of the model (Fig. 5.5). Disease reduces the average feeding rate of the host population, yielding more resources. Then, because spore production (σ) increases with resource density, infected hosts produce more spores, which amplifies the spread of disease. This escalation of disease results in much higher infection prevalence in scenario 2 (Fig. C.4D), compared to scenario 1 (Fig. C.4A), for given values of u and σ_1.

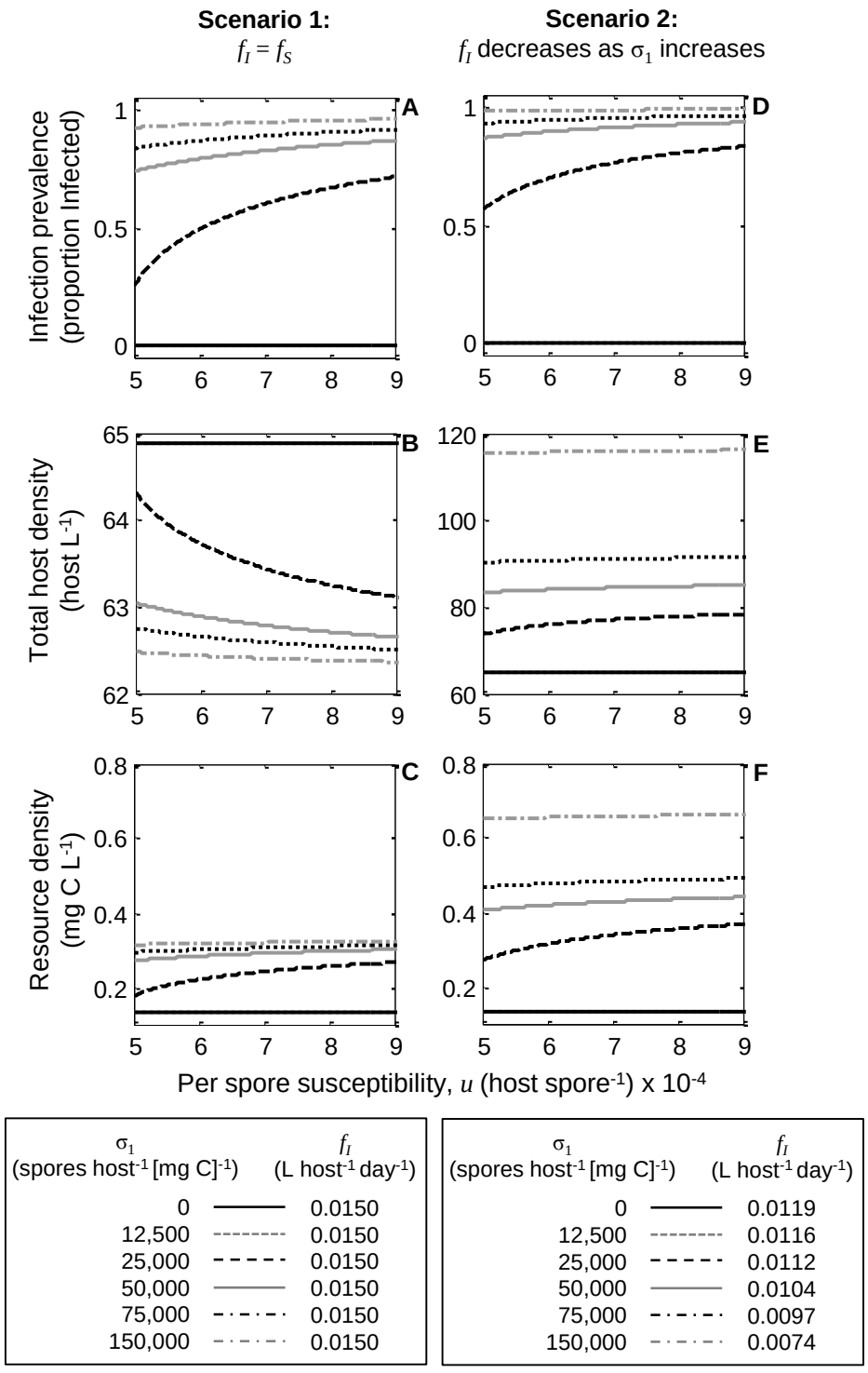

Figure C.4. Equilibrium results of the dynamic epidemiological model with resource-dependent spore production (equ. C.2), simulated over a range of values of per spore susceptibility, u (x-axis) and slope of spore production with resources, σ_1 (contours). (A–C) *Scenario 1, DMIE:* infection does not alter feeding rate ($f_I = f_S$). As u or σ_1 increases,

(A) infection prevalence increases, (B) host density decreases, and (C) resource density increases. (D–F) *Scenario 2, TMIE:* feeding rate of infected hosts (f_I) decreases linearly with σ_1. As u increases, or as f_I decreases with increasing σ_1, (D) infection prevalence increases to higher levels than in Scenario 1 because infected hosts remove fewer spores from the water. In contrast to Scenario 1, (E) host density increases with infection prevalence because the average grazing rate of the population decreases, (F) allowing resource density to increase. In both scenarios, note that when σ_1 is low, resource density is also low. Therefore, spore yield per host is low, and epidemics are inhibited.

REFERENCES

Abrams, P. A. 2009. When does greater mortality increase population size? The long history and diverse mechanisms underlying the hydra effect. Ecology Letters **12**:462-474.

Adamo, S. A., A. Bartlett, J. Le, N. Spencer, and K. Sullivan. 2010. Illness-induced anorexia may reduce trade-offs between digestion and immune function. Animal Behaviour **79**:3-10.

Ali, M. I., G. W. Felton, T. Meade, and S. Y. Young. 1998. Influence of interspecific and intraspecific host plant variation on the susceptibility of heliothines to a baculovirus. Biological Control **12**:42-49.

Allan, B. F., F. Keesing, and R. S. Ostfeld. 2003. Effect of forest fragmentation on Lyme disease risk. Conservation Biology **17**:267-272.

Allen, A. P. and J. F. Gillooly. 2009. Towards an integration of ecological stoichiometry and the metabolic theory of ecology to better understand nutrient cycling. Ecology Letters **12**:369-384.

Andersen, T. and D. O. Hessen. 1991. Carbon, nitrogen, and phosphorus content of freshwater zooplankton. Limnology and Oceanography **36**:807-814.

Anderson, R. M. and R. M. May. 1992. Infectious Diseases of Humans: Dynamics and Control Oxford University Press, Oxford.

Anderson, T. R. and D. O. Hessen. 2005. Threshold elemental ratios for carbon versus phosphorus limitation in *Daphnia*. Freshwater Biology **50**:2063-2075.

Anderson, T. R., D. O. Hessen, J. J. Elser, and J. Urabe. 2005. Metabolic stoichiometry and the fate of excess carbon and nutrients in consumers. American Naturalist **165**:1-15.

Arias-Gonzalez, J. E. and S. Morand. 2006. Trophic functioning with parasites: a new insight for ecosystem analysis. Marine Ecology-Progress Series **320**:43-53.

Babin, A., C. Biard, and Y. Moret. 2010. Dietary supplementation with carotenoids improves immunity without increasing its cost in a crustacean. American Naturalist **176**:234-241.

Bachmann, R. W. and D. E. Canfield. 1996. Use of an alternative method for monitoring total nitrogen concentrations in Florida lakes. Hydrobiologia **323**:1-8.

Bailey, G. N. A. 1975. Energetics of a host-parasite system: A preliminary report. International Journal for Parasitology **5**:609-613.

Beldomenico, P. M. and M. Begon. 2010. Disease spread, susceptibility and infection intensity: Vicious circles? Trends in Ecology & Evolution **25**:21-27.

Bernot, R. J. and G. A. Lamberti. 2008. Indirect effects of a parasite on a benthic community: an experiment with trematodes, snails and periphyton. Freshwater Biology **53**:322-329.

Bertram, C. R., M. Pinkowski, S. R. Hall, M. A. Duffy, and C. E. Cáceres. 2013. Trait-mediated indirect effects, predators, and disease: test of a size-based model. Oecologia **173**:1023-1032.

Bishara, A. J. and J. B. Hittner. 2012. Testing the significance of a correlation with nonnormal data: Comparison of Pearson, Spearman, transformation, and resampling approaches. Psychological Methods **17**:399-417.

Booth, D. T., D. H. Clayton, and B. A. Block. 1993. Experimental demonstration of the energetic cost of parasitism in free-ranging hosts. Proceedings of the Royal Society B-Biological Sciences **253**:125-129.

Brookes, J. D., J. Antenucci, M. Hipsey, M. D. Burch, N. J. Ashbolt, and C. Ferguson. 2004. Fate and transport of pathogens in lakes and reservoirs. Environment International **30**:741-759.

Bruno, J. F., L. E. Petes, C. D. Harvell, and A. Hettinger. 2003. Nutrient enrichment can increase the severity of coral diseases. Ecology Letters **6**:1056-1061.

Burdon, J. J., P. H. Thrall, and L. Ericson. 2006. The current and future dynamics of disease in plant communities. Pages 19-39 Annual Review of Phytopathology.

Burnham, K. P. and D. R. Anderson. 2002. Model selection and multimodel inference: a practical information-theoretic approach, 2nd ed. Springer-Verlag, New York.

Cáceres, C. E., S. R. Hall, M. A. Duffy, A. J. Tessier, C. Helmle, and S. MacIntyre. 2006. Physical structure of lakes constrains epidemics in *Daphnia* populations. Ecology **87**:1438-1444.

Cáceres, C. E., C. J. Knight, and S. R. Hall. 2009. Predator-spreaders: Predation can enhance parasite success in a planktonic host-parasite system. Ecology **90**:2850-2858.

Careau, V., D. W. Thomas, and M. M. Humphries. 2010. Energetic cost of bot fly parasitism in free-ranging eastern chipmunks. Oecologia **162**:303-312.

Carey, C. C., B. W. Ibelings, E. P. Hoffmann, D. P. Hamilton, and J. D. Brookes. 2012. Eco-physiological adaptations that favour freshwater cyanobacteria in a changing climate. Water Research **46**:1394-1407.

Chen, C. T. and F. J. Millero. 1977. Use and misuse of pure water PVT properties for lake waters. Nature **266**:707-708.

Civitello, D. J., P. Forys, A. P. Johnson, and S. R. Hall. 2012. Chronic contamination decreases disease spread: a *Daphnia*-fungus-copper case study. Proceedings of the Royal Society B-Biological Sciences **279**:3146-3153.

Civitello, D. J., S. Pearsall, M. A. Duffy, and S. R. Hall. 2013a. Parasite consumption and host interference can inhibit disease spread in dense populations. Ecology Letters **16**:626-634.

Civitello, D. J., R. M. Penczykowski, J. L. Hite, M. A. Duffy, and S. R. Hall. 2013b. Potassium stimulates fungal epidemics in *Daphnia* by increasing host and parasite reproduction. Ecology **94**:380-388.

Collinge, S. K., W. C. Johnson, C. Ray, R. Matchett, J. Grensten, J. F. Cully, K. L. Gage, M. Y. Kosoy, J. E. Loye, and A. P. Martin. 2005. Landscape structure and plague occurrence in black-tailed prairie dogs on grasslands of the western USA. Landscape Ecology **20**:941-955.

Coors, A. and L. De Meester. 2011. Fitness and virulence of a bacterial endoparasite in an environmentally stressed crustacean host. Parasitology **138**:122-131.

Cory, J. S. and K. Hoover. 2006. Plant-mediated effects in insect-pathogen interactions. Trends in Ecology & Evolution **21**:278-286.

Cotter, S. C., S. J. Simpson, D. Raubenheimer, and K. Wilson. 2011. Macronutrient balance mediates trade-offs between immune function and life history traits. Functional Ecology **25**:186-198.

Crumpton, W. G., T. M. Isenhart, and P. D. Mitchell. 1992. Nitrate and organic N analyses with second-derivative spectroscopy. Limnology and Oceanography **37**:907-913.

Cruz-Rivera, E. and M. E. Hay. 2003. Prey nutritional quality interacts with chemical defenses to affect consumer feeding and fitness. Ecological Monographs **73**:483-506.

Daniels, R. R., S. Beltran, R. Poulin, and C. Lagrue. 2013. Do parasites adopt different strategies in different intermediate hosts? Host size, not host species, influences *Coitocaecum parvum* (Trematoda) life history strategy, size and egg production. Parasitology **140**:275-283.

Darchambeau, F. and I. Thys. 2005. In situ filtration responses of *Daphnia galeata* to changes in food quality. Journal of Plankton Research **27**:227-236.

Daszak, P., A. A. Cunningham, and A. D. Hyatt. 2000. Emerging infectious diseases of wildlife - Threats to biodiversity and human health. Science **287**:1756-1756.

de Roode, J. C., A. B. Pedersen, M. D. Hunter, and S. Altizer. 2008. Host plant species affects virulence in monarch butterfly parasites. Journal of Animal Ecology **77**:120-126.

De Stasio, B. T., D. K. Hill, J. M. Kleinhans, N. P. Nibbelink, and J. J. Magnuson. 1996. Potential effects of global climate change on small north-temperate lakes: Physics, fish, and plankton. Limnology and Oceanography **41**:1136-1149.

Decaestecker, E., L. De Meester, and D. Ebert. 2002. In deep trouble: Habitat selection constrained by multiple enemies in zooplankton. Proceedings of the National Academy of Sciences of the United States of America **99**:5481-5485.

DeMott, W. R., E. N. McKinney, and A. J. Tessier. 2010. Ontogeny of digestion in *Daphnia*: implications for the effectiveness of algal defenses. Ecology **91**:540-548.

DeMott, W. R. and D. C. Muller-Navarra. 1997. The importance of highly unsaturated fatty acids in zooplankton nutrition: evidence from experiments with *Daphnia*, a cyanobacterium and lipid emulsions. Freshwater Biology **38**:649-664.

Demott, W. R., Q. X. Zhang, and W. W. Carmichael. 1991. Effects of toxic cyanobacteria and purified toxins on the survival and feeding of a copepod and three species of *Daphnia*. Limnology and Oceanography **36**:1346-1357.

Droop, M. R. 1968. Vitamin B12 and marine ecology. IV. The kinetics of uptake, growth, and inhibition in *Monochrysis lutheri*. Journal of the Marine Biological Association of the United Kingdom **48**:689-733.

Duffy, M. A. 2007. Selective predation, parasitism, and trophic cascades in a bluegill-*Daphnia*-parasite system. Oecologia **153**:453-460.

Duffy, M. A. and S. R. Hall. 2008. Selective predation and rapid evolution can jointly dampen effects of virulent parasites on *Daphnia* populations. American Naturalist **171**:499-510.

Duffy, M. A., S. R. Hall, A. J. Tessier, and M. Huebner. 2005. Selective predators and their parasitized prey: are epidemics in zooplankton under top-down control? Limnology and Oceanography **50**:412-420.

Duffy, M. A., J. M. Housley, R. M. Penczykowski, C. E. Cáceres, and S. R. Hall. 2011. Unhealthy herds: indirect effects of predators enhance two drivers of disease spread. Functional Ecology **25**:945-953.

Duffy, M. A. and L. Sivars-Becker. 2007. Rapid evolution and ecological host-parasite dynamics. Ecology Letters **10**:44-53.

Dunn, A. M., M. E. Torchin, M. J. Hatcher, P. M. Kotanen, D. M. Blumenthal, J. E. Byers, C. A. C. Coon, V. M. Frankel, R. D. Holt, R. A. Hufbauer, A. R. Kanarek, K. A. Schierenbeck, L. M. Wolfe, and S. E. Perkins. 2012. Indirect effects of parasites in invasions. Functional Ecology **26**:1262-1274.

Dwyer, G., J. Firestone, and T. E. Stevens. 2005. Should models of disease dynamics in herbivorous insects include the effects of variability in host-plant foliage quality? American Naturalist **165**:16-31.

Ebert, D. 2005. Ecology, epidemiology and evolution of parasitism in *Daphnia*. National Library of Medicine (US), National Center for Biotechnology Information, Bethesda, MD.

Ebert, D., H. J. Carius, T. Little, and E. Decaestecker. 2004. The evolution of virulence when parasites cause host castration and gigantism. American Naturalist **164**:S19-S32.

Ebert, D., C. D. Zschokke-Rohringer, and H. J. Carius. 2000. Dose effects and density-dependent regulation of two microparasites of *Daphnia magna*. Oecologia **122**:200-209.

Elser, J. J., D. R. Dobberfuhl, N. A. MacKay, and J. H. Schampel. 1996. Organism size, life history, and N:P stoichiometry. Bioscience **46**:674-684.

Elser, J. J., W. F. Fagan, A. J. Kerkhoff, N. G. Swenson, and B. J. Enquist. 2010. Biological stoichiometry of plant production: metabolism, scaling and ecological response to global change. New Phytologist **186**:593-608.

Elser, J. J. and J. Urabe. 1999. The stoichiometry of consumer-driven nutrient recycling: Theory, observations, and consequences. Ecology **80**:735-751.

Fee, E. J. 1979. A relation between lake morphometry and primary productivity and its use in interpreting whole-lake eutrophication experiments. Limnology and Oceanography **24**:401-416.

Fee, E. J., R. E. Hecky, S. E. M. Kasian, and D. R. Cruikshank. 1996. Effects of lake size, water clarity, and climatic variability on mixing depths in Canadian Shield lakes. Limnology and Oceanography **41**:912-920.

Fels, D. 2005. The effect of food on microparasite transmission in the waterflea *Daphnia magna*. Oikos **109**:360-366.

Felton, G. W. and S. S. Duffey. 1990. Inactivation of baculovirus by quinones formed in insect-damaged plant tissues. Journal of Chemical Ecology **16**:1221-1236.

Ferrer, M. and J. J. Negro. 2004. The near extinction of two large European predators: Super specialists pay a price. Conservation Biology **18**:344-349.

Fink, P. and E. Von Elert. 2006. Physiological responses to stoichiometric constraints: nutrient limitation and compensatory feeding in a freshwater snail. Oikos **115**:484-494.

Foley, J. A., R. DeFries, G. P. Asner, C. Barford, G. Bonan, S. R. Carpenter, F. S. Chapin, M. T. Coe, G. C. Daily, H. K. Gibbs, J. H. Helkowski, T. Holloway, E. A. Howard, C. J. Kucharik, C. Monfreda, J. A. Patz, I. C. Prentice, N. Ramankutty, and P. K. Snyder. 2005. Global consequences of land use. Science **309**:570-574.

Forshay, K. J., P. T. J. Johnson, M. Stock, C. Peñalva, and S. I. Dodson. 2008. Festering food: Chytridiomycete pathogen reduces quality of *Daphnia* host as a food resource. Ecology **89**:2692-2699.

Fowler, D., M. Coyle, U. Skiba, M. A. Sutton, J. N. Cape, S. Reis, L. J. Sheppard, A. Jenkins, B. Grizzetti, J. N. Galloway, P. Vitousek, A. Leach, A. F. Bouwman, K. Butterbach-Bahl, F. Dentener, D. Stevenson, M. Amann, and M. Voss. 2013. The global nitrogen cycle in the twenty-first century. Philosophical Transactions of the Royal Society B-Biological Sciences **368**.

Frost, P. C., D. Ebert, and V. H. Smith. 2008a. Bacterial infection changes the elemental composition of Daphnia magna. Journal of Animal Ecology **77**:1265-1272.

Frost, P. C., D. Ebert, and V. H. Smith. 2008b. Responses of a bacterial pathogen to phosphorus limitation of its aquatic invertebrate host. Ecology **89** 313-318.

Frost, P. C., M. A. Xenopoulos, and J. H. Larson. 2004. The stoichiometry of dissolved organic carbon, nitrogen, and phosphorus release by a planktonic grazer, Daphnia. Limnology and Oceanography **49**:1802-1808.

Gachon, C. M. M., T. Sime-Ngando, M. Strittmatter, A. Chambouvet, and G. H. Kim. 2010. Algal diseases: spotlight on a black box. Trends in Plant Science **15**:633-640.

Gorham, E. and F. M. Boyce. 1989. Influence of lake surface area and depth upon thermal stratification and the depth of the summer thermocline. Journal of Great Lakes Research **15**:233-245.

Gotelli, N. J. and A. M. Ellison. 2004. A Primer of Ecological Statistics. Sinauer Associates, Inc., Sunderland, MA.

Green, J. 1974. Parasites and epibionts of *Cladocera*. Transactions of the Zoological Society of London **32**:417-515.

Gsell, A. S., L. N. D. Domis, S. M. H. Naus-Wiezer, N. R. Helmsing, E. Van Donk, and B. W. Ibelings. 2013. Spatiotemporal variation in the distribution of chytrid parasites in diatom host populations. Freshwater Biology **58**:523-537.

Hall, S. R. 2009. Stoichiometrically explicit food webs: Feedbacks between resource supply, elemental constraints, and species diversity. Annual Review of Ecology Evolution and Systematics **40**:503-528.

Hall, S. R., C. R. Becker, M. A. Duffy, and C. E. Caceres. 2010a. Variation in resource acquisition and use among host clones creates key epidemiological trade-offs. American Naturalist **176**:557-565.

Hall, S. R., C. R. Becker, M. A. Duffy, and C. E. Caceres. 2012. A power-efficiency trade-off in resource use alters epidemiological relationships. Ecology **93**:645-656.

Hall, S. R., C. R. Becker, M. A. Duffy, and C. E. Cáceres. 2011. Epidemic size determines population-level effects of fungal parasites on *Daphnia* hosts. Oecologia **166**:833-842.

Hall, S. R., C. R. Becker, J. L. Simonis, M. A. Duffy, A. J. Tessier, and C. E. Cáceres. 2009a. Friendly competition: evidence for a dilution effect among competitors in a planktonic host-parasite system. Ecology **90**:791-801.

Hall, S. R., C. J. Knight, C. R. Becker, M. A. Duffy, A. J. Tessier, and C. E. Cáceres. 2009b. Quality matters: resource quality for hosts and the timing of epidemics. Ecology Letters **12**:118-128.

Hall, S. R., M. A. Leibold, D. A. Lytle, and V. H. Smith. 2007a. Grazers, producer stoichiometry, and the light : nutrient hypothesis revisited. Ecology **88**:1142-1152.

Hall, S. R., R. M. Nisbet, J. Simonis, and C. E. Cáceres. 2006a. Parasites as consumers of resources: models for disease based on dynamic energy budgets. Integrative and Comparative Biology **46**:E54-E54.

Hall, S. R., J. L. Simonis, R. M. Nisbet, A. J. Tessier, and C. E. Cáceres. 2009c. Resource ecology of virulence in a planktonic host-parasite system: an explanation using dynamic energy budgets. American Naturalist **174**:149-162.

Hall, S. R., L. Sivars-Becker, C. Becker, M. A. Duffy, A. J. Tessier, and C. E. Cáceres. 2007b. Eating yourself sick: transmission of disease as a function of foraging ecology. Ecology Letters **10**:207-218.

Hall, S. R., R. Smyth, C. R. Becker, M. A. Duffy, C. J. Knight, S. MacIntyre, A. J. Tessier, and C. E. Cáceres. 2010b. Why are *Daphnia* in some lakes sicker? Disease ecology, habitat structure, and the plankton. Bioscience **60**:363-375.

Hall, S. R., A. J. Tessier, M. A. Duffy, M. Huebner, and C. E. Cáceres. 2006b. Warmer does not have to mean sicker: temperature and predators can jointly drive timing of epidemics. Ecology **87**:1684-1695.

Hart, B. L. 1990. Behavioral adaptations to pathogens and parasites: Five strategies. Neuroscience and Biobehavioral Reviews **14**:273-294.

Harvell, C. D., K. Kim, J. M. Burkholder, R. R. Colwell, P. R. Epstein, D. J. Grimes, E. E. Hofmann, E. K. Lipp, A. Osterhaus, R. M. Overstreet, J. W. Porter, G. W. Smith, and G. R. Vasta. 1999. Emerging marine diseases - Climate links and anthropogenic factors. Science **285**:1505-1510.

Hatcher, M. J., J. T. A. Dick, and A. M. Dunn. 2012. Diverse effects of parasites in ecosystems: linking interdependent processes. Frontiers in Ecology and the Environment **10**:186-194.

Hatcher, M. J. and A. M. Dunn. 2011. Parasites in ecological communities: From interactions to ecosystems. Cambridge University Press, New York.

Hechinger, R. F., K. D. Lafferty, J. P. McLaughlin, B. L. Fredensborg, T. C. Huspeni, J. Lorda, P. K. Sandhu, J. C. Shaw, M. E. Torchin, K. L. Whitney, and A. M. Kuris. 2011. Food webs including parasites, biomass, body sizes, and life stages for three California/Baja California estuaries. Ecology **92**:791.

Hernandez, A. D. and M. V. K. Sukhdeo. 2008a. Parasite effects on isopod feeding rates can alter the host's functional role in a natural stream ecosystem. International Journal for Parasitology **38**:683-690.

Hernandez, A. D. and M. V. K. Sukhdeo. 2008b. Parasites alter the topology of a stream food web across seasons. Oecologia **156**:613-624.

Hessen, D. O. and A. Lyche. 1991. Interspecific and intraspecific variations in zooplankton element composition. Archiv Fur Hydrobiologie **121**:343-353.

Holdo, R. M., A. R. E. Sinclair, A. P. Dobson, K. L. Metzger, B. M. Bolker, M. E. Ritchie, and R. D. Holt. 2009. A disease-mediated trophic cascade in the Serengeti and its implications for ecosystem C. PLoS Biology **7**:-.

Hudson, P. J., A. P. Dobson, and K. D. Lafferty. 2006. Is a healthy ecosystem one that is rich in parasites? Trends in Ecology & Evolution **21**:381-385.

Hudson, P. J., A. P. Dobson, and D. Newborn. 1998. Prevention of population cycles by parasite removal. Science **282**:2256-2258.

Hutchings, M. R., I. Kyriazakis, and I. J. Gordon. 2001. Herbivore physiological state affects foraging trade-off decisions between nutrient intake and parasite avoidance. Ecology **82**:1138-1150.

Ibelings, B. W., A. S. Gsell, W. M. Mooij, E. van Donk, S. van den Wyngaert, and L. N. D. Domis. 2011. Chytrid infections and diatom spring blooms: Paradoxical effects of climate warming on fungal epidemics in lakes. Freshwater Biology **56**:754-766.

Johnson, C. K., M. T. Tinker, J. A. Estes, P. A. Conrad, M. Staedler, M. A. Miller, D. A. Jessup, and J. A. K. Mazet. 2009a. Prey choice and habitat use drive sea otter pathogen exposure in a resource-limited coastal system. Proceedings of the National Academy of Sciences of the United States of America **106**:2242-2247.

Johnson, P. T. J., J. M. Chase, K. L. Dosch, R. B. Hartson, J. A. Gross, D. J. Larson, D. R. Sutherland, and S. R. Carpenter. 2007. Aquatic eutrophication promotes pathogenic infection in amphibians. Proceedings of the National Academy of Sciences of the United States of America **104**:15781-15786.

Johnson, P. T. J., A. Dobson, K. D. Lafferty, D. J. Marcogliese, J. Memmott, S. A. Orlofske, R. Poulin, and D. W. Thieltges. 2010a. When parasites become prey: ecological and epidemiological significance of eating parasites. Trends in Ecology & Evolution **25**:362-371.

Johnson, P. T. J., A. R. Ives, R. C. Lathrop, and S. R. Carpenter. 2009b. Long-term disease dynamics in lakes: causes and consequences of chytrid infections in *Daphnia* populations. Ecology **90**:132-144.

Johnson, P. T. J., D. E. Stanton, E. R. Preu, K. J. Forshay, and S. R. Carpenter. 2006. Dining on disease: How interactions between parasite infection and environmental conditions affect host predation risk. Ecology **87**:1973-1980.

Johnson, P. T. J., A. R. Townsend, C. C. Cleveland, P. M. Glibert, R. W. Howarth, V. J. McKenzie, E. Rejmankova, and M. H. Ward. 2010b. Linking environmental nutrient enrichment and disease emergence in humans and wildlife. Ecological Applications **20**:16-29.

Karvonen, A., B. Lundsgaard-Hansen, J. Jokela, and O. Seehausen. 2013. Differentiation in parasitism among ecotypes of whitefish segregating along depth gradients. Oikos **122**:122-128.

Keesing, F., L. K. Belden, P. Daszak, A. Dobson, C. D. Harvell, R. D. Holt, P. Hudson, A. Jolles, K. E. Jones, C. E. Mitchell, S. S. Myers, T. Bogich, and R. S. Ostfeld. 2010. Impacts of biodiversity on the emergence and transmission of infectious diseases. Nature **468**:647-652.

Keesing, F., R. D. Holt, and R. S. Ostfeld. 2006. Effects of species diversity on disease risk. Ecology Letters **9**:485-498.

Kilpatrick, A. M., C. J. Briggs, and P. Daszak. 2010. The ecology and impact of chytridiomycosis: an emerging disease of amphibians. Trends in Ecology & Evolution **25**:109-118.

King, K. C., L. F. Delph, J. Jokela, and C. M. Lively. 2009. The geographic mosaic of sex and the Red Queen. Current Biology **19**:1438-1441.

Kirillin, G., H. P. Grossart, and K. W. Tang. 2012. Modeling sinking rate of zooplankton carcasses: Effects of stratification and mixing. Limnology and Oceanography **57**:881-894.

Kitchell, J. A. and J. F. Kitchell. 1980. Size-selective predation, light transmission, and oxygen stratification: Evidence from the recent sediments of manipulated lakes. Limnology and Oceanography **25**:389-402.

Kling, G. W. 1988. Comparative transparency, depth of mixing, and stability of stratification in lakes of Cameroon, West Africa. Limnology and Oceanography **33**:27-40.

Klüttgen, B., U. Dulmer, M. Engels, and H. T. Ratte. 1994. ADaM, an artificial freshwater for the culture of zooplankton. Water Research **28**:743-746.

Kooijman, S.A.L.M. (1986) Energy budgets can explain body size relations. Journal of Theoretical Biology **121**:269-282.

Kooijman, S., T. Sousa, L. Pecquerie, J. van der Meer, and T. Jager. 2008. From food-dependent statistics to metabolic parameters, a practical guide to the use of dynamic energy budget theory. Biological Reviews **83**:533-552.

Kooijman, S. A. L. M. 2010. Dynamic Energy Budget theory for metabolic organisation. Cambridge University Press, Great Britain.

Krebs, J. R., J. C. Ryan, and E. L. Charnov. 1974. Hunting by expectation or optimal foraging - Study of patch use by chickadees. Animal Behaviour **22**:953-964.

Kuris, A. M., R. F. Hechinger, J. C. Shaw, K. L. Whitney, L. Aguirre-Macedo, C. A. Boch, A. P. Dobson, E. J. Dunham, B. L. Fredensborg, T. C. Huspeni, J. Lorda, L. Mababa, F. T. Mancini, A. B. Mora, M. Pickering, N. L. Talhouk, M. E. Torchin, and K. D. Lafferty. 2008. Ecosystem energetic implications of parasite and free-living biomass in three estuaries. Nature **454**:515-518.

Lafferty, K. D. 2009. The ecology of climate change and infectious diseases. Ecology **90**:888-900.

Lafferty, K. D., S. Allesina, M. Arim, C. J. Briggs, G. De Leo, A. P. Dobson, J. A. Dunne, P. T. J. Johnson, A. M. Kuris, D. J. Marcogliese, N. D. Martinez, J. Memmott, P. A. Marquet, J. P. McLaughlin, E. A. Mordecai, M. Pascual, R. Poulin, and D. W. Thieltges. 2008. Parasites in food webs: the ultimate missing links. Ecology Letters **11**:533-546.

Lafferty, K. D., A. P. Dobson, and A. M. Kuris. 2006. Parasites dominate food web links. Proceedings of the National Academy of Sciences of the United States of America **103**:11211-11216.

Lafferty, K. D. and R. D. Holt. 2003. How should environmental stress affect the population dynamics of disease? Ecology Letters **6**:654-664.

Lafferty, K. D. and A. M. Kuris. 2009a. Parasites reduce food web robustness because they are sensitive to secondary extinction as illustrated by an invasive estuarine snail. Philosophical Transactions of the Royal Society B-Biological Sciences **364**:1659-1663.

Lafferty, K. D. and A. M. Kuris. 2009b. Parasitic castration: the evolution and ecology of body snatchers. Trends in Parasitology **25**:564-572.

Lafferty, K. D. and A. K. Morris. 1996. Altered behavior of parasitized killifish increases susceptibility to predation by bird final hosts. Ecology **77**:1390-1397.

Lagrue, C., N. Kaldonski, M. J. Perrot-Minnot, B. Motreuil, and L. Bollache. 2007. Modification of hosts' behavior by a parasite: Field evidence for adaptive manipulation. Ecology **88**:2839-2847.

Lampert, W. 2006. *Daphnia*: Model herbivore, predator and prey. Polish Journal of Ecology **54**:607-620.

Lefèvre, T., C. Lebarbenchon, M. Gauthier-Clerc, D. Misse, R. Poulin, and F. Thomas. 2009. The ecological significance of manipulative parasites. Trends in Ecology & Evolution **24**:41-48.

Lefèvre, T., L. Oliver, M. D. Hunter, and J. C. de Roode. 2010. Evidence for trans-generational medication in nature. Ecology Letters **13**:1485-1493.

Lürling, M. and E. van der Grinten. 2003. Life-history characteristics of *Daphnia* exposed to dissolved microcystin-LR and to the cyanobacterium *Microcystis aeruginosa* with and without microcystins. Environmental Toxicology and Chemistry **22**:1281-1287.

MacIntyre, S. and J. M. Melack. 1995. Vertical and horizontal transport in lakes: Linking littoral, benthic, and pelagic habitats. Journal of the North American Benthological Society **14**:599-615.

Malinen, T., J. Horppila, and A. Liljendahl-Nurminen. 2001. Langmuir circulations disturb the low-oxygen refuge of phantom midge larvae. Limnology and Oceanography **46**:689-692.

Marcogliese, D. J. 2001. Implications of climate change for parasitism of animals in the aquatic environment. Canadian Journal of Zoology-Revue Canadienne De Zoologie **79**:1331-1352.

Martin-Creuzburg, D., E. von Elert, and K. H. Hoffmann. 2008. Nutritional constraints at the cyanobacteria-*Daphnia magna* interface: The role of sterols. Limnology and Oceanography **53**:456-468.

May, R. M. 1983. Parasitic infections as regulators of animal populations. American Scientist **71**:36-45.

Mazumder, A., W. D. Taylor, D. J. McQueen, and D. R. S. Lean. 1990. Effects of fish and plankton on lake temperature and mixing depth. Science **247**:312-315.

McCallum, H., D. Harvell, and A. Dobson. 2003. Rates of spread of marine pathogens. Ecology Letters **6**:1062-1067.

McCallum, H., M. Jones, C. Hawkins, R. Hamede, S. Lachish, D. L. Sinn, N. Beeton, and B. Lazenby. 2009. Transmission dynamics of Tasmanian devil facial tumor disease may lead to disease-induced extinction. Ecology **90**:3379-3392.

McKenzie, V. J. and A. R. Townsend. 2007. Parasitic and infectious disease responses to changing global nutrient cycles. EcoHealth **4**:384-396.

Millennium Ecosystem Assessment. 2005. Ecosystems and Human Well-being: Synthesis. Island Press, Washington, DC.

Moore, J. 1995. The behavior of parasitized animals. Bioscience **45**:89-96.

Moore, M. V. 1988. Differential use of food resources by the instars of *Chaoborus punctipennis*. Freshwater Biology **19**:249-268.

Neter, J., M. H. Kutner, C. J. Nachtsheim, and W. Wasserman. 1996. Applied linear statistical models, 4th ed. McGraw-Hill/Irwin, Chicago.

Niquil, N., M. Kagami, J. Urabe, U. Christaki, E. Viscogliosi, and T. Sime-Ngando. 2011. Potential role of fungi in plankton food web functioning and stability: a simulation analysis based on Lake Biwa inverse model. Hydrobiologia **659**:65-79.

Nisbet, R. M., M. Jusup, T. Klanjscek, and L. Pecquerie. 2012. Integrating dynamic energy budget (DEB) theory with traditional bioenergetic models. Journal of Experimental Biology **215**:892-902.

Nisbet, R. M., E. B. Muller, K. Lika, and S. Kooijman. 2000. From molecules to ecosystems through dynamic energy budget models. Journal of Animal Ecology **69**:913-926.

O'Neil, J. M., T. W. Davis, M. A. Burford, and C. J. Gobler. 2012. The rise of harmful cyanobacteria blooms: The potential roles of eutrophication and climate change. Harmful Algae **14**:313-334.

Ostfeld, R. S., G. E. Glass, and F. Keesing. 2005. Spatial epidemiology: an emerging (or re-emerging) discipline. Trends in Ecology & Evolution **20**:328-336.

Ostfeld, R. S., F. Keesing, and V. T. Eviner, editors. 2008. Infectious Disease Ecology: Effects of Ecosystems on Disease and of Disease on Ecosystems. Princeton University Press, Princeton, NJ.

Overholt, E. P., S. R. Hall, C. E. Williamson, C. K. Meikle, M. A. Duffy, and C. E. Cáceres. 2012. Solar radiation decreases parasitism in *Daphnia*. Ecology Letters **15**:47-54.

Park, T. 1948. Interspecies competition in populations of *Tribolium confusum* Duval and *Tribolium castaneum* Herbst. Ecological Monographs **18**:265-307.

Patz, J. A., P. Daszak, G. M. Tabor, A. A. Aguirre, M. Pearl, J. Epstein, N. D. Wolfe, A. M. Kilpatrick, J. Foufopoulos, D. Molyneux, D. J. Bradley, and D. Working Grp Land Use Change. 2004. Unhealthy landscapes: Policy recommendations on land use change and infectious disease emergence. Environmental Health Perspectives **112**:1092-1098.

Peñalva-Arana, D. C., K. Forshay, P. T. J. Johnson, J. R. Strickler, and S. I. Dodson. 2011. Chytrid infection reduces thoracic beat and heart rate of *Daphnia pulicaria*. Hydrobiologia **668**:147-154.

Penczykowski, R. M., S. R. Hall, D. J. Civitello, and M. A. Duffy. in press. Habitat structure and ecological drivers of disease. Limnology and Oceanography.

Penczykowski, R. M., J. L. Hite, M. S. Shocket, S. R. Hall, and M. A. Duffy. in prep.-a. Nutrient enrichment, habitat structure, and disease in the plankton.

Penczykowski, R. M., B. C. P. Lemanski, R. D. Sieg, S. R. Hall, J. H. Ochs, J. Kubanek, and M. A. Duffy. in review. Poor resource quality lowers transmission potential by changing foraging behaviour. Functional Ecology.

Penczykowski, R. M., J. H. Ochs, H. Sundar, M. S. Shocket, B. C. P. Lemanski, S. R. Hall, and M. A. Duffy. in prep.-b. Disease reduces host foraging rate: Trait-mediated indirect effects of disease on resources.

Persaud, A. D. and N. D. Yan. 2003. UVR sensitivity of *Chaoborus* larvae. Ambio **32**:219-224.

Piñeiro, G., S. Perelman, J. P. Guerschman, and J. M. Paruelo. 2008. How to evaluate models: Observed vs. predicted or predicted vs. observed? Ecological Modelling **216**:316-322.

Plath, K. and M. Boersma. 2001. Mineral limitation of zooplankton: Stoichiometric constraints and optimal foraging. Ecology **82**:1260-1269.

Ploutno, A. and S. Carmeli. 2002. Modified peptides from a water bloom of the cyanobacterium *Nostoc* sp. Tetrahedron **58**:9949-9957.

Plowright, R. K., P. Foley, H. E. Field, A. P. Dobson, J. E. Foley, P. Eby, and P. Daszak. 2011. Urban habituation, ecological connectivity and epidemic dampening: the emergence of Hendra virus from flying foxes (Pteropus spp.). Proceedings of the Royal Society B-Biological Sciences **278**:3703-3712.

Power, A. G. 1987. Plant community diversity, herbivore movement, and an insect-transmitted disease of maize. Ecology **68**:1658-1669.

Preston, D. L., S. A. Orlofske, J. P. McLaughlin, and P. T. J. Johnson. 2012. Food web including infectious agents for a California freshwater pond. Ecology **93**:1760.

Pulkkinen, K., L. R. Suomalainen, A. F. Read, D. Ebert, P. Rintamaki, and E. T. Valtonen. 2010. Intensive fish farming and the evolution of pathogen virulence: the case of columnaris disease in Finland. Proceedings of the Royal Society B-Biological Sciences **277**:593-600.

Ravet, J. L., M. T. Brett, and D. C. Muller-Navarra. 2003. A test of the role of polyunsaturated fatty acids in phytoplankton food quality for *Daphnia* using liposome supplementation. Limnology and Oceanography **48**:1938-1947.

Rhodes, C. J. and A. P. Martin. 2010. The influence of viral infection on a plankton ecosystem undergoing nutrient enrichment. Journal of Theoretical Biology **265**:225-237.

Rohr, J. R., A. P. Dobson, P. T. J. Johnson, A. M. Kilpatrick, S. H. Paull, T. R. Raffel, D. Ruiz-Moreno, and M. B. Thomas. 2011. Frontiers in climate change-disease research. Trends in Ecology & Evolution **26**:270-277.

Rohrlack, T., M. Henning, and J. G. Kohl. 1999. Mechanisms of the inhibitory effect of the cyanobacterium *Microcystis aeruginosa* on *Daphnia galeata*'s ingestion rate. Journal of Plankton Research **21**:1489-1500.

Saraiva, S., J. van der Meer, S. Kooijman, and T. Sousa. 2011. DEB parameters estimation for Mytilus edulis. Journal of Sea Research **66**:289-296.

Sarnelle, O. and A. E. Wilson. 2008. Type III functional response in *Daphnia*. Ecology **89**:1723-1732.

Sato, T., T. Egusa, K. Fukushima, T. Oda, N. Ohte, N. Tokuchi, K. Watanabe, M. Kanaiwa, I. Murakami, and K. D. Lafferty. 2012. Nematomorph parasites indirectly alter the food web and ecosystem function of streams through behavioural manipulation of their cricket hosts. Ecology Letters **15**:786-793.

Sato, T., K. Watanabe, M. Kanaiwa, Y. Niizuma, Y. Harada, and K. D. Lafferty. 2011. Nematomorph parasites drive energy flow through a riparian ecosystem. Ecology **92**:201-207.

Schindler, D. W., R. E. Hecky, D. L. Findlay, M. P. Stainton, B. R. Parker, M. J. Paterson, K. G. Beaty, M. Lyng, and S. E. M. Kasian. 2008. Eutrophication of lakes cannot be controlled by reducing nitrogen input: Results of a 37-year whole-

ecosystem experiment. Proceedings of the National Academy of Sciences **105**:11254-11258.

Schindler, D. W. and J. R. Vallentyne. 2008. The Algal Bowl: Overfertilization of the world's freshwaters and estuaries. University of Alberta Press, Alberta.

Seppälä, O., K. Liljeroos, A. Karvonen, and J. Jokela. 2008. Host condition as a constraint for parasite reproduction. Oikos **117**:749-753.

Smith, D. L., B. Lucey, L. A. Waller, J. E. Childs, and L. A. Real. 2002. Predicting the spatial dynamics of rabies epidemics on heterogeneous landscapes. Proceedings of the National Academy of Sciences of the United States of America **99**:3668-3672.

Smith, V. H. 2003. Eutrophication of freshwater and coastal marine ecosystems: A global problem. Environmental Science and Pollution Research **10**:126-139.

Smith, V. H., T. P. Jones, and M. S. Smith. 2005. Host nutrition and infectious disease: an ecological view. Frontiers in Ecology and the Environment **3**:268-274.

Smyth, R. L. 2010. Stratification and turbulent mixing in small strongly stratified lakes with implications for planktonic disease dynamics. PhD Thesis. University of California, Santa Barbara.

Snucins, E. and J. Gunn. 2000. Interannual variation in the thermal structure of clear and colored lakes. Limnology and Oceanography **45**:1639-1646.

Soranno, P. A., S. R. Carpenter, and R. C. Lathrop. 1997. Internal phosphorus loading in Lake Mendota: response to external loads and weather. Canadian Journal of Fisheries and Aquatic Sciences **54**:1883-1893.

Sterner, R. W. and J. J. Elser. 2002. Ecological stoichiometry: The biology of elements from molecules to the biosphere. Princeton University Press, Princeton, NJ.

Sterner, R. W., J. J. Elser, E. J. Fee, S. J. Guildford, and T. H. Chrzanowski. 1997. The light:nutrient ratio in lakes: The balance of energy and materials affects ecosystem structure and process. American Naturalist **150**:663-684.

Sterner, R. W. and D. O. Hessen. 1994. Algal nutrient limitation and the nutrition of aquatic herbivores. Annual Review of Ecology and Systematics **25**:1-29.

Sullivan, L. L., B. L. Johnson, L. A. Brudvig, and N. M. Haddad. 2011. Can dispersal mode predict corridor effects on plant parasites? Ecology **92**:1559-1564.

Sumpter, D. J. T. and S. J. Martin. 2004. The dynamics of virus epidemics in Varroa-infested honey bee colonies. Journal of Animal Ecology **73**:51-63.

Tessier, A. J. and J. Welser. 1991. Cladoceran assemblages, seasonal succession and the importance of a hypolimnetic refuge. Freshwater Biology **25**:85-93.

Tessier, A. J. and P. Woodruff. 2002. Cryptic trophic cascade along a gradient of lake size. Ecology **83**:1263-1270.

Thomas, F., F. Renaud, T. de Meeus, and R. Poulin. 1998. Manipulation of host behaviour by parasites: ecosystem engineering in the intertidal zone? Proceedings of the Royal Society B-Biological Sciences **265**:1091-1096.

Thompson, R. M., K. N. Mouritsen, and R. Poulin. 2005. Importance of parasites and their life cycle characteristics in determining the structure of a large marine food web. Journal of Animal Ecology **74**:77-85.

Threlkeld, S. T. 1979. The midsummer dynamics of two *Daphnia* species in Wintergreen Lake, Michigan. Ecology **60**:165-179.

Tompkins, D. M., A. M. Dunn, M. J. Smith, and S. Telfer. 2011. Wildlife diseases: from individuals to ecosystems. Journal of Animal Ecology **80**:19-38.

Tompkins, D. M., A. R. White, and M. Boots. 2003. Ecological replacement of native red squirrels by invasive greys driven by disease. Ecology Letters **6**:189-196.

Urabe, J., J. Clasen, and R. W. Sterner. 1997. Phosphorus limitation of *Daphnia* growth: Is it real? Limnology and Oceanography **42**:1436-1443.

van de Waal, D. B., A. M. Verschoor, J. M. H. Verspagen, E. van Donk, and J. Huisman. 2010. Climate-driven changes in the ecological stoichiometry of aquatic ecosystems. Frontiers in Ecology and the Environment **8**:145-152.

van der Meer, J. 2006. An introduction to Dynamic Energy Budget (DEB) models with special emphasis on parameter estimation. Journal of Sea Research **56**:85-102.

Venesky, M. D., T. E. Wilcoxen, M. A. Rensel, L. Rollins-Smith, J. L. Kerby, and M. J. Parris. 2012. Dietary protein restriction impairs growth, immunity, and disease resistance in southern leopard frog tadpoles. Oecologia **169**:23-31.

von Elert, E. and F. Jüttner. 1997. Phosphorus limitation and not light controls the extracellular release of allelopathic compounds by *Trichormus doliolum* (cyanobacteria). Limnology and Oceanography **42**:1796-1802.

von Elert, E., L. Oberer, P. Merkel, T. Huhn, and J. F. Blom. 2005. Cyanopeptolin 954, a chlorine-containing chymotrypsin inhibitor of *Microcystis aeruginosa* NIVA Cya 43. Journal of Natural Products **68**:1324-1327.

von Elert, E., A. Zitt, and A. Schwarzenberger. 2012. Inducible tolerance to dietary protease inhibitors in *Daphnia magna*. Journal of Experimental Biology **215**:2051-2059.

Von Ende, C. N. 1979. Fish predation, interspecific predation, and the distribution of two *Chaoborus* species. Ecology **60**:119-128.

Vrede, T., D. R. Dobberfuhl, S. Kooijman, and J. J. Elser. 2004. Fundamental connections among organism C : N : P stoichiometry, macromolecular composition, and growth. Ecology **85**:1217-1229.

Wang, T., C. C. Y. Hung, and D. J. Randall. 2006. The comparative physiology of food deprivation: From feast to famine. Pages 223-251 Annual Review of Physiology. Annual Reviews, Palo Alto.

Warren, C. P., M. Pascual, K. D. Lafferty, and A. M. Kuris. 2010. The inverse niche model for food webs with parasites. Theoretical Ecology **3**:285-294.

Washburn, J. O., D. R. Mercer, and J. R. Anderson. 1991. Regulatory role of parasites: Impact on host population shifts with resource availability. Science **253**:185-188.

Webb, D. J., B. K. Burnison, A. M. Trimbee, and E. E. Prepas. 1992. Comparison of chlorophyll *a* extractions with ethanol and dimethyl sulfoxide/acetone, and a concern

about spectrophotometric phaeopigment correction. Canadian Journal of Fisheries and Aquatic Sciences **49**:2331-2336.

Welschmeyer, N. A. 1994. Fluorometric analysis of chlorophyll *a* in the presence of chlorophyll *b* and pheopigments. Limnology and Oceanography **39**:1985-1992.

Wilson, A. E., O. Sarnelle, and A. R. Tillmanns. 2006. Effects of cyanobacterial toxicity and morphology on the population growth of freshwater zooplankton: Meta-analyses of laboratory experiments. Limnology and Oceanography **51**:1915-1924.

Winder, M. and U. Sommer. 2012. Phytoplankton response to a changing climate. Hydrobiologia **698**:5-16.

Wood, C. L., J. E. Byers, K. L. Cottingham, I. Altman, M. J. Donahue, and A. M. H. Blakeslee. 2007. Parasites alter community structure. Proceedings of the National Academy of Sciences of the United States of America **104**:9335-9339.